January 2015

Immunotherapy of Folate Receptor Expressing Cancers

Nimalka Achini Bandara
Purdue University

Graduate School Form 30
(Updated 11/20/2014)

PURDUE UNIVERSITY
GRADUATE SCHOOL
Thesis/Dissertation Acceptance

This is to certify that the thesis/dissertation prepared

By Nimalka Achini Bandara

Entitled

IMMUNOTHERAPY OF FOLATE RECEPTOR EXPRESSING CANCERS

For the degree of Doctor of Philosophy

Is approved by the final examining committee:

Philip S. Low

David H. Thompson

Timothy L. Ratliff

Jean A. Chmielewski

To the best of my knowledge and as understood by the student in the Thesis/Dissertation Agreement, Publication Delay, and Certification/Disclaimer (Graduate School Form 32), this thesis/dissertation adheres to the provisions of Purdue University's "Policy on Integrity in Research" and the use of copyrighted material.

Philip S. Low

Approved by Major Professor(s): _____

_____

Approved by: R. E. Wild 02/06/2015

Head of the Department Graduate Program Date

IMMUNOTHERAPY OF FOLATE RECEPTOR EXPRESSING CANCERS

A Dissertation

Submitted to the Faculty

of

Purdue University

by

Nimalka Achini Bandara

In Partial Fulfillment of the

Requirements for the Degree

of

Doctor of Philosophy

May 2015

Purdue University

West Lafayette, Indiana

For my Amma and Appachchi

ACKNOWLEDGEMENTS

I grew up in countries where children are raised by the extended families, the neighbors, and the other adults on the street where your house was built. I must have had my meals in three different homes on any given day and been disciplined by every aunt and uncle in my family. The one common value instilled in me by every individual who raised me as a child was the desire to pursue as high an education as I could attain. So, first I would like to thank my parents who planned for my education since before I was born; who taught me at home so that I was always a step ahead at school, and who gave up many of their own pursuits in order to make the best education they could offer available to me. Second, I would like to thank my maternal grandmother and grandfather as well as my aunts and uncles for raising me and teaching me the values that one must live by in life.

All my teachers from elementary school through high school were instrumental in making learning a positive experience for me. From the little notes on tests when I did well (‘bombs come in little packages’ comes to mind) to the brilliant books that I was assigned to read, I look back to the time in school as a pleasant phase of life. My college professors at Wofford College were dedicated educators and loving mentors who made me want to grow up and be like them, and to them I owe a debt of gratitude that will never be repaid.

I thank Dr. Philip Low for welcoming me into his group as a zero year student in the summer of 2009 and for keeping me on as a graduate student for the following five years. Dr. Low taught me to work independently, to think critically, and to be thorough in the research that I conducted in his lab. I also thank Prof. David Thompson, Prof. Jean Chmielewski, and Prof. Tim Ratliff for being members of my committee and for taking the time to guide my development as a researcher. Much gratitude goes out to Drs. June Lu and Leroy Wheeler at Endocyte, Inc. for providing conversation, offering suggestions, donating supplies, and most importantly for helping me with my thesis projects. Your advice, guidance, and friendship are truly appreciated.

My years in the Low lab would not have been as memorable as it is without the lab members who colored my life with their presence. Drs. Charity Wayua and Lindsay Kelderhouse who dealt with my daily frustrations, jokes, and general ridiculousness helped make my time in the lab exciting and light-hearted, and taught me a great many of the techniques that I know today. Drs. Michael Hansen and Johnny Shen provided excellent conversation and a myriad of cultural knowledge. I thank Jyoti Roy, Dr. Haiyan Chu, and Dr. Bingbing Wang for being such wonderful friends who were always being willing to help when I was in a tight spot. I am grateful to Greg Jarvis for providing many interesting conversations over the years and to all the younger lab members for being delightful faces of positive hopefulness during my last few years. All the past and present postdocs in the lab (Drs. Venkatesh Chelvam, Madduri Srinivasarao, Sakkarapalayam Mahalingam, Srinivasa Tennetti, Bo Liang, Guo Li, Ananda Kanduluru, Qingshou Chen, and Pengcheng Lu) have been brilliant resources and synthetic gurus who never hesitated to help with an experiment, so I thank each of you for your

generousness of time and caring towards younger students. I thank Dr. Christopher Galliford for helping me with the completion of manuscripts for publication and for being positive through that challenging process. Last but not at all least, I express my sincere gratitude to Patti Cauble for being a phenomenal administrative assistant, a patient listener, and a solver of problems. Your friendship is more valuable than we ever get to tell you about.

My tenure as a graduate student in the Department of Chemistry was made significantly easier by the wealth of knowledge, advice, and general helpfulness offered by Betty Hatfield, Lynn Rider, Debbie Packer, Trisha Herrera, and Rob Reason. They are each such wonderful and genuinely friendly individuals whose smiling faces I will miss dearly when I leave Purdue. I thank Nancy Petretic for helping with my many cell culture questions and Karen Wethington for caring so well for the animals that I housed in her facility.

My years in Indiana would have been devoid of happiness had it not been for a fabulous group of friends. I will forever be grateful to Kelsey Bohn for the many walks, the many failed attempts at training for races, for making me laugh helplessly with the situations we managed to get into, and for standing in solidarity with me about our hopeless dogs. I thank Patty Wiley for being a consistent, loyal friend and roommate who could always be counted upon for serious conversations on serious matters and for a very fun evening when it was time to relax and celebrate. Dr. Zach Davis, your exuberantly positive personality, excellent appetite, love for a cultured life, and good taste in wine made it possible for me to get through many a difficult day over the past five years and for that, I am indebted to you. Drs. William McGee and Scott Toth, I will always cherish

our nights of spaghetti and meat sauce, pumpkin pie, Monty Python, and grading lab reports.

The last and most difficult two years of my graduate school career was made bearable by the spontaneous outings, long walks, incredible conversations, and contagious sense of humor supplied by Dr. Josh Wiley and the unconditional love and loyalty provided by our foster dogs, Emma and Delilah. You make my life a vibrant adventure and I am continually grateful for your support!

TABLE OF CONTENTS

Page

Page

Page

Page

LIST OF TABLES

LIST OF FIGURES

Figure Page

Figure Page

Figure Page

LIST OF ABBREVIATIONS

ADCC	antibody dependent cellular cytotoxicity
AF	Alexa Fluor
AIDS	acquired immune deficiency syndrome
APC	antigen presenting cells ***or*** allophycocyanin fluorophore
AU	antibody fluorescence units
BSA	bovine serum albumin
CAR	chimeric antigen receptor
CCR5	chemokine receptor 5
CD	cluster of differentiation
CHO	Chinese hamster ovary
CMC	carboxymethylcellulose
CNS	central nervous system
CpG	regions of DNA where a guanine follows a cytosine
cpm	counts per minute
CTL	cytotoxic T cell
CTLA4	cytotoxic T-lymphocyte-associated protein 4

DC	dendritic cell
DMEM	Dulbecco’s modified Eagle’s medium
DMSO	dimetylsulfoxide
DNA	deoxyribonucleic acid
DNP	dinitrophenol
EDA	ethylenediamine
ELISA	enzyme-linked immunosorbent assay
FACS	fluorescence-activated cell sorting
FBP	folate binding protein
FBS	fetal bovine serum
FD	folate deficient
FDA	food and drug administration
FEFITC	folate-EDA-FITC
FITC	fluorescein isothiocyanate
FR	folate receptor
g	grams
GPCR	G-protein coupled receptor
GPI	glycosylphosphatidylinositol
h	hours
HIV	human immunodeficiency virus
HPLC	high-performance liquid chromatography

HRP	horse radish peroxidase
IC_{50}	concentration at 50% inhibition
IFN	interferon
IgG	immunoglobulin gamma
IL	interleukin
i.p.	intraperitoneal
i.v.	intravenous
kDa	kiloDaltons
kg	kilograms
KLH	keyhole limpet hemocyanin
mAB	monoclonal antibody
MDSC	myeloid derived suppressor cell
MHC	major histocompatibility complex
mg	milligrams
min	minutes
ml	milliliters
µL	microliter
mm	millimeters
mM	millimolar
µg	micrograms
µM	micromolar

µmol	micromoles
NIH	national institutes of health
NK	natural killer cell
nm	nanometers
nM	nanomolar
nmol	nanomoles
O.D.	optical density
ODN	oligodeoxynucleotide
OPD	*o*-phenylenediamine dihydrochloride
OVA	ovalbumin
PBS	phosphate buffered saline, pH 7.4
PD-1	programmed cell death protein-1
PE	phycoerythrin
PEG	polyethyleneglycol
p.o.	per os *or* by mouth
RFC	reduced folate carrier
RPM	revolutions per minute
RPMI	culture medium developed at Roswell Park Memorial Institute
RT	room temperature
rtk	receptor tyrosine kinase
s	seconds

s.c.	subcutaneous
scFv	single-chain antibody fragment
SEM	standard error mean
sst	somatostatin
TAA	tumor associated antigen
TCR	T cell receptor
TLR	toll like receptor
TSA	tumor specific antigen
T_{reg}	regulatory T cell
VEGFR	vascular endothelial growth factor receptor

ABSTRACT

Bandara, Nimalka Achini, Ph.D., Purdue University, May 2015. Immunotherapy of Folate Receptor Expressing Cancers. Major Professor: Philip S. Low.

The folate receptor (FR) is a GPI anchored cell surface glycoprotein that functions to facilitate folic acid uptake and mediate signal transduction. With the introduction of multiple folate-targeted drugs into the clinic, the question has arisen regarding how frequently a patient can be dosed with a FR-targeted drug or antibody, and whether dosing frequency exerts any impact on the availability of FR for subsequent rounds of FR-mediated drug uptake. Although the rate of FR recycling has been examined in murine tumor models, little or no information exists on the impact of FR occupancy on its rate of endocytosis. The studies described in chapter two of this thesis quantitates the number of cell surface FR-α and FR-β following exposure to saturating concentrations of a variety of folate-linked molecules and anti-FR antibodies, including the unmodified vitamin, folate-linked drug mimetics, multi-folate derivatized nanoparticles, and monoclonal antibodies to FR. The collected data indicate that FR occupancy has no impact on the rate of FR internalization. The results also demonstrate that multivalent conjugates that bind and cross-link FRs at the cell surface internalize at the same rate as monovalent folate conjugates that have no impact on FR clustering, even though the multivalent conjugates traffic through a different endocytic pathway.

Having described early, fundamental studies regarding the mechanism of action of cell surface folate receptors, the remaining chapters in this thesis will focus on the design and evaluation of combination immunotherapy techniques for the treatment of FR expressing cancers. Cancer immunotherapy relies on harnessing the power of the body's immune system and directing its killing power towards a patient's malignant tumor while avoiding toxicity to healthy tissues. Since physiological folates play a critical role in DNA synthesis and cell division, and since uncontrolled proliferation of cells is a trademark of malignant cancers, FR is overexpressed by a variety of tumors in order to meet the demand for larger quantities of the vitamin. Therefore, the folate receptor has been successfully exploited for the delivery of folic acid linked imaging and therapeutic agents to a variety of cancer cell types. Chapters 3 and 4 of this thesis describes experiments aimed towards evaluating immunotherapy combinations that could have clinically translatable effects on FR positive cancers. By using *in vivo* mouse models of kidney cancer, lung cancer, and lymphoma these studies demonstrate that vascular endothelial growth factor receptor (VEGFR) inhibitors as well as T cell check point inhibitors synergize with folate-hapten mediated immunotherapy to slow tumor progression, reduce tumor cell metastasis, and prolong survival. We then proceed to answer the more challenging question of why this observed synergy occurs by evaluating resected tumor and spleen tissues from treated mice for changes in immune cell components and microenvironment composition. It is apparent from the collected data that the physiological mechanism of synergy is multi-fold and includes the combination's ability to better activate immune effector cells, recruit cytotoxic cells to the tumor site, down regulate immune suppressor cells, and slow the growth of tumor vasculature.

LIST OF PATENTS AND PUBLICATIONS

LIST OF PATENTS AND PUBLICATIONS

1. N. Achini Bandara, Michael J. Hansen, and Philip S. Low. Effect of Receptor Occupancy on Folate Receptor Internalization. *Mol. Pharmaceutics*, 2014, 11: 1007–1013.

2. N. Achini Bandara and Philip S. Low. Method of Treatment Using Folate Conjugates and Tyrosine Kinase Inhibitors. US Patent Application 62/091, 437, filed December 12, 2014.

3. Michael J. Hansen, N. Achini Bandara, and Philip S. Low. Folate Receptor Expression on Murine and Human Adipose Tissue Macrophages. Accepted. *Inflamm. Res*. 2015.

4. Venkatesh Chelvam, Ananda K. Kanduluru, N. Achini Bandara, and Philip S. Low. Stimulation of Endosomal Release of Entrapped Drugs by a Novel Mechanism. (Invited by *AAPS J*. and submitted)

5. N. Achini Bandara, Cody D. Bates, Yingjuan Lu, Emily K. Hoylman, and Philip S. Low. Folate-hapten mediated immunotherapy synergizes with vascular endothelial growth factor receptor (VEGFR) inhibitors for the treatment of cancer. (Manuscript in preparation)

6. N. Achini Bandara and Philip S. Low. Antibody inhibitors of the T cell checkpoints, PD-1 and CTLA4, synergize with folate-hapten mediated immunotherapy in folate receptor expressing cancers. (Manuscript in preparation)

7. N. Achini Bandara and Philip S. Low. Method of Treatment Using Folate Conjugates and T cell checkpoint inhibitors. (Patent in preparation)

molecular pharmaceutics

Article

pubs.acs.org/molecularpharmaceutics

Effect of Receptor Occupancy on Folate Receptor Internalization

N. Achini Bandara, Michael J. Hansen, and Philip S. Low*

Department of Chemistry, Purdue University, West Lafayette, Indiana 47907, United States

ABSTRACT: The folate receptor (FR) is a GPI anchored cell surface glycoprotein that functions to facilitate folic acid uptake and mediate signal transduction. With the introduction of multiple folate-targeted drugs into the clinic, the question has arisen regarding how frequently a patient can be dosed with a FR-targeted drug or antibody and whether dosing frequency exerts any impact on the availability of FR for subsequent rounds of FR-mediated drug uptake. Although the rate of FR recycling has been examined in murine tumor models, little or no information exists on the impact of FR occupancy on its rate of endocytosis. The present study quantitates the number of cell surface FR-α and FR-β following exposure to saturating concentrations of a variety of folate-linked molecules and anti-FR antibodies, including the unmodified vitamin, folate-linked drug mimetics, multifolate derivatized nanoparticles, and monoclonal antibodies to FR. We report here that FR occupancy has no impact on the rate of FR internalization. We also demonstrate that multivalent conjugates that bind and cross-link FRs at the cell surface internalize at the same rate as monovalent folate conjugates that have no impact on FR clustering, even though the multivalent conjugates traffic through a different endocytic pathway.

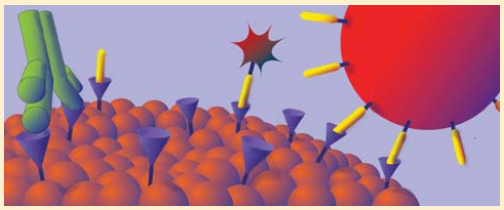

KEYWORDS: *receptor recycling, folate receptor endocytosis, ligand targeted drugs, antibodies to folate receptors, ligand valency on nanomedicines*

INTRODUCTION

The folate receptor (FR) constitutes a family of four homologous proteins that are thought to bind folic acid and its physiologic congeners.[1,2] FR-α is found on the apical surfaces of certain epithelial cells, where it is largely inaccessible to folates in the bloodstream.[3,4] It is also overexpressed on a variety of epithelial-derived cancers, where it can be readily targeted by intravenously injected folate-linked drugs.[5−7] FR-β is primarily expressed on activated macrophages[8] which populate almost all autoimmune and inflamed tissues and mediate many of the destructive processes responsible for disease symptoms.[9−11] Examples of inflammatory diseases caused or worsened by FR+ activated macrophages include rheumatoid arthritis, ulcerative colitis, atherosclerosis, multiple sclerosis, and psoriasis among others.[12−18] FR-γ has been detected in the bone marrow from whence it may be released into circulation,[19] but whether it facilitates folate uptake is not known. FR-δ has been found primarily on regulatory T cells[20] and like FR-γ has no known function. Only FR-α has been shown to be involved in signal transduction,[21] but the possible participation of FR-β, FR-γ, or FR-δ in transmembrane signaling has never been examined.

Because of the limited expression and/or accessibility of FR in healthy human tissues, both FR-α and FR-β have been exploited for targeted drug delivery to cancer tissues and sites of inflammation, respectively.[22] For this purpose, folate is linked to a therapeutic or imaging agent and injected into the diseased host, where it is either captured by FR on the pathologic cell surface or rapidly excreted from the body. Radioactive[13,15] and fluorescent[23,24] folate conjugates have been used to visualize sites of inflammation[25] and localize malignant disease,[23,26,27] whereas folate-conjugated therapeutic agents have been exploited to destroy FR-α expressing tumor cells[28,29] and inactivate FR-β expressing inflammatory macrophages.[14,16] A variety of folate-targeted molecules are currently undergoing human clinical trials.

Because the rate of FR internalization and trafficking can influence the frequency of folate conjugate dosing (i.e., there is no merit in injecting a patient with a folate−drug conjugate more frequently than empty FR return to the pathologic cell surface following endocytosis), several studies have examined the rate and routes of FR trafficking in physiologically relevant systems.[24,30−32] Results from these studies demonstrate that FR traffic through different intracellular compartments depending on the number of folates tethered to the targeted conjugate, with monovalent folate−drug conjugates trafficking through a recycling center before returning to the cell surface,[24,31,33] and multivalent FR ligands trafficking through multivesicular bodies prior to deposition in lysosomes.[34−37] Importantly, despite the detailed nature of the above studies, the effect of folate conjugate size and valency on its rate of internalization and recycling has never been examined. In this paper, we explore the kinetics of internalization of both FR-α and FR-β following their ligation to a variety of folate-linked molecules and antifolate receptor antibodies, including the free unligated

Received: November 4, 2013
Revised: January 16, 2014
Accepted: January 21, 2014
Published: January 21, 2014

dx.doi.org/10.1021/mp400659t | *Mol. Pharmaceutics* 2014, 11, 1007−1013

vitamin, folate-linked small molecules, multifolate derivatized nanoparticles, and monoclonal antibodies to FR.

EXPERIMENTAL PROCEDURES

Cell Lines and Culture. All FR positive cell lines were maintained in the Cell Culture Facility of the Purdue University Department of Chemistry. KB and IGROV cells were maintained in folate-deficient RPMI 1640 medium (Invitrogen, Grand Island, NY) supplemented with 10% heat inactivated fetal bovine serum (Sigma Aldrich, St. Louis, MO), penicillin (50 units/mL), and streptomycin (50 μg/mL). Chinese hamster ovary (CHO) cells stably transfected with human FR-β (generous gift from Manohar Ratnam, Karmanos Cancer Center, Detroit, MI) were maintained in folate-deficient RPMI 1640 medium (Invitrogen, Grand Island, NY) supplemented with 10% heat inactivated fetal bovine serum (Sigma Aldrich, St. Louis, MO), 0.15 mg/mL L-proline, 10 nmol/L N^5-formyl tetrahydrofolate, 100 units/mL penicillin, and 100 μg/mL streptomycin (Sigma Aldrich, St. Louis, MO). All cell lines were passaged continuously in a monolayer and cultured at 37 °C in a humidified atmosphere containing 5% CO_2.

Antibodies and Reagents. Folic acid was purchased from Sigma Aldrich (St. Louis, MO) and dissolved in pH adjusted deionized water. The hybridoma cell line that produces a mouse monoclonal antibody to human FR-α (mAb 343) was a generous gift from Wilbur Franklin (University of Colorado), and folate-fluorescein (EC17) was kindly provided by Endocyte, Inc. (West Lafayette, IN). Fluorescein-labeled goat antimouse IgG antibody was purchased from Santa Cruz Biotechnology, Inc. (Dallas, TX). Human antihuman mAb against FR-β (m909) was developed in collaboration with Dr. Dimiter Dimitrov (National Institutes of Health, Frederick, MD) and labeled with fluorescein isothiocyanate.[9]

Folate Conjugates. A water-soluble monovalent folate-rhodamine conjugate with nanomolar FR affinity (Figure 1A) was synthesized as previously described.[24,26] Folate-targeted polyethylene glycol-derivatized liposomes were also prepared according to previous procedures,[35] with ~3.5% of the phospholipids derivatized with PEG and ~10% of the PEGylated lipids further conjugated to folic acid. Assuming ~80 000 lipids per liposome, this calculates to ~280 folate targeting ligands per liposome for a folate-targeted lipid concentration of ~1.5 μM in the stock suspension.

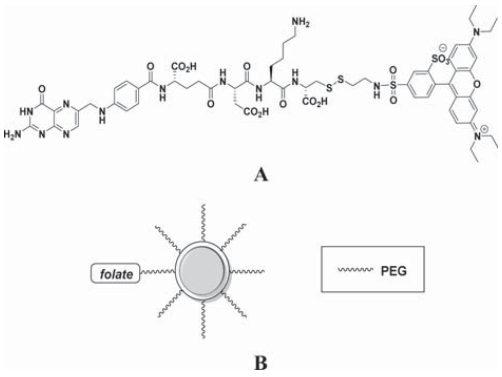

Figure 1. General structures of (A) folate−rhodamine conjugate and (B) folate−PEG liposomes.

Evaluation of the Effect of Receptor Occupancy on Receptor Internalization. Each cell type to be investigated was plated in a six-well plate at a density of 50 000 cells/well and allowed to adhere overnight. Individual wells were either left untreated (controls) or incubated in 100 nM folic acid or folate rhodamine for 20 min, 4 h, or 24 h at 37 °C. For analyses of liposome uptake, 100 μL of 2 mg/mL folate-conjugated liposome stock suspension was added to each well prior to execution of the same incubation procedure. Following incubation, wells were washed thoroughly with PBS to remove unbound ligand, after which cells were removed from the plate by scraping, centrifuged to form a pellet, and resuspended in cold (4 °C) folate-deficient culture medium to block further FR trafficking. Folate receptors accessible on the cell surface were then labeled with either mAb343 followed by fluorescein-labeled goat antimouse secondary antibody (KB and IGROV cells) or m909-FITC (CHO-β cells) by further incubation at 4 °C for 1 h. After washing with PBS to remove unbound antibody, fluorescently labeled FR in all cell samples were quantitated on a Becton Dickinson FACS Caliber flow cytometer. Ten thousand cells were counted from each sample, and three samples from each treatment condition were evaluated. CellQuest software was used for data collection, and FlowJo software was employed for data analysis. Graphing and statistical calculations of the analyzed data were performed using GraphPad Prism software.

RESULTS

Effect of Folic Acid on the Kinetics of FR-α Internalization. For many cell surface receptors, the rate of receptor internalization is strongly dependent on both receptor number and receptor occupancy.[38,39] Although previous studies have demonstrated that the rate of FR internalization is independent of receptor number,[30] no information is currently available on the impact of receptor occupancy on the rate of FR endocytosis. To obtain this information, KB and IGROV cells (which express high and low levels of FR-α, respectively) were incubated *in vitro* with a saturating concentration (100 nM) of free folic acid for 20 min, 4 h, or 24 h at 37 °C. Cell surface FR were then quantitated by flow cytometry using a noncompeting anti-FR-α primary antibody (mAb343) followed by labeling with a fluorescein-conjugated goat antimouse secondary antibody. If folic acid binding were to induce FR internalization, a decrease in available FR on the cell surface would be expected as exposure to folate/folate conjugate proceeded. Moreover, if resting state FR levels were to impact the rate of ligand-induced receptor endocytosis, differences between FR internalization by KB and IGROV cells would be anticipated. As seen in Figure 2, the rate of FR-α internalization is not altered by folic acid binding, since cell surface FR-α numbers remain similar to their levels in untreated cells at all of the time points tested. Furthermore, the level of FR expression in untreated cells must exert little influence over the kinetics of receptor internalization, since cell lines that express high and low levels of FR display the same insensitivity to receptor saturation.

Effect of Folic Acid on the Kinetics of FR-β Internalization. Although FR-β exhibits similar nanomolar affinity for folic acid to FR-α,[40] its greatly reduced level of expression,[41] its unique manifestation on activated immune cells,[8−11] and its rapid rate of internalization[12,30] raise the question of whether the response of FR-β to saturation with folic acid might differ

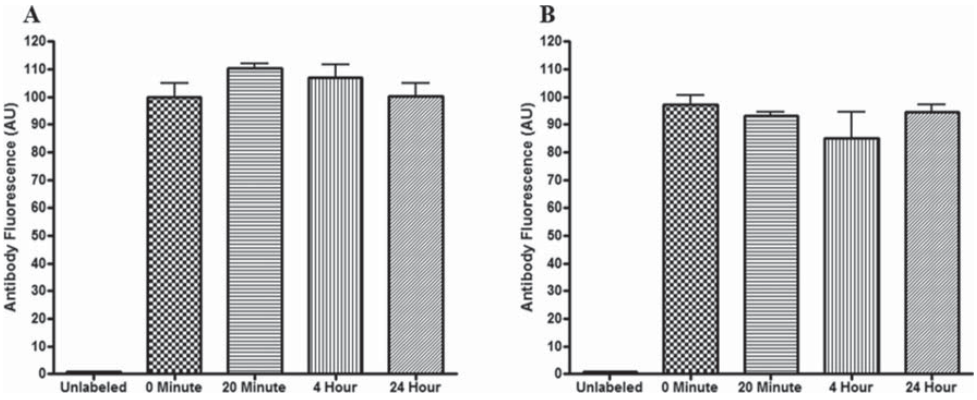

Figure 2. Quantitation of cell surface FR-α after incubating KB cells (A) and IGROV cells (B) with a saturating concentration (100 nM) of folic acid for 20 min, 4 h, and 24 h. Cell surface FR were quantitated by flow cytometry using a noncompeting monoclonal anti-FR-α antibody, as described in the Methods. Mean fluorescent intensities from three samples were averaged and graphed as a percentage of the average fluorescence intensity measured at the 0 min time point, that is, before addition of free folic acid.

from that of FR-α. To evaluate the impact of FR-β occupancy on its rate of internalization, a CHO-K1 strain that was stably transfected with human FR-β was incubated with a saturating concentration of folic acid and examined for cell surface FR-β using a noncompeting monoclonal antibody to FR-β (m909).[9] As seen in Figure 3, the level of FR-β on CHO-β cell surfaces is

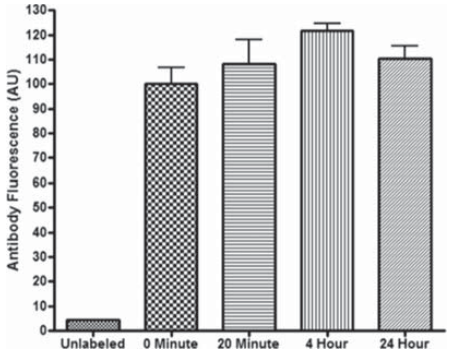

Figure 3. Quantitation of cell surface FR-β after incubating CHO-β cells with saturating folic acid for 20 min, 4 h, and 24 h, as determined by flow cytometry following labeling of extracellular receptors with m909-FITC. Mean fluorescent intensities from three different samples were averaged and graphed as a percentage of the average fluorescence intensity measured at the 0 min time point, that is, before addition of free folic acid.

independent of the time and extent of FR-β saturation with folic acid. Thus, m909-FITC binding remains essentially the same in the absence of added folic acid (0 min time point) as seen following 24 h exposure to saturating levels of folic acid (24 h time point). Moreover, there is no significant difference in cell surface FR-β between cells incubated for 20 min in saturating folic acid and those incubated for 4 or 24 h with the vitamin. Based on these observations, we suggest that the rate of internalization of FR-β, like that of FR-α, is not altered by changes in the level folic acid binding, but instead recycles at a steady rate, regardless of receptor occupancy.

Effect of Folate Conjugate Valency on the Kinetics of Receptor Endocytosis. Cross-linking or clustering of cell surface receptors using multivalent ligands has been known for years to accelerate receptor endocytosis and trafficking to lysosomes.[34,36,42] For example, multivalent lectins and antibodies that can bind multiple receptors simultaneously have been observed to induce localized receptor "patching" followed by a more global receptor "capping" prior to receptor internalization and degradation.[43] Because many laboratories have exploited folate to target nanoparticles to pathologic cells, invariably derivatizing their nanomedicines with multiple folates to increase binding avidity, the concern has naturally arisen whether such multivalent formulations might induce accelerated depletion of FR from the cell surface, preventing or at least delaying the ability to target additional nanomedicines to the same FR-expressing cells. To address this concern, we have compared the number of cell surface FR following incubation of cells with a monovalent ligand (folate–rhodamine) to their number following incubation with a multivalent ligand (folate-targeted liposomes). As seen in Figure 4, only minor differences are seen in the number of residual cell surface FR following incubation with either monovalent (panel A) or multivalent (panel B) folate conjugates, suggesting that cell surface receptor depletion commonly observed with other multivalent ligands does not occur when FR is the targeted receptor. In the case of monovalent folate–rhodamine, the detected variation in cell surface FR-α (KB) and FR-β (CHO-β) levels following different incubation times are minor and probably a consequence of experimental variability. Even in the case of the multivalent liposomes, the decrease in cell surface FR at early time points is reversed at 24 h, suggesting any real effect may be transient at best. Moreover, although receptor numbers differ significantly with IGROV cells and the receptor sequence differs in CHO-β cells, similar insensitivities to folate conjugate valency are observed. We, therefore, conclude that conjugate valency does not have a significant effect on the rate of FR internalization.

Impact of Antibody Binding on FR Endocytosis. Because several anti-FR antibodies have recently entered clinical trials,[44] and since antibodies commonly induce the endocytosis of their targeted receptors,[45] we felt it might be

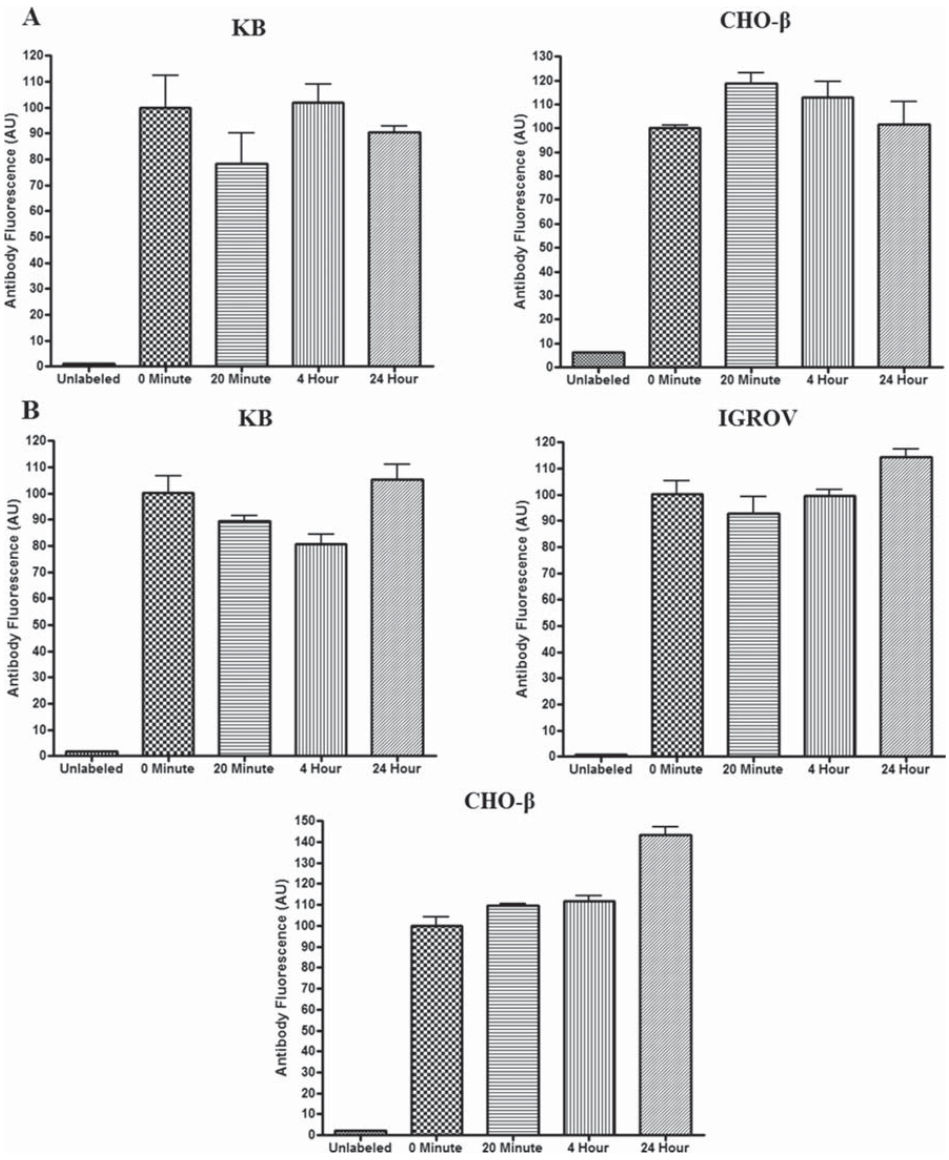

Figure 4. Quantitation of cell surface FR-α and FR-β following incubation of cells with folate−rhodamine (A) or folate-labeled liposomes (B) for the indicated times. As in previous figures, cell surface FR were labeled with mAb343 or m909-FITC and quantitated by flow cytometry. Mean fluorescent intensities from three samples were averaged and graphed as a percentage of the average fluorescence intensity measured at the 0 min time point, that is, before the addition of free folic acid.

prudent to include in our study an examination of the impact of antibody binding on FR endocytosis. For this purpose, KB and CHO-β cells were incubated with saturating concentrations of mAb343 and m909, respectively, and subsequently labeled with folate−fluorescein (EC17) to quantitate the number of cell surface FR. As seen in Figure 5, no differences in cell surface FR were observed following incubation with either antibody at any of the three incubation times, demonstrating that antibody binding also has no impact on FR internalization.

■ DISCUSSION

The rate of internalization and trafficking of most cell surface receptors may depend on multiple parameters, including: (i) the nature of the ligand,[46] (ii) the level of receptor occupancy,[38,47] and (iii) the degree of receptor clustering

dx.doi.org/10.1021/mp400659t | *Mol. Pharmaceutics* 2014, 11, 1007−1013

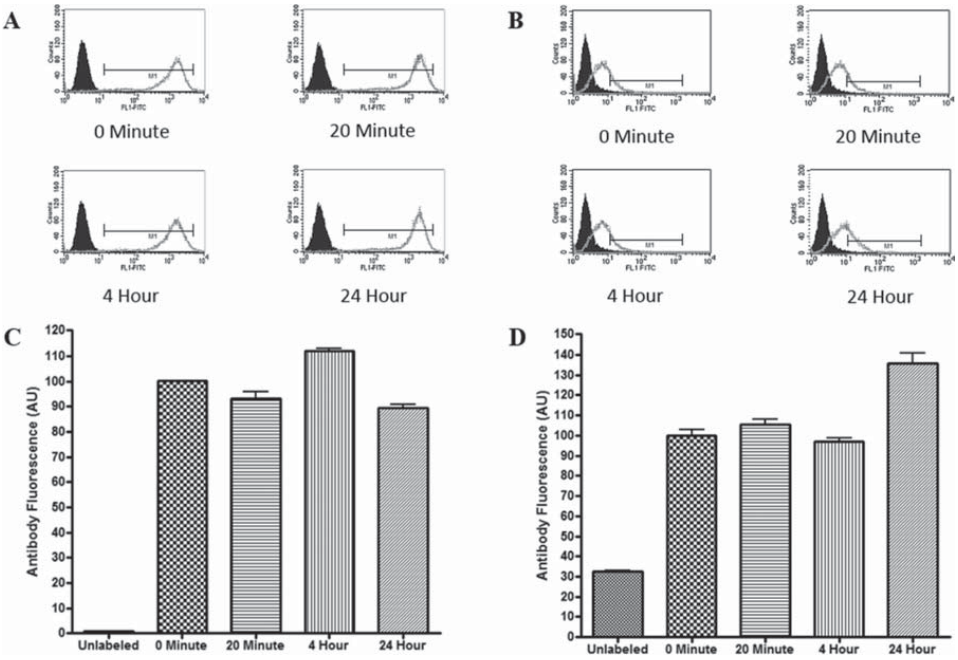

Figure 5. Evaluation of cell surface FR after incubation of KB (A, C) and CHO-β (B, D) cells with mAb343 or m909, respectively, for 20 min, 4 h, or 24 h. Cell surface FR was quantitated by incubation of the cells with saturating folate–fluorescein followed by measurement of FITC fluorescence by flow cytometry. Histograms of representative samples from each incubation time (open histograms) are overlaid with the histograms of unlabeled control cells (filled histograms). The 0 min incubation plot shows representative histograms from cells not incubated with antibody. C (KB) and D (CHO-β) are graphical representations of the flow cytometry histograms A and B, respectively.

induced by its binding ligand.[48] Thus, natural agonists commonly promote rapid receptor endocytosis, while antagonists generally do not.[49,50] High levels of receptor occupancy may also induce internalization and destruction of some occupied receptors, while low levels of receptor saturation may stimulate greater receptor trafficking to recycling endosomes and subsequent return of the receptor to the cell surface.[51] Finally, the degree of ligand-induced receptor clustering can also influence receptor fate, with some clustered receptors further aggregating into cell surface patches prior to endocytosis[43] and others either internalizing immediately or not endocytosing at all. Not surprisingly, with the many possible effects that different ligands can exert on the endocytosis and trafficking of their cognate receptors, we wondered whether the amount or nature of an injected folate-targeted drug would impact the availability of FR on the targeted cell surface. Thus, if folate–drug conjugate binding were to lead to significant receptor down-regulation, the interval between folate conjugate dosing might have to be lengthened to allow for cell surface FR levels to recover.

The unanticipated result from this study was that neither FR occupancy nor folate conjugate valency has any significant effect on FR levels at the cell surface. These data suggest that FR endocytosis occurs at a constitutive rate, regardless of FR occupancy or cross-linking due to multivalent ligand binding. They also suggest that if FR cross-linking induces FR trafficking to lysosomes, as suggested by studies with multivalent folate-targeted nanoparticles,[35,36] the synthesis of new FR must compensate for any FR that are degraded. As a consequence, selection of an optimal frequency for folate conjugate dosing need not involve consideration of folate conjugate concentration or valency. Rather, the only variable that must apparently be evaluated when dosing frequency is optimized constitutes the rate at which the FR naturally recycles in each particular tumor type. Based on previous studies of several human tumor xenografts in live mice, this recycling rate may vary from 8 to 12 h.[30]

■ AUTHOR INFORMATION

Corresponding Author

*Purdue University, Department of Chemistry, 560 Oval Drive, West Lafayette, IN 47907-2084. Phone: 765-494-5273. Fax: 765-494-5272. E-mail: plow@purdue.edu.

Present Address

M.J.H.: BASF, 26701 Telegraph Road, Southfield, MI 48034–2442.

Notes

The authors declare the following competing financial interest(s): The studies reported in this publication were supported by a grant from Endocyte, Inc. Endocyte, Inc. is a biopharmaceutical company that develops folate targeted therapies for the treatment of cancer.

■ ACKNOWLEDGMENTS

We thank Endocyte Inc. (West Lafayette, IN) for their generous financial support and the gift of folate-FITC (EC-17). We are grateful to Dr. Dimitri Dimitrov for providing the

m909-FITC antibody. We are also grateful to Drs. Venkatesh Chelvam and Scott Poh for synthesizing the folate-rhodamine conjugate and the folate-targeted liposomes used in the experiments. Furthermore, we thank Robert Reason for his indispensable help with creating the table of contents figure.

REFERENCES

(1) Elnakat, H.; Ratnam, M. Distribution, functionality and gene regulation of folate receptor isoforms: implications in targeted therapy. *Adv. Drug Delivery Rev.* **2004**, *56*, 1067−1084.
(2) Salazar, M. D.; Ratnam, M. The folate receptor: What does it promise in tissue-targeted therapeutics? *Cancer Metastasis Rev.* **2007**, *26*, 141−152.
(3) Sadasivan, E.; Rothenberg, S. P. The complete amino acid sequence of a human folate binding protein from KB cells determined from the cDNA. *J. Biol. Chem.* **1989**, *264*, 5806−5811.
(4) Ratnam, M.; Marquardt, H.; Duhring, J. L.; Freisheim, J. H. Homologous membrane folate binding proteins in human placenta: cloning and sequence of a cDNA. *Biochemistry* **1989**, *28*, 8249−8254.
(5) Leamon, C. P.; Low, P. S. Membrane folate-binding proteins are responsible for folate-protein conjugate endocytosis into cultured cells. *Biochem. J.* **1993**, *291*, 855−860.
(6) Reddy, J. A.; Low, P. S. Folate-mediated targeting of therapeutic and imaging agents in cancers. *Crit. Rev. Ther. Drug Carrier Syst.* **1998**, *15*, 587−627.
(7) Wang, S.; Low, P. S. Folate-mediated targeting of antineoplastic drugs, imaging agents and nucleic acids to cancer cells. *J. Controlled Release* **1988**, *53*, 39−48.
(8) Shen, F.; Ross, J. F.; Wang, X.; Ratnam, M. Identification of a novel folate receptor, a truncated receptor, and receptor type beta in hematopoietic cells: cDNA cloning, expression, immunoreactivity, and tissue specificity. *Biochemistry* **1994**, *33*, 1209−1215.
(9) Feng, Y.; Shen, J.; Streaker, E. D.; Lockwood, M.; Zhu, Z.; Low, P. S.; Dimitrov, D. S. A folate receptor beta-specific human monoclonal antibody recognizes activated macrophage of rheumatoid patients and mediates antibody dependent cell-mediated cytotoxicity. *Arth. Res. Ther.* **2011**, *13*, R59.
(10) Heijden, J.; Oerlemans, R.; Dijkmans, B.; et al. Folate receptor beta as a potential delivery route for novel folate antagonists to macrophages in the synovial tissue of rheumatoid arthritis patients. *Arth. Rheum.* **2009**, *60*, 12−21.
(11) Nakashima-Matsushita, N.; Homma, T.; Yu, S.; et al. Selective expression of folate receptor beta and its possible role in methotrexate transport in synovial macrophages from patients with rheumatoid arthritis. *Arth. Rheum.* **1999**, *42*, 1609−1616.
(12) Xia, W.; Hilgenbrink, A.; Matteson, E.; et al. A functional folate receptor is induced during macrophage activation and can be used to target drugs to activated macrophages. *Blood* **2009**, *113*, 438−446.
(13) Turk, M. J.; Breur, G. J.; Widmer, W. R.; Paulos, C. M.; Xu, L. C.; Grote, L. A.; Low, P. S. Folate-targeted imaging of activated macrophages in rats with adjuvant-induced arthritis. *Arth. Rheum.* **2002**, *46*, 1947−1955.
(14) Paulos, C.; Varghese, B.; Widmer, W.; et al. Folate-targeted immunotherapy effectively treats established adjuvant and collagen-induced arthritis. *Arth. Res. Ther.* **2006**, *8*, R77.
(15) Ayala-López, W.; Xia, W.; Varghese, B.; et al. Imaging of atherosclerosis in apoE−/− mice: targeting of a folate-conjugated radiopharmaceutical to activated macrophages. *J. Nucl. Med.* **2010**, *51*, 768−774.
(16) Ahtohe, F.; Radulescu, L.; Puchianu, E.; Kennedy, M. D.; Low, P. S.; Simionescu, M. Increased uptake of folate conjugates by activated macrophages in experimental hyperlipemia. *Cell Tissue Res.* **2005**, *320*, 277−285.
(17) Grip, O.; Janciauskiene, S.; Lindgren, S. Macrophages in inflammatory bowel disease. *Curr. Drug Targets Inflamm. Allergy* **2003**, *2*, 155−160.
(18) Wang, H.; Peters, T.; Kess, D.; et al. Activated macrophages are essential in a murine model for T cell-mediated chronic psoriasiform skin inflammation. *J. Clin. Invest.* **2006**, *116*, 2105−2114.
(19) Shen, F.; Wu, M.; Ross, J. F.; Miller, D.; Ratnam, M. Folate receptor type gamma is primarily a secretory protein due to lack of an efficient signal for glycosylphosphatidylinositol modification: protein characterization and cell type specificity. *Biochemistry* **1995**, *34*, 5660−5665.
(20) Yamaguchi, T.; Hirota, K.; Nagahama, K.; Ohkawa, K.; Takahashi, T.; Nomura, T.; Sakaguchi, S. Control of Immune Responses by Antigen-Specific Regulatory T Cells Expressing the Folate Receptor. *Immunity* **2007**, *27*, 145−159.
(21) Boshnjaku, V.; Shim, K.-W.; Tsurubuchi, T.; Ichi, S.; Szany, E. V.; Xi, G.; Mania-Farnell, B.; McLone, D. G.; Tomita, T.; Mayanil, C. S. Nuclear localization of folate receptor alpha: a new role as a transcription factor. *Sci. Rep.* **2012**, *2*, 980.
(22) Low, P.; Henne, W.; Doorneweerd, D. Discovery and development of folic-acid-based receptor targeting for imaging and therapy of cancer and inflammatory diseases. *Acc. Chem. Res.* **2008**, *41*, 120−129.
(23) Kelderhouse, L. E.; Chelvam, V.; Wayua, C.; Mahalingam, S.; Poh, S.; Kularathne, S. A.; Low, P. S. Development of Tumor-Targeted Near Infrared Probes for Fluorescence Guided Surgery. *Bioconjugate Chem.* **2013**, *24*, 1075−1080.
(24) Yang, J.; Chen, H.; Vlahov, I. R.; Cheng, J.; Low, P. S. Evaluation of disulfide reduction during receptor-mediated endocytosis by using FRET imaging. *Proc. Natl. Acad. Sci.* **2006**, *103*, 13872−13877.
(25) Matteson, E.; Lowe, V.; Prendergast, F.; et al. Assessment of disease activity in rheumatoid arthritis using a novel folate targeted radiopharmaceutical Folatescan. *Clin. Exp. Rheumatol.* **2009**, *27*, 253−259.
(26) Vlashi, E.; Sturgis, J. E.; Thomas, M.; Low, P. S. Real Time, Noninvasive Imaging and Quantitation of the Accumulation of Ligand-Targeted Drugs into Receptor-Expressing Solid Tumors. *Mol. Pharmaceutics* **2009**, *6*, 1868−1875.
(27) Leamon, C. P.; Parker, M. A.; Vlahov, I. R.; Xu, L. C.; Reddy, J. A.; Vetzel, M.; Douglas, N. Synthesis and biological evaluation of EC20: a new folate-derived, ^{99m}Tc-based radiopharmaceutical. *Bioconjugate Chem.* **2002**, *13*, 1200−1210.
(28) Lu, Y.; Low, P. S. Folate-mediated delivery of macromolecular anticancer therapeutic agents. *Adv. Drug Delivery Rev.* **2002**, *54*, 675−693.
(29) Reddy, J. A.; Dorton, R.; Dawson, A.; et al. In Vivo Structural Activity and Optimization Studies of Folate−Tubulysin Conjugates. *Mol. Pharmaceutics* **2009**, *6*, 1518−1525.
(30) Paulos, C. M.; Reddy, J. A.; Leamon, C. P.; Turk, M. J.; Low, P. S. Ligand Binding and Kinetics of Folate Receptor Recycling in Vivo: Impact on Receptor-Mediated Drug Delivery. *Mol. Pharmacol.* **2004**, *66*, 1406−1414.
(31) Kamen, B. A.; Wang, M.-T.; Streckfuss, A. J.; Peryea, X.; Anderson, R. G. W. Delivery of Folates to the Cytoplasm of MA104 Cells is Mediated by a Surface Membrane Receptor That Recycles. *J. Biol. Chem.* **1988**, *263*, 13602−13609.
(32) Rothberg, K. G.; Ying, Y.; Kolhouse, J. F.; Kamen, B. A.; Anderson, R. G. W. The Glycophospholipid-linked Folate Receptor Internalizes Folate without Entering the Clathrin-coated Pit Endocytic Pathway. *J. Cell Biol.* **1990**, *110*, 637−649.
(33) Mayor, S.; Sabharanjak, S.; Maxfield, F. R. Cholesterol-dependent retention of GPI-anchored proteins in endosomes. *EMBO J.* **1998**, *17*, 4626−4638.
(34) Mislick, K. A.; Baldeschwieler, J. D.; Kayyem, J. F.; Meade, T. J. Transfection of Folate-Polylysine DNA Complexes: Evidence for Lysosomal Delivery. *Bioconjugate Chem.* **1995**, *6*, 512−515.
(35) Lee, R. J.; Low, P. S. Delivery of Liposomes into Cultured KB Cells via Folate Receptor-mediated Endocytosis. *J. Biol. Chem.* **1994**, *269*, 3198−3204.

(36) Turek, J. J.; Leamon, C. P.; Low, P. S. Endocytosis of folate-protein conjugates: ultrastructural localization in KB cells. *J. Cell Sci.* **1993**, *106*, 423−430.
(37) Gruenberg, J.; Maxfield, F. R. Membrane Transport in the Endocytic Pathway. *Curr. Opin. Cell Biol.* **1995**, *7*, 552−563.
(38) Marshall, S. Kinetics of Insulin Receptor Internalization and Recycling in Adipocytes. *J. Biol. Chem.* **1985**, *260*, 4136−4144.
(39) Sorkin, A.; Waters, C. M. Endocytosis of Growth Factor Receptors. *Bio Essays* **1993**, *15*, 375−382.
(40) Sudimack, J.; Lee, R. J. Targeted Drug Delivery via the Folate Receptor. *Adv. Drug Delivery Rev.* **2000**, *41*, 147−162.
(41) Nakashima-Matsushita, N.; Homma, T.; Yu, S.; et al. Selective expression of folate receptor β and its possible role in methotrexate transport in synovial macrophages from patients with rheumatoid arthritis. *Arth. Rheum.* **1999**, *42*, 1609−1616.
(42) York, S. J.; Arneson, L. S.; Gregory, W. T.; Dahms, N. M.; Kornfeld, S. The Rate of Internalization of the Mannose 6-Phosphate/Insulin-like Growth Factor II Receptor is Enhanced by Multivalent Ligand Binding. *J. Biol. Chem.* **1999**, *274*, 1164−1171.
(43) Santoso, S.; Zimmermann, U.; Neppert, J.; Mueller-Eckhardt, C. Receptor patching and capping of platelet membranes induced by monoclonal antibodies. *Blood* **1986**, *67*, 343−349.
(44) Konner, J. A.; Bell-McGuinn, K. M.; Sebbatini, P.; et al. Farletuzumab, a Humanized Monoclonal Antibody against Folate Receptor α, in Epithelial Ovarian Cancer: a Phase I Study. *Clin. Cancer Res.* **2010**, *16*, 5288−5295.
(45) Press, O. W.; Farr, A. G.; Borroz, K. I.; Anderson, S. K.; Martin, P. J. Endocytosis and Degradation of Monoclonal Antibodies Targeting Human B-Cell Malignancies. *Cancer Res.* **1989**, *49*, 4906−4912.
(46) Guillemard, V.; Nedev, H. N.; Berezov, A.; Murali, R.; Saragovi, H. U. HER2-Mediated Internalization of a Targeted Produrg Cytotoxic Conjugate Is Dependent on the Valency of the Targeting Ligand. *DNA Cell Biol.* **2005**, *24*, 350−358.
(47) Zandstra, P. W.; Jervis, E.; Haynes, C. A.; Kilburn, D. G.; Eaves, C. J.; Piret, J. M. Concentration-Dependent Internalization of a Cytokine/Cytokine Receptor Complex in Human Hematopoietic Cells. *Biotechnol. Bioeng.* **1999**, *63*, 493−500.
(48) Managit, C.; Kawakami, S.; Yamashita, F.; Hashida, M. Effect of Galactose Density on Asialoglycoprotein Receptor-Mediated Uptake of Galactosylated Liposomes. *J. Pharm. Sci.* **2005**, *94*, 2266−2275.
(49) Finch, A. R.; Caunt, C. J.; Armstrong, S. P.; McArdle, C. A. Agonist-induced internalization and downregulation of gonadotropin-releasing hormone receptors. *Am. J. Physiol.* **2009**, *297*, C591−C600.
(50) Cescato, R.; Schulz, S.; Waser, B.; et al. Internalization of sst_2, sst_3, and sst_5 Receptors: Effects of Somatostatin Agonists and Antagonists. *J. Nucl. Med.* **2006**, *47*, 502−511.
(51) Roettger, B. F.; Rentsch, R. U.; Pinon, D.; Holicky, E.; Hadac, E.; Larkin, J. M.; Miller, L. J. Dual pathways of internalization of the cholecystokinin receptor. *J. Cell Biol.* **1995**, *128*, 1029−1041.

CHAPTER 1:

TARGETING THE FOLATE RECEPTOR FOR CANCER IMMUNOTHERAPY

1.1 Introduction

Mark Horn, a former graduate student in the Low lab was studying receptor-mediated-endocytosis when he serendipitously discovered that biotin, a small vitamin molecule, could mediate the uptake of large animal proteins into live plant cells.[1] To follow up this exciting new finding, a variety of other vitamins were examined for their ability to transport macromolecules into the cytoplasm of mammalian cells. These experiments led to the observation that folic acid, a B vitamin, could facilitate the internalization of large proteins into animal cells and subsequently opened the door to folate-conjugate chemistry.[1-2] Although folic acid is a synthetic version of naturally found folates, it can be converted by enzymes into the biologically active form once it enters the body.[3] More importantly, it can readily be conjugated to any number of different molecules for delivery into folate receptor (FR) expressing cells.

Physiological folates are necessary for the synthesis of new nucleotide bases as well as for DNA and histone methylation. Therefore, folates are essential molecules for growth and division of all cells.[4-6] Since animals lack the ability to biosynthesize folates, its uptake is sorely based on diet and its appropriation is carefully regulated.[6] This normal dietary uptake of folic acid is mediated by either the reduced folate carrier (RFC) or

proton coupled folate transporter in the majority of healthy cells.[7-8] However, folate receptors, which bind folates with significantly higher affinity than the two aforementioned transporters, are also expressed by a select few types of cells.[7] Folate receptors bind physiological folates as well as folic acid with a K_D of ~10^{-10} M, which contrasts dramatically with the much lower affinity of ~10^{-5} M demonstrated by the reduced folate carrier to the same molecules.[7,9] As shown in chapter 2 of this thesis, the folate receptor is also a constitutively recycling glycophophatidylinositol (GPI) anchored cell surface protein that enables the transport of extracellular free folate or folate-conjugates by receptor-mediated-endocytosis into the cytoplasm. Figure 1.1 summarizes the path taken by folate receptors during the internalization and release of bound cargo. Currently, four homologous proteins, FR-α, FR-β, FR-γ, and FR-δ, are known to constitute the folate receptor family.[10-11] Although folate receptors are extensively studied, little information is yet available regarding the exact role played by these receptors in cellular signaling and communication.

Many of the aforementioned characteristics, when combined with the knowledge that the receptor is overexpressed by a variety of cancer cells, make FR a great target for drug delivery purposes. Tumors are believed to elevate their FR expression level in order to capture the amount of folate necessary for the uncontrolled cell divisions that are a trademark of cancer cells.[12] Exploiting this receptor overexpression in order to mediate the death of malignant cells allows for both therapeutic efficacy and tissue selectivity. Since cancer by nature is a condition allowed to thrive by a malfunction of the immune system's sentinel cells that are charged with the destruction of mutated or abnormal cells, harnessing the powers of the immune system to combat the disease is an endeavor that is

crucial for long-term success in the battle against cancer. Therefore, the major portion of this thesis focuses on our attempts at awakening the immune system and directing its activity to sites of cancer by using a folate-hapten conjugate as an immunotherapeutic drug. Furthermore, we explore the possibility of augmenting this immunotherapy approach by combining the folate-hapten conjugate with other known immunomodulatory drugs. Chapter 3 delves into the combination of receptor tyrosine kinase inhibitors with folate-FITC for the treatment of animal models of FR+ solid tumors and chapter 4 reports on the synergy observed when folate receptor-mediated immunotherapy is combined with antibody inhibitors of the two main T cell check points, cytotoxic T lymphocyte associated protein 4 (CTLA-4) and programmed cell death protein 1 (PD-1).

1.2 Folate Receptor Expression in Healthy and Diseased Tissues

Although the four isoforms of the folate receptor display significant peptide sequence homology, their physiological expression appears to be distinctly tissue specific.[10-13] FR-α is expressed on the apical, lumen facing side of polarized cells of epithelial origin including those of the choroid plexus, esophagus, proximal tubules of the kidney, and alveolar cells of the lungs.[14-18] Folate receptors on these healthy tissue are not accessible to folate conjugates injected into the blood stream since the tight junctions between polarized cells prevent the passage of conjugates between the circulation and the luminal surface.[16] In the kidneys, the folate receptors serve as a strainer that prevent/delay the excretion of folates in the urine by binding the molecules and transporting them back to the blood stream.[10,17,19]

Besides the healthy tissues mentioned earlier, FR-α is also expressed by approximately 1/3 of human cancers of epithelial origin, and this upregulation has been shown to become more pronounced with disease progression.[13,20-21] In certain cancers where the primary solid tumor does not have noticeably elevated FR expression, upregulation of the receptor has been observed on its metastatic nodules. Some examples of FR-α expressing cancers include those of the brain, kidney, ovary, uterus, lung, breast, and endometrium. [13,17,22-24] Fortunately for researchers, the FR on cancer cells are readily accessible to drug molecules in the blood stream due to a breakdown of tight junctions between the uncontrollably proliferating tumor cells.[25-26]

FR-β is most commonly expressed on activated macrophages and neutrophils. More recently, the receptor has also been observed on tumor-associated myeloid derived suppressor cells (MDCSs).[9,22,27-28] FR-β can be used as an identification marker for the pro-inflammatory, activated macrophages that play an important role in the development and persistence of many autoimmune and inflammatory conditions including rheumatoid arthritis, atherosclerosis, pulmonary fibrosis, psoriasis, and ulcerative colitis among a myriad others.[29-35] FR-β is also expressed by some cancers of hematopoietic and nonepithelial origin such as myelogenous leukemias.[22,27]

FR-γ is a secreted protein that has mainly been observed in the bone marrow,[36] while FR-δ is reported to be primarily expressed by regulatory T cells.[37] These two isoforms of the receptor have not yet been studied in great detail and their specific functions or whether they play a role in any malignancies have not been reported in the literature. However, the field of folate-related research has attracted many investigators over the decades and the number of groups conducting studies aimed at better

understanding the fundamental mechanism of receptor function or at better targeting the receptor for drug delivery is continuing to grow annually.

1.3 Targeting the Folate Receptor for the Treatment of Diseases

Cell surface receptors are most commonly targeted with the use of either a receptor-specific antibody (including any variations of antibody fragments) or receptor-specific small molecules. The folate receptor monoclonal antibodies, MOv18 and MOv19, have been conjugated and evaluated for therapeutic efficacy against several cancers at the preclinical stage, and a MOv18 radioimmunotherapy construct even progressed so far as to be tested on ovarian cancer patients in clinical trials.[38-40] However, antibody therapeutics pose a number of disadvantages, the most important of which is the diminished tumor penetration capability resulting from their large size.[41-42] Therefore, folate receptor-targeting has focused mainly on the development of small molecule drug constructs.

Over the years, a large number of therapeutic compounds and imaging agents have been conjugated to folic acid for the purposes of identifying, visualizing, and treating the many FR+ cancers and inflammatory diseases. The basic structure of most folate conjugates is very similar and the final construct is usually composed of a folic acid molecule bound to a drug or imaging agent via a releasable or non-releasable linker. Releasable linkers are almost always used when the payload is a cell-killing agent while non-releasable linkers are generally used with imaging agents. These spacer chains are generally composed of simple molecules such as amino acids, sugar units, polyethylene glycol units (PEGs), etc. and serve a range of purposes including enhancing water-

solubility, adding to the flexibility or rigidity of the final compound, and can even enhance affinity to the receptor. To date, folic acid has been linked to toxic proteins,[43] chemotherapeutic molecules,[44] radionuclides for both imaging and therapy,[45-47] antisense oligonucleotides,[48] liposomes and dendrimers,[48-51] near infrared dyes,[52] and haptens and antibodies for immunotherapy[53-55] to name a few. These conjugates have been tested in animal models of cancer and inflammation and have shown efficacy in treating both types of conditions with complete eradication of symptoms resulting in certain instances.[44-45,47,52,54-55] Folate-targeted imaging agents have been used successfully to detect and stage inflammation in mice, rats, dogs, and horses, as well as in humans,[1,52,56-59] and the visualization of FR-α positive tumors has been so successful that surgeons have used fluorescent folate conjugates to aid in tumor resection surgeries.[60] With the development of tissue penetrating near infrared dye conjugates, this technique has the hope of becoming a routine component of cancer surgeries. More than eight folate-conjugates are currently in human clinical trials, and given the specificity displayed by folic acid conjugates to the folate receptor, these compounds offer great promise as highly potent treatment options with low toxicity profiles.

1.4 Folate Receptor Mediated Immunotherapy of Cancer and Inflammatory Diseases

Dr. William B. Coley, a bone surgeon at Memorial Hospital in New York City, is credited with pioneering the field of modern cancer immunotherapy. In the 1890s, while reviewing cases of cancer patients who had undergone surgery, Dr. Coley noticed that patients who developed bacterial infections following tumor resection tended to have better therapeutic outcomes.[61] These observations led him to conclude that the

inflammatory response stimulated by an infection can aid the body to combat cancer. He initially tested his hypothesis by injecting live bacterial strains directly into the tumor mass of patients, but due to the risk associated with such a treatment approach he later transitioned to using bacterial products.[62] Although a great deal of controversy surrounded his experimental therapies, Coley toxins were used until mid-20th century.

During the early 1900s immunotherapy took a backseat to the excitement that surrounded the development of radiation therapy,[62] but more recently over the past several decades significant attention has been paid to the fundamental understanding of the immune system as well as the development of therapies that could mobilize a patient's immune cells against their cancer.[63] These research endeavors have led to the discovery of tumor specific antigens (TSA) and tumor associated antigens (TAA) that can be used as immunotherapeutic targets. TSAs are, by definition, present only on cancer cells whereas TAAs are present on both cancer cells and some normal cells.[64-65] The importance of these finding lies in the ability of TSAs and TAAs to be recognized by antibodies and T cells in the body as 'non-self' foreign substances. However, cancers manage to survive and thrive because these TAAs are not always recognized and destroyed by the immune system due to a complicated mechanism that has been credited by Hanahan and Weinberg as an emerging hallmark of all cancers: evading immune destruction.[66] Cancers evade immune recognition by 1) downregulating antigen presentation, 2) secreting immune inhibitory cytokines, 3) stimulating the cell-surface expression of immune inhibitory receptors while hindering the expression of immune cell activating receptors, 4) promoting anergy in immune cells, and even 5) inducing immune cell death.

In order to neutralize and overcome these stealth mechanisms, researchers must keep several important considerations in mind as they design new immunotherapeutic drugs. A good immunotherapeutic should be capable of improving the immune system's ability to recognize the tumor, activate a full immune response (humoral and cellular) against the tumor, educate immune cells to distinguish between malignant and healthy cells, attract a robust and sustained flow of activated immune cells to the site of disease, and lastly, to induce a long-term memory against the cancer.[67-68] The idea of targeting folate-hapten conjugates to FR positive cancers in order to facilitate their immune-mediated destruction was conceived with the hope of meeting these goals.

Haptens are small (< 1kDa), non-immunogenic molecules that are capable of eliciting an immune response when attached to a large, highly immunogenic carrier protein.[69] Although some metal ions can also perform the functions of a hapten, small molecules are used preferentially in research. The molecules that are most commonly used as haptens are oxazolone, dinitrophenol (DNP), urushiol, and fluorescein.[69] Bovine serum albumin (BSA), ovalbumin (OVA), and keyhole limpet hemocyanin (KLH) are the most widely used carrier proteins.[69]

In folate-hapten mediated immunotherapy, a patient is vaccinated several times with a hapten-carrier conjugate to elicit an immune response leading to the generation of anti-hapten antibodies before treating the disease with regular administrations of the folic acid-hapten conjugate. The resulting reduction in tumor burden is achieved in part by antibody-dependent cellular cytotoxicity (ADCC) where the FR bound hapten is recognized by anti-hapten antibodies in the immunized patient's blood stream leading to the recruitment of immune effector cells that can destroy the antibody decorated cancer

cells. The particular immunotherapy experiments described in chapters 3 and 4 of this thesis were conducted in immunocompetent mice using KLH-FITC as the carrier conjugate and folate-FITC as the therapeutic hapten drug.

Previous studies conducted within the Low group have shown that when folate-hapten immunotherapy is administered in combination with small doses of IL-2 and IFN-α, ionizing radiation, and oligodeoxynucleotides containing CpG motifs (CpG-ODN), significant extension of survival and reduction in tumor burden is observed.[53-54] Furthermore, experiments aimed at elucidating the mechanism of this therapeutic success have shown that ADCC mediated cancer cell phagocytosis is the main cause of tumor elimination, and that this process leads to the development of an anti-cancer memory within the treated animals.[67] The removal of NK cell, T cell, and macrophage activity by inhibitory antibodies have proven detrimental to the efficacy of folate-hapten immunotherapy showing that these effector cells play a major role in tumor recognition.[53] This therapeutic approach has been evaluated with promising results in both ascites and solid tumor models, as well as in some models of inflammation.[53-55,70-71] However, since IL-2 and IFN- α can cause undesirable side effects in patients and ionizing radiation is difficult to target specifically to the tumor site, better combination options with low toxicity profiles that can positively augment folate-hapten immunotherapy would be needed in order to move the area of FR-targeted immunotherapy further forward.

Outside the realm of hapten-mediated immunotherapy and in addition to the MOv18 mediated radioimmunotherapy described earlier, several other techniques of FR-targeted immunotherapy have also been tested over the years. Examples include the conjugation of folic acid to anti-CD3 antibodies and the development of anti-FR and anti-

T cell receptor (TCR) bispecific antibodies with the goal of recruiting cytotoxic T cells to the site of the tumor,[72-75] as well as the synthesis of MOv18 bound immune stimulating cytokine constructs (MOv18-IL-2) to activate immune cells that find their way to the tumor microenvironment.[76] More recently, with the increasing popularity of chimeric antigen receptor (CAR) T cells, several varieties of FR-targeted CAR T cell constructs have been produced and tested in animal models and one is currently been evaluated against ovarian cancers in human clinical trials.[77-78]

1.5 Current State of Immunotherapy in Clinical Cancer Treatment

A wide variety of immunotherapeutic drugs have been developed for the treatment of cancer over the eleven or so decades since Dr. Coley's success with toxin-based therapies. Some of the vaccine-type antibody therapeutics have even obtained approval from the FDA and a growing number of immunotherapies are entering clinical trials every year. The most well-known FDA approved antibody drugs include Campath®, Zevalin®, Avastin®, Erbitux®, Mylotarg®, Yervoy®, Arzera®, Rituxan®, Herceptin®, Provenge®, and most recently Keytruda®, approved in September 2014. Most of these drugs are currently being used to treat cancers of hematopoietic origin; the two main exceptions being Herceptin® for the treatment of Her2+ breast cancers and Provenge® for the treatment of hormone refractory prostate cancer.

Aside from anti-tumor antibodies, antibody conjugates, and tumor vaccines, other immunotherapies currently under evaluation include chimeric antigen receptor T cells, dendritic cell-dependent vaccines, tumor-associated protein therapies, DNA vaccines,

immune cell checkpoint inhibitors, toll like receptor (TLR) stimulators, and chemokines.[79-80] These drugs have shown significant promise in a variety of different cancers, but have particularly been successful in immunogenic tumors such as melanoma, renal cell carcinoma, and lymphomas.[80-81] However, many of the above listed immunotherapy techniques are unsuccessful at eliminating solid tumors when administered on their own, which make them only a minor fraction of the cancer drugs used in clinic today. Therefore, in the hopes of using immunotherapy to treat patients afflicted with the more common and aggressive cancers, these drugs are being evaluated in combination with chemotherapy and radiotherapy as well as with other immunotherapy drugs. For example, dendritic cell vaccines have been tested in combination with VEGF receptor inhibitors to produce significant synergy in *in vivo* tumor models,[82] and T cell check point inhibitors have been tested in combination with other checkpoint inhibitors as well as with natural killer cell stimulators to show similar anti-tumor therapeutic effects.[83] In addition, checkpoint inhibitor antibodies and immunomodulatory VEGF inhibitors have been shown to synergize with chemotherapeutic drugs such as cisplatin and docetaxel in murine models of cancer.[84-85] The possibility of cancer immunotherapy moving forward to become a significant subset of the clinically administered drug cohort will depend on the discovery of highly potent and minimally toxic immunotherapy combinations.

1.6 References

1. Low P, Henne W, Doorneweerd D (2008) Discovery and development of folic-acid-based receptor targeting for imaging and therapy of cancer and inflammatory diseases. Acc Chem Res 41:120-129

2. Leamon C, Jackman A (2008) Exploitation of the folate receptor in the management of cancer and inflammatory disease. Vitam Horm 79:203-233

3. Stranger O (2002) Physiology of folic acid in health and disease. Curr Drug Metab 3: 211-223

4. Kim Y (2005) Nutritional Epigenetics: impact of folate deficiency on DNA methylation and colon cancer susceptibility. J Nutr 135:2703-2709

5. Loenen W (2006) S-adenosylmethionine: jack of all trades and master of everything? Biochem Soc Trans 34:330-333

6. Lucock, M (2000) Folic Acid: Nutritional Biochemistry, Molecular Biology, and Role in Disease Processes. Mol Genet Metab 71: 121-138

7. Antony A (1992) The biological chemistry of folate receptors. Blood 79:2807-2820

8. Matherly L, Goldman D (2003) Membrane transport of folates. Vitam Horm 66:403-456

9. Nakashima-Matsushita N, Homma T, Yu S et al (1999) Selective expression of folate receptor beta and its possible role in methotrexate transport in synovial macrophages from patients with rheumatoid arthritis. Arth Rheum 42:1609-1616

10. Elnakat H, Ratnam M (2004) Distribution, functionality and gene regulation of folate receptor isoforms: implications in targeted therapy. Adv Drug Deliver Rev 56: 1067–1084.

11. Salazar M D, Ratnam M (2007) The folate receptor: What does it promise in tissue-targeted therapeutics? Cancer Metastasis Rev 26: 141-152.

12. Reddy J A, Low P S (1998) Folate-mediated targeting of therapeutic and imaging agents in cancers. Crit Rev Ther Drug Carrier Syst 15: 587-627.

13. Weitman S D, Lark R H, Coney L R, Fort D W, Frasca V, Zurawski V R, Kamen B A (1992) Distribution of the folate receptor GP38 in normal and malignant cell lines and tissues. Cancer Res 52: 3396-3401

14. Morshed K M, Ross D M, McMartin K E (1997) Folate Transport Proteins Mediate the Bidirectional Transport of 5-methyltetrahydrofolate in Cultured Human Proximal Tubule Cells J Nutr 127: 1137-1147

15. Kennedy M D, Jallad K N, Lu J, Low P S, Ben-Amotz D (2003) Evaluation of Folate Conjugate Uptake and Transport by the Choroid Plexus of Mice. Pharm Res 20: 714-719

16. Yang X, Mackins J Y Li Q, Antony A C (1981) Isolation and Characterization of a Folate Receptor from Human Placenta. J Biol Chem 256: 9684-9692

17. Weitman S D, Weinberg A G, Coney L R, Zurawski V R, Jennings D S, Kamen B A (1992) Cellular Localization of the Folate Receptor: Potential Role in Drug Toxicity and Folate Homeostasis. Cancer Res 52: 6708-6711

18. Ratnam M, Marquardt H, Duhring J L, Freisheim J H (1989) Homologous membrane folate binding proteins in human placenta: cloning and sequence of a cDNA. Biochemistry 28: 8249 – 8254

19. Sandoval R, Kennedy M, Low P et al (2004) Uptake and trafficking of fluorescent conjugates of folic acid in intact kidney determined using intravital two-photon microscopy. Am J Physiol Cell Physiol 287:C517-C526

20. Toffoli G, Cernigoi C, Russo A, Gallo A, Bagnoli M, Boiocchi M (1997) Overexpression of folate binding protein in ovarian cancers. Int J Cancer 74: 193-198

21. Iwakiri S, Sonobe M, Nagai S, Hirata T, Wada H, Miyahara R (2008) Expression Status of Folate Receptor is Significantly Correlated with Prognosis in Non-Small-Cell Lung Cancers. Annals Surg Oncol 15: 889-899

22. Ross J, Chaudhuri P, Ratnam M (1994) Differential regulation of folate receptor isoforms in normal and malignant tissues in vivo and in established cell lines. Cancer 73:2432-2443

23. Parker N, Turk M, Westrick E et al (2005) Folate receptor expression in carcinomas and normal tissues determined by a quantitative radioligand binding assay. Anal Biochem 338:284-93

24. Weitman S D, Frazier K M, Kamen B A (1994) The folate receptor in central nervous system malignancies of childhood. J Neurooncol 21: 107-112

25. Martin T A, Jiang W G (2009) Loss of tight junction barrier function and its role in cancer metastasis. Biochem Biophys Acta-Biomembranes 1788: 872-891

26. Soller A P, Miller R D, Laughlin K V, Karp N Z, Klurfeld D M, Mullin J M (1999) Increased tight junction permeability is associated with the development of colon cancer. Carcinogenesis 20: 1425-1432

27. Ross J, Wang H, Behm F et al (1999) Folate receptor type β is a neutrophilic lineage marker and is differentially expressed in myeloid leukemia. Cancer 85:348-357

28. Reddy J, Haneline L, Srour E et al (1999) Expression and functional characterization of the beta-isoform of the folate receptor on CD34(+) cells. Blood 93:3940-3948

29. Xia W, Hilgenbrink A, Matteson E et al (2009) A functional folate receptor is induced during macrophage activation and can be used to target drugs to activated macrophages. Blood 113:438-446

30. Turk M, Breur G, Widmer W et al (2002) Folate-targeted imaging of activated macrophages in rats with adjuvant-induced arthritis. Arthritis Rheumatoid 46:1947-1955

31. Paulos C, Turk M, Breur G et al (2004) Folate receptor-mediated targeting of therapeutic and imaging agents to activated macrophages in rheumatoid arthritis. Adv Drug Deliv Rev 56:1205-1217

32. Varghese B, Haase N, Low P (2007) Depletion of folate-receptor-positive macrophages leads to alleviation of symptoms and prolonged survival in two murine models of systemic lupus erythematosus. Mol Pharm 4:679-85

33. Antohe F, Radulescu L, Puchianu E et al (2005) Increased uptake of folate conjugates by activated macrophages in experimental hyperlipemia. Cell Tissue Res 320:277-285

34. Grip O, Janciauskiene S, Lindgren S (2003) Macrophages in inflammatory bowel disease. Curr Drug Targets Inflamm Allergy 2: 155-160

35. Wang H, Peters T, Kess D, et al. (2006) Activated macrophages are essential in a murine model for T cell-mediated chronic psoriasiform skin inflammation. J Clin Invest 116: 2105-2114

36. Shen F, Wu M, Ross J F, Miller D, Ratnam M (1995) Folate receptor type gamma is primarily a secretory protein due to lack of an efficient signal for glycosylphosphatidylinositol modification: protein characterization and cell type specificity. Biochemistry 34: 5660-5665

37. Yamaguchi T, Hirota K, Nagahama K, Ohkawa K, Takahashi T, Nomura T, Sakaguchi S (2007) Control of Immune Responses by Antigen-Specific Regulatory T Cells Expressing the Folate Receptor. Immunity 27: 145-159

38. Gruner B A, Weitman S D (1999) The folate receptor as a potential therapeutic anticancer target. Invest New Drugs 16: 205-2019

39. Crippa F, Buraggi G L,Di Re E, Gasparini, M et al. (1991) Radioimmunoscintigraphy of ovarian cancer with the MOv18 monoclonal antibody. Eur J Cancer 27: 724-729

40. Crippa F, Bolis G, Seregni E, Gavoni N et al. (1995) Single-dose intraperitoneal radioimmunotherapy with the murine monoclonal antibody I-131 MOv18: clinical results in patients with minimal residual disease of ovarian cancer. Eur J Cancer 31A: 686-690

41. Dreher M R, Liu W, Michelich C R, Dewhirst M W, Yuan F, Chilkoti A (2006) Tumor vascular permeability, accumulation and penetration of macromolecular drug carriers. J Natl Cancer Inst 98: 335-344

42. Lu Y, Yang J, Sega E (2006) Issues related to targeted delivery of proteins and peptides. AAPS J 8: E466-E478

43. Leamon C P, Low P S (1992) Cytotoxicity of momordin-folate conjugates in cultured human cells. J Biol Chem 267: 24966-24971

44. Reddy, J. A.; Dorton, R.; Dawson, A.; et al. (2009) In Vivo Structural Activity and Optimization Studies of Folate−Tubulysin Conjugates. Mol Pharmaceutics 6: 1518-1525

45. Leamon C P, Parker M A, Vlahov I R, Xu L C, et al. (2002) Synthesis and Biological Evaluation of EC20: A New Folate-Derived, (99m)Tc-Based Radiopharmaceutical. Bioconjug Chem 13: 1200-1210

46. Wang S, Luo J, Lantrip D A, Waters D J, et al. (1997) Design and Synthesis of [111In]DTPA-Folate for Use as a Tumor-Targeting Radiopharmaceutical. Bioconjug Chem 8: 673-679

47. Mathias C J, Wang S, Low P S, Waters D J, Green M A (1999) Receptor mediated targeting of 67Ga-deferoxamine-folate to folate-receptor-positive human KB tumor xenografts. Nucl Med Biol 26: 23-25

48. Wang S, Lee R J, Cauchon G, Gorenstein D G, Low P S (1995) Delivery of antisense oligodeoxyribonucleotides against the human epidermal growth factor receptor into cultured KB cells with liposomes conjugated to folate via polyethyleneglycol. Proc Natl Acad Sci USA 92: 3318-3322

49. Lee R J, Low P S (1995) Folate-mediated tumor cell targeting of liposome-entrapped doxorubicin in vitro. Biochem Biophys Acta 1233: 134-144

50. Lee R J, Huang L (1996) Folate-targeted, anionic liposome-entrapped polylysine-condensed DNA for tumor cell-specific gene transfer. J Biol Chem 271: 8481-8487

51. Quintana A, Raczka E, Piehler L, Lee I, et al. (2002) Design and Function of a Dendrimer-Based Therapeutic Nanodevice Targeted to Tumor Cells Through the Folate Receptor. Pharmaceutic Res 19: 1310-1316

52. Kelderhouse L E, Chelvam V, Wayua C, Mahalingam S, et al. (2013) Development of Tumor-Targeted Near Infrared Probes for Fluorescence Guided Surgery. Bioconjugate Chem 24: 1075-1080

53. Lu Y, Sega E, Leamon C P, Low, P S (2004) Folate receptor-targeted immunotherapy of cancer: mechanism and therapeutic potential. Adv Drug Del Rev 56: 1161-1176

54. Lu Y, Sega E, Low P S (2005) Folate receptor-targeted immunotherapy: induction of humoral and cellular immunity against hapten-decorated cancer cells. Int J Cancer 116: 710-719.

55. Paulos C, Varghese B, Widmer W et al (2006) Folate-targeted immunotherapy effectively treats established adjuvant and collagen-induced arthritis. Arthritis Res Ther 8:R77

56. Matteson E, Lowe V, Prendergast F et al (2009) Assessment of disease activity in rheumatoid arthritis using a novel folate targeted radiopharmaceutical Folatescan. Clin Exp Rheumatol 27:253-259

57. Saborowski, O, Simon G, Raatschen H et al (2007) MR imaging of antigen-induced arthritis with a new, folate receptor-targeted contrast agent. Contrast Media Mol Imaging 2:72-81

58. Chen W, Khazaie K, Zhang G et al (2005) Detection of dysplastic intestinal adenomas using a fluorescent folate imaging probe. Mol Imaging 4:67-74

59. Chen W, Mahmood U, Weissleder et al (2005) Arthritis imaging using a near-infrared fluorescence folate-targeted probe. Arthritis Res Ther 7:R310-317

60. Van Dam G M, Themelis G, Crane L M, Harlaar N J, et al. (2011) Intraoperative tumor-specific fluorescence imaging in ovarian cancer by folate receptor-α targeting: first in-human results. Nat Med 17: 1315-1319

61. Coley W B (1893) The treatment of malignant tumors by repeated inoculation of erysipelas: with a report of ten original cases. Am J Med Sci 105: 487-510

62. McCarthy E F (2006) The Toxins of William B. Coley and the Treatment of Bone and Soft-Tissue Sarcomas. Iowa Orthop J 26: 154-158

63. Foss F M (2002) Immunologic mechanisms of antitumor activity. Semin Oncol 29: 5-11

64. Mitchell M S (2002) Cancer vaccines, a critical review—Part I. Curr Opin Investig Drugs 3: 140-149

65. Mitchell M S (2002) Cancer vaccines, a critical review—Part II. Curr Opin Investig Drugs 3: 150-158

66. Hanahan D, Weinberg R A (2011) Hallmarks of Cancer: The Next Generation. Cell 144: 646-674

67. Lu Y, Low P S (2003) Targeted immunotherapy of cancer: development of antibody-induced cellular immunity. J Pharm Pharmacol 55: 163-167

68. Reilly R T, Emens L A, Jaffee E M (2001) Humoral and cellular immune responses: independent forces or collaborators in the fight against cancer? Curr Opin Investig Drugs 2: 133-135

69. Erkes D A, Selvan S R (2014) Hapten-induced contact hypersensitivity, autoimmune reactions, and tumor regressions: plausibility of mediating antitumor immunity. J Immunol Res Article ID 175265, 28 pages

70. Yi Y, Ayala-Lopez W, Kularatne S et al (2009) Folate-targeted hapten immunotherapy of adjuvant-induced arthritis: comparison of hapten potencies. Mol Pharm 6:1228-1236

71. Lu Y, Low, P. S. (2003) Immunotherapy of folate receptor-expressing tumors: review of recent advances and future prospect. J Control Release 91: 17-29.

72. Cho B K, Roy E J, Patrick T A, Kranz D M (1997) Single-chain Fv/folate conjugates mediate efficient lysis of folate-receptor-positive tumor cells. Bioconjug Chem 8: 338-346

73. Kranz D M, Manning T C, Rund L A, Cho B K, et al. (1998) Targeting tumor cells with bispecific antibodies and T cells. J Control Release 53: 77-84

74. Roy E J, Cho B K, Rund L A, Patrick T A, Kranz D M (1998) Targeting T cells against brain tumors with a bispecific ligand-antibody conjugate. Int J Cancer 76: 761-766

75. Kranz D M, Patrick T A, Brigle K E, Spinella M J, Roy E J (1995) Conjugates of folate and anti-T-cell-receptor antibodies specifically target folate-receptor-positive tumor cells for lysis. Proc Natl Acad Sci USA 92: 9057-9061

76. Melani C, Figini M, Nicosia D, Luison E, et al. (1998) Targeting of interleukin 2 to human ovarian carcinoma by fusion with a single-chain Fv of antifolate receptor antibody. Cancer Res 58: 4146-4154

77. Urbanska K, Lanitis E, Poussin M, Lynn R C, et al. (2012) A universal strategy for adoptive immunotherapy of cancer through use of a novel T-cell antigen receptor. Cancer Res 72: 1844-1852

78. Kandalaft L E, Powell D J, Coukos G (2012) A phase I clinical trial of adoptive transfer of folate receptor-alpha redirected autologous T cells for recurrent ovarian cancer. J Transl Med 10:157

79. Blattman J N, Greenberg P D (2004) Cancer Immunotherapy: A Treatment for the Masses. Science 305: 200-205

80. Mellman I, Coukos G, Dranoff G (2011) Cancer immunotherapy comes of age. Nature 480: 480–489

81. Sharma P, Wagner K, Wolchok J D, Allison J P (2011) Novel cancer immunotherapy agent with survival benefit: recent successes and next steps. Nature Rev Cancer 11: 805-812

82. Bose A, Lowe D B, Rao A, Storkus W J (2012) Combined vaccine + axitinib therapy yields superior anti-tumor efficacy in a murine melanoma model. Melanoma Res 22: 236-243

83. Kohrt H E, Houot R, Weiskopf K, Goldstein M J, et al. (2012) Stimulation of natural killer cells with a CD137-specific antibody enhances trastuzumab efficacy in xenotransplant models of breast cancer. J Clin Invest 122:1066–1075

84. Guerin O, Formento P, Lo Nigro C, et al. (2008) Supra-additive antitumor effect of sunitinib malate (SU11248, Sutent®) combined with docetaxel. A new therapeutic perspective in hormone refractory prostate cancer. J Cancer Res Clin Oncol 134: 51-57

85. Wei H, Zhao L, Li W, Fan K, et al. (2013) Combinatorial PD-1 Blockade and CD137 Activation Has Therapeutic Efficacy in Murine Cancer Models and Synergizes with Cisplatin. PLOS one 8: e84927

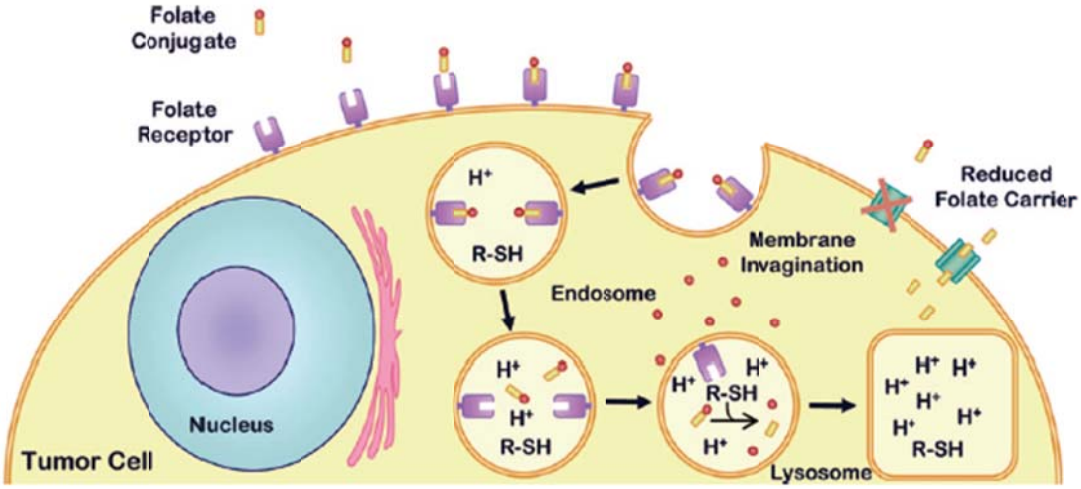

Figure 1.1. Path of folate conjugate internalization and payload release. Folate conjugates are recognized by folate receptors expressed on the surface of certain cells and transported to the cell interior by receptor mediated endocytosis. The therapeutic or imaging cargo is then released from the folic acid in the endosomal compartments and the receptor is either destroyed or recycled back to the cell surface. The reduced folate carrier is incapable of transporting folate conjugates and can only mediate the internalization of free folates. Image credit: Low, Henne, and Doorneweerd, *Accounts of Chemical Research*, **2008**, 41, 120-129.

Table 1.1. The average expression levels of folate receptor on healthy human and animal tissues. Each tissue was analyzed from at least 2 animals of each species (except primate liver, where n was 1) and FR expression values is expressed in picomoles FR/mg of solubilized membrane protein. This table was reproduced based on a published figure from *Analytical Biochemistry*. Parker, N.; Turk, M. J.; Westrick, E.; Lewis, J. D.; Low, P. S.; Leamon, C. P. Folate receptor expression in carcinomas and normal tissues determined by a quantitative radioligand binding assay. *Anal. Biochem*., **2005**, 338: 284-293.

Tissue	Mouse	Rat	Guinea Pig	Rabbit	Dog	Primate	Human
Heart	0.31	0.00	1.02	0.19	0.18	0.45	1.87
Lung	0.17	0.00	1.56	0.53	0.19	0.50	7.79
Liver	0.06	0.02	0.03	0.90	0.23	0.22	1.23
Intestine	0.11	0.60	2.16	0.22	0.07	0.41	2.74
Kidney	12.74	6.00	2.20	9.46	1.25	1.29	14.40
Spleen	0.21	0.44	2.42	6.72	0.52	2.12	0.55
Muscle	0.68	0.57	0.59	0.52	0.00	0.19	0.97
Brain	0.45	0.20	ND	0.46	0.03	0.17	0.32

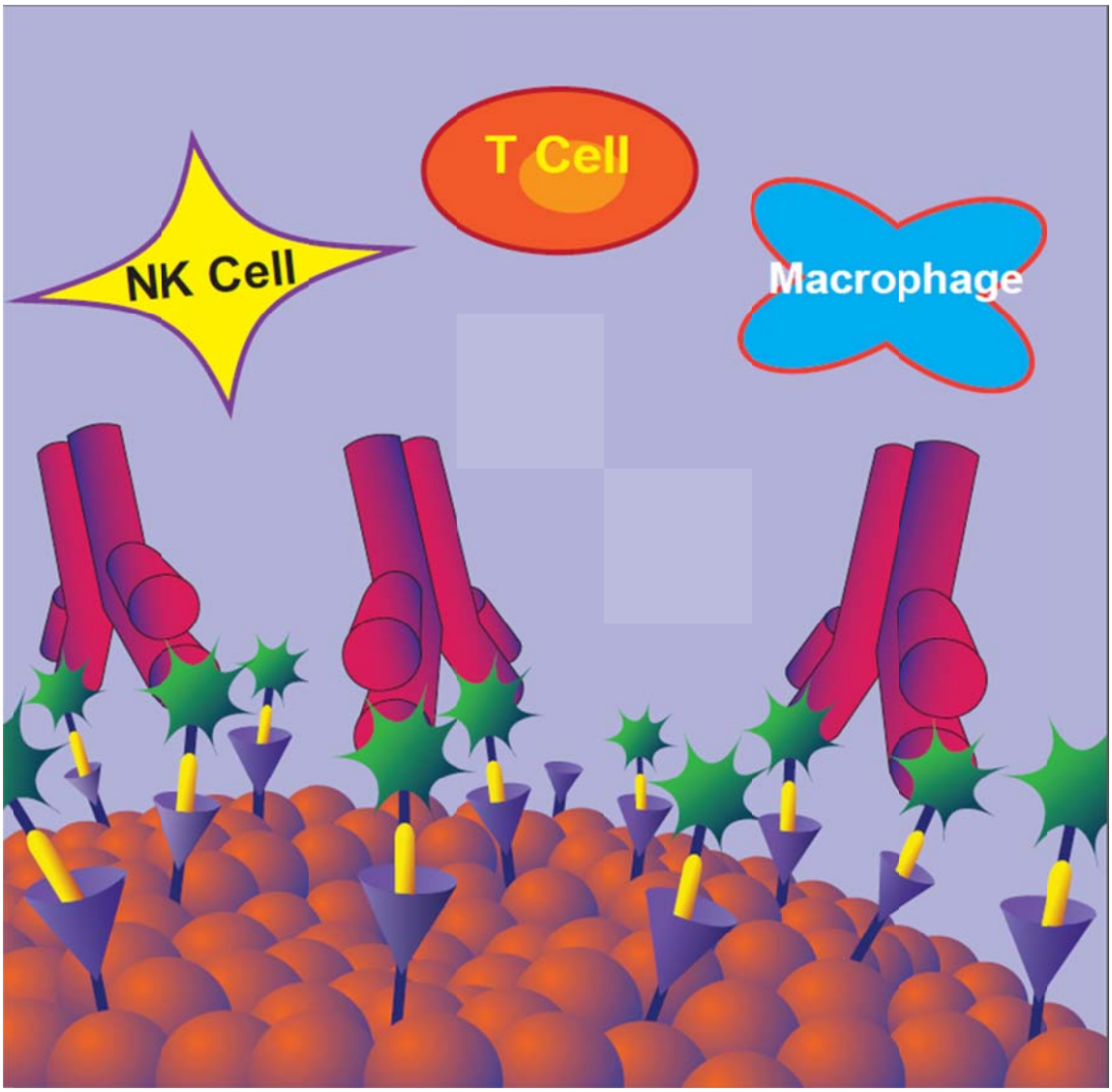

Figure 1.2. A simplified representation of the folate-FITC mediated attraction of anti-FITC antibodies to folate receptor expressing cancer cell surfaces. These antibodies will then be recognized by the F_c receptors on activated effector cells in the body (e.g. macrophages and NK cells), which will mediate the destruction of antibody bound cancer cells while also releasing immune attractants that recruit and activate cytotoxic immune cells (e.g. CD8+ T cells).

1.7 Copyright Permission

CHAPTER 2:

EFFECT OF RECEPTOR OCCUPANCY ON FOLATE RECEPTOR INTERNALIZATION

2.1 Introduction

The folate receptor (FR) constitutes a family of four homologous proteins that are thought to bind folic acid and its physiologic congeners.[1,2] FR-α is found on the apical surfaces of certain epithelial cells, where it is largely inaccessible to folates in the blood stream.[3,4] It is also over-expressed on a variety of epithelial-derived cancers, where it can be readily targeted by intravenously injected folate-linked drugs.[5-7] FR-β is primarily expressed on activated macrophages[8] which populate almost all autoimmune and inflamed tissues and mediate many destructive processes responsible for disease symptoms.[9-11] Examples of inflammatory diseases caused or worsened by FR+ activated macrophages include rheumatoid arthritis, ulcerative colitis, atherosclerosis, multiple sclerosis and psoriasis among others.[12-18] FR-γ has been detected in the bone marrow from whence it may be released into circulation[19], but whether it facilitates folate uptake is not known. FR-δ has been found primarily on regulatory T cells[20] and like FR-γ has no known function. Only FR-α has been shown to be involved in signal transduction[21], but the possible participation of FR-β, FR-γ, or FR-δ in transmembrane signaling has never been examined.

Because of the limited expression and/or accessibility of FR in healthy human tissues, both FR-α and FR-β have been exploited for targeted drug delivery to cancer tissues and sites of inflammation, respectively.[22] For this purpose, folate is linked to a therapeutic or imaging agent and injected into the diseased host, where it is either captured by FR on the pathologic cell surface or rapidly excreted from the body. Radioactive[13,15] and fluorescent[23,24] folate conjugates have been used to visualize sites of inflammation[25] and localize malignant disease,[23,26,27] whereas folate-conjugated therapeutic agents have been exploited to destroy FR-α expressing tumor cells[28,29] and inactivate FR-β expressing inflammatory macrophages.[14,16] A variety of folate-targeted molecules are currently undergoing human clinical trials.

Because the rate of FR internalization and trafficking can influence the frequency of folate conjugate dosing (i.e. there is no merit in injecting a patient with a folate-drug conjugate more frequently than empty FR return to the pathologic cell surface following endocytosis), several studies have examined the rate and routes of FR trafficking in physiologically relevant systems.[24,30-32] Results from these studies demonstrate that FR traffic through different intracellular compartments depending on the number of folates tethered to the targeted conjugate, with monovalent folate-drug conjugates trafficking through a recycling center before returning to the cell surface,[24,31,33] and multivalent FR ligands trafficking through multivesicular bodies prior to deposition in lysosomes.[34-37] Importantly, despite the detailed nature of the above studies, the effect of folate conjugate size and valency on its rate of internalization and recycling has never been examined. In this paper, we explore the kinetics of internalization of both FR-α and FR-β following their ligation to a variety of folate-linked molecules and anti-folate receptor antibodies,

including the free unligated vitamin, folate-linked small molecules, multi-folate derivatized nanoparticles, and monoclonal antibodies to FR.

2.2 Materials and Methods

2.2.1 Cell Lines and Culture

All FR positive cell lines were maintained in the Cell Culture Facility of the Purdue University Department of Chemistry. KB and IGROV cells were maintained in folate-deficient RPMI 1640 medium (Invitrogen, Grand Island, NY) supplemented with 10% heat inactivated fetal bovine serum (Sigma Aldrich, St. Louis, MO), penicillin (50 units/mL) and streptomycin (50μg/mL). Chinese Hamster Ovary (CHO) cells stably transfected with human FR-β (generous gift from Manohar Ratnam, Karmanos Cancer Center, Detroit, MI) were maintained in folate-deficient RPMI 1640 medium (Invitrogen, Grand Island, NY) supplemented with 10% heat inactivated fetal bovine serum (Sigma Aldrich, St. Louis, MO), 0.15mg/mL L-proline, 10nmol/L N^5-formyl tetrahydrofolate, 100units/mL penicillin and 100μg/mL streptomycin (Sigma Aldrich, St. Louis, MO). All cell lines were passaged continuously in a monolayer and cultured at 37°C in a humidified atmosphere containing 5% CO_2.

2.2.2 Antibodies and Reagents

Folic acid was purchased from Sigma Aldrich (St. Louis, MO) and dissolved in pH adjusted deionized water. The hybridoma cell line that produces a mouse monoclonal antibody to human FR-α (MAb 343) was a generous gift from Wilbur Franklin

(University of Colorado), and folate-fluorescein (EC17) was kindly provided by Endocyte, Inc. (West Lafayette, IN). Fluorescein-labeled goat anti-mouse IgG antibody was purchased from Santa Cruz Biotechnology, Inc. (Dallas, TX). Human anti-human mAb against FR-β (m909) was developed in collaboration with Dr. Dimiter Dimitrov (National Institutes of Health, Frederick, MD) and labeled with fluorescein isothiocyanate.[9]

2.2.3 Folate Conjugates

A water-soluble monovalent folate-rhodamine conjugate with nanomolar FR affinity (Figure 2.1 A) was synthesized as previously described.[24,26] Folate-targeted polyethylene glycol-derivatized liposomes were also prepared according to previous procedures,[35] with ~3.5% of the phospholipids derivatized with PEG and ~10% of the PEGylated lipids further conjugated to folic acid. Assuming ~80,000 lipids per liposome, this calculates to ~280 folate targeting ligands per liposome for a folate-targeted lipid concentration of ~1.5μM in the stock suspension.

2.2.4 Evaluation of the Effect of Receptor Occupancy on Receptor Internalization

Each cell type to be investigated was plated in a six well plate at a density of 50,000 cells/well and allowed to adhere overnight. Individual wells were either left untreated (controls) or incubated in 100nM folic acid or folate rhodamine for 20 minutes, 4 hours or 24 hours at 37°C. For analyses of liposome uptake, 100μL of 2mg/mL folate-conjugated liposome stock suspension was added to each well prior to execution of the same incubation procedure. Following incubation, wells were washed thoroughly with

PBS to remove unbound ligand, after which cells were removed from the plate by scraping, centrifuged to form a pellet and resuspended in cold (4°C) folate-deficient culture medium to block further FR trafficking. Folate receptors accessible on the cell-surface were then labeled with either mAb343 followed by fluorescein-labeled goat anti-mouse secondary antibody (KB and IGROV cells) or m909-FITC (CHO-β cells) by further incubation at 4°C for 1 hour. After washing with PBS to remove unbound antibody, fluorescently labeled FR in all cell samples were quantitated on a Becton Dickinson FACS Caliber flow cytometer. Ten thousand cells were counted from each sample and three samples from each treatment condition were evaluated. CellQuest software was used for data collection and FlowJo software was employed for data analysis. Graphing and statistical calculations of the analyzed data were performed using GraphPad Prism software.

2.3 Results

2.3.1 Effect of Folic Acid on the Kinetics of FR-α Internalization

For many cell surface receptors, the rate of receptor internalization is strongly dependent on both receptor number and receptor occupancy.[38,39] Although previous studies have demonstrated that the rate of FR internalization is independent of receptor number,[30] no information is currently available on the impact of receptor occupancy on the rate of FR endocytosis. To obtain this information, KB and IGROV cells (which express high and low levels of FR-α, respectively) were incubated *in vitro* with a saturating concentration (100nM) of free folic acid for 20 minutes, 4 hours, or 24 hours at

37˚C. Cell surface FR were then quantitated by flow cytometry using a noncompeting anti-FR-α primary antibody (mAb343) followed by labeling with a fluorescein-conjugated goat anti-mouse secondary antibody. If folic acid binding were to induce FR internalization, a decrease in available FR on the cell surface would be expected as exposure to folate/folate conjugate proceeded. Moreover, if resting state FR levels were to impact the rate of ligand-induced receptor endocytosis, differences between FR internalization by KB and IGROV cells would be anticipated. As seen in Fig. 2.2, the rate of FR-α internalization is not altered by folic acid binding, since cell surface FR-α numbers remain similar to their levels in untreated cells at all the time points tested. Furthermore, the level of FR expression in untreated cells must exert little influence over the kinetics of receptor internalization, since cell lines that express high and low levels of FR display the same insensitivity to receptor saturation.

2.3.2 Effect of Folic Acid on the Kinetics of FR-β Internalization

Although FR-β exhibits similar nanomolar affinity for folic acid to FR-α,[40] its greatly reduced level of expression,[41] its unique manifestation on activated immune cells,[8-11] and its rapid rate of internalization[12,30] raise the question of whether the response of FR-β to saturation with folic acid might differ from that of FR-α. In order to evaluate the impact of FR-β occupancy on its rate of internalization, a CHO-K1 strain that was stably transfected with human FR-β was incubated with a saturating concentration of folic acid and examined for cell surface FR-β using a noncompeting monoclonal antibody to FR-β (m909).[9] As seen in Fig. 2.3, the level of FR-β on CHO-β cell surfaces is independent of the time and extent of FR-β saturation with folic acid. Thus, m909-FITC

binding remains essentially the same in the absence of added folic acid (0 minute time point) as seen following 24 hour exposure to saturating levels of folic acid (24 hour time point). Moreover, there is no significant difference in cell surface FR-β between cells incubated for 20 minutes in saturating folic acid and those incubated for 4 hours or 24 hours with the vitamin. Based on these observations, we suggest that the rate of internalization of FR-β, like that of FR-α, is not altered by changes in the level folic acid binding, but instead recycles at a steady rate, regardless of receptor occupancy.

2.3.3 Effect of Folate Conjugate Valency on the Kinetics of Receptor Endocytosis

Cross-linking or clustering of cell surface receptors using multivalent ligands has been known for years to accelerate receptor endocytosis and trafficking to lysosomes.[34,36,42] For example, multivalent lectins and antibodies that can bind multiple receptors simultaneously have been observed to induce localized receptor "patching" followed by a more global receptor "capping" prior to receptor internalization and degradation.[43] Because many labs have exploited folate to target nanoparticles to pathologic cells, invariably derivatizing their nanomedicines with multiple folates in order to increase binding avidity, the concern has naturally arisen whether such multivalent formulations might induce accelerated depletion of FR from the cell surface, preventing or at least delaying the ability to target additional nanomedicines to the same FR-expressing cells. To address this concern, we have compared the number of cell surface FR following incubation of cells with a monovalent ligand (folate-rhodamine) to their number following incubation with a multivalent ligand (folate-targeted liposomes). As seen in Fig. 2.4 and Fig. 2.5, only minor differences are seen in the number of residual

cell surface FR following incubation with either monovalent (Fig. 2.4) or multivalent (Fig. 2.5) folate conjugates, suggesting that cell surface receptor depletion commonly observed with other multivalent ligands does not occur when FR is the targeted receptor. In the case of monovalent folate-rhodamine, the detected variation in cell surface FR-α (KB) and FR-β (CHO-β) levels following different incubation times are minor and probably a consequence of experimental variability. Even in the case of the multivalent liposomes, the decrease in cell surface FR at early time points is reversed at 24 hours, suggesting any real effect may be transient at best. Moreover, although receptor numbers differ significantly with IGROV cells and receptor sequence differs in CHO-β cells, similar insensitivities to folate conjugate valency are observed. We, therefore, conclude that conjugate valency does not have a significant effect on the rate of FR internalization.

2.3.4 Analysis of the Impact of Antibody Binding on FR Endocytosis

Because several anti-FR antibodies have recently entered clinical trials,[44] and since antibodies commonly induce the endocytosis of their targeted receptors,[45] we felt it might be prudent to include in our study an examination of the impact of antibody binding on FR endocytosis. For this purpose, KB and CHO-β cells were incubated with saturating concentrations of mAb343 and m909, respectively, and subsequently labeled with folate-fluorescein (EC17) to quantitate the number of cell surface FR. As seen in Fig. 2 .6, no differences in cell surface FR were observed following incubation with either antibody at any of the three incubation times, demonstrating that antibody binding also has no impact on FR internalization.

2.4 Discussion

The rate of internalization and trafficking of most cell surface receptors may depend on multiple parameters, including: i) the nature of the ligand,[46] ii) the level of receptor occupancy,[38,47] and iii) the degree of receptor clustering induced by its binding ligand.[48] Thus, natural agonists commonly promote rapid receptor endocytosis, while antagonists generally do not.[49,50] High levels of receptor occupancy may also induce internalization and destruction of some occupied receptors, while low levels of receptor saturation may stimulate greater receptor trafficking to recycling endosomes and subsequent return of the receptor to the cell surface.[51] Finally, the degree of ligand-induced receptor clustering can also influence receptor fate, with some clustered receptors further aggregating into cell surface patches prior to endocytosis[43] and others either internalizing immediately or not endocytosing at all. Not surprisingly, with the many possible effects that different ligands can exert on the endocytosis and trafficking of their cognate receptors, we wondered whether the amount or nature of an injected folate-targeted drug would impact the availability of FR on the targeted cell surface. Thus, if folate-drug conjugate binding were to lead to significant receptor down-regulation, the interval between folate conjugate dosing might have to be lengthened to allow for cell surface FR levels to recover.

The unanticipated result from this study was that neither FR occupancy nor folate conjugate valency has any significant effect on FR levels at the cell surface. These data suggest that FR endocytosis occurs at a constitutive rate, regardless of FR occupancy or cross-linking due to multivalent ligand binding. They also suggest that if FR cross-linking induces FR trafficking to lysosomes, as suggested by studies with multivalent

folate-targeted nanoparticles,[35,36] the synthesis of new FR must compensate for any FR that are degraded. As a consequence, selection of an optimal frequency for folate conjugate dosing need not involve consideration of folate conjugate concentration or valency. Rather, the only variable that must apparently be evaluated when dosing frequency is optimized constitutes the rate at which the FR naturally recycles in each particular tumor type. Based on previous studies of several human tumor xenografts in live mice, this recycling rate may vary from 8 to 12 hours.[30]

2.5 References

1. Elnakat, H.; Ratnam, M. Distribution, functionality and gene regulation of folate receptor isoforms: implications in targeted therapy. *Adv. Drug Deliver. Rev*. **2004**, 56, 1067–1084.

2. Salazar, M. D.; Ratnam, M. The folate receptor: What does it promise in tissue-targeted therapeutics? *Cancer Metastasis Rev.* **2007**, 26, 141-152.

3. Sadasivan, E.; Rothenberg, S. P. The complete amino acid sequence of a human folate binding protein from KB cells determined from the cDNA. *J. Biol. Chem.* **1989**, 264, 5806 – 5811.

4. Ratnam, M.; Marquardt, H.; Duhring, J. L.; Freisheim, J. H. Homologous membrane folate binding proteins in human placenta: cloning and sequence of a cDNA. *Biochemistry* **1989**, 28, 8249 – 8254.

5. Leamon, C. P.; Low, P. S. Membrane folate-binding proteins are responsible for folate-protein conjugate endocytosis into cultured cells. *Biochem J*. **1993**, 291, 855-860.

6. Reddy, J. A.; Low, P. S. Folate-mediated targeting of therapeutic and imaging agents in cancers. *Crit. Rev. Ther. Drug Carrier Syst.* **1998**, 15, 587-627.

7. Wang, S.; Low, P. S. Folate-mediated targeting of antineoplastic drugs, imaging agents and nucleic acids to cancer cells. *J. Control. Release* **1988**, 53, 39-48.

8. Shen, F.; Ross, J. F.; Wang, X.; Ratnam, M. Identification of a novel folate receptor, a truncated receptor, and receptor type beta in hematopoietic cells: cDNA cloning, expression, immunoreactivity, and tissue specificity. *Biochemistry* **1994**, 33, 1209-1215.

9. Feng, Y.; Shen, J.; Streaker, E. D.; Lockwood, M. Zhu, Z.; Low, P. S.; Dimitrov, D. S. A folate receptor beta-specific human monoclonal antibody recognizes activated macrophage of rheumatoid patients and mediates antibody dependent cell-mediated cytotoxicity. *Arthritis Res. Ther*. **2011**, 13, R59.

10. Heijden J.; Oerlemans R.; Dijkmans B.; et al Folate receptor beta as a potential delivery route for novel folate antagonists to macrophages in the synovial tissue of rheumatoid arthritis patients. *Arth. Rheum.* **2009**, 60, 12-21.

11. Nakashima-Matsushita N.; Homma T.; Yu S.; et al Selective expression of folate receptor beta and its possible role in methotrexate transport in synovial macrophages from patients with rheumatoid arthritis. *Arth. Rheum*. **1999**, 42, 1609-1616.

12. Xia W.; Hilgenbrink A.; Matteson E.; et al A functional folate receptor is induced during macrophage activation and can be used to target drugs to activated macrophages. *Blood* **2009**, 113, 438-446.

13. Turk, M. J.; Breur, G. J.; Widmer, W. R.; Paulos, C. M.; Xu, L. C.; Grote, L. A.; Low, P. S. Folate-targeted imaging of activated macrophages in rats with adjuvant-induced arthritis. *Arthritis Rheum*. **2002**, 46, 1947-1955.

14. Paulos C.; Varghese B.; Widmer W.; et al Folate-targeted immunotherapy effectively treats established adjuvant and collagen-induced arthritis. *Arthritis Res.Ther.* **2006**, 8, R77.

15. Ayala-López W.; Xia W.; Varghese B.; et al Imaging of atherosclerosis in apoE-/- mice: targeting of a folate-conjugated radiopharmaceutical to activated macrophages. *J. Nuc. Med.* **2010**, 51, 768-774.

16. Antohe, F.; Radulescu, L.; Puchianu, E.; Kennedy, M. D.; Low, P. S.; Simionescu, M. Increased uptake of folate conjugates by activated macrophages in experimental hyperlipemia. *Cell Tissue Res*. **2005**, 320, 277-285.

17. Grip, O.; Janciauskiene, S.; Lindgren, S. Macrophages in inflammatory bowel disease. *Curr. Drug Targets Inflamm. Allergy* **2003**, 2, 155-160.

18. Wang, H.; Peters, T.; Kess, D.; et al. Activated macrophages are essential in a murine model for T cell-mediated chronic psoriasiform skin inflammation. *J. Clin. Invest*. **2006**, 116, 2105-2114.

19. Shen, F.; Wu, M.; Ross, J. F.; Miller, D.; Ratnam, M. Folate receptor type gamma is primarily a secretory protein due to lack of an efficient signal for glycosylphosphatidylinositol modification: protein characterization and cell type specificity. *Biochemistry* **1995**, 34, 5660-5665.

20. Yamaguchi, T.; Hirota, K.; Nagahama, K.; Ohkawa, K.; Takahashi,T.; Nomura,T.; Sakaguchi, S. Control of Immune Responses by Antigen-Specific Regulatory T Cells Expressing the Folate Receptor. *Immunity* **2007**, 27, 145-159.

21. Boshnjaku, V.; Shim, K.-W.; Tsurubuchi, T.; Ichi, S.; Szany, E. V.; Xi, G.; Mania-Farnell, B.; McLone, D. G.; Tomita, T.; Mayanil, C. S. Nuclear localization of folate receptor alpha: a new role as a transcription factor. *Sci. Rep.* **2012**, 2, 980.

22. Low P.; Henne W.; Doorneweerd D.; Discovery and development of folic-acid-based receptor targeting for imaging and therapy of cancer and inflammatory diseases. *Acc. Chem. Res.* **2008**, 41, 120-129.

23. Kelderhouse, L. E.; Chelvam, V.; Wayua, C.; Mahalingam, S.; Poh, S.; Kularathne, S. A.; Low, P. S. Development of Tumor-Targeted Near Infrared Probes for Fluorescence Guided Surgery. *Bioconjugate Chem*. **2013**, 24, 1075-1080.

24. Yang, J.; Chen, H.; Vlahov, I. R.; Cheng, J.; and Low, P. S. Evaluation of disulfide reduction during receptor-mediated endocytosis by using FRET imaging. *Proc. Natl. Acad. Sci.* **2006**, 103, 13872-13877.

25. Matteson E.; Lowe V.; Prendergast F.; et al Assessment of disease activity in rheumatoid arthritis using a novel folate targeted radiopharmaceutical Folatescan. *Clin. Exp. Rheumatol.* **2009**, 27, 253-259.

26. Vlashi, E.; Sturgis, J. E.; Thomas, M.; Low, P. S. Real Time, Noninvasive Imaging and Quantitation of the Accumulation of Ligand-Targeted Drugs into Receptor-Expressing Solid Tumors. *Mol. Pharmaceutics* **2009**, 6, 1868-1875.

27. Leamon, C. P.; Parker, M. A.; Vlahov, I. R.; Xu, L. C.; Reddy, J. A.; Vetzel, M.; Douglas, N. Synthesis and biological evaluation of EC20: a new folate-derived, ^{99m}Tc-based radiopharmaceutical. *Bioconjugate Chem*. **2002**, 13, 1200-1210.

28. Lu, Y.; Low, P. S. Folate-mediated delivery of macromolecular anticancer therapeutic agents. *Adv. Drug Deliv. Rev*. **2002**, 54, 675-693.

29. Reddy, J. A.; Dorton, R.; Dawson, A.; et al. In Vivo Structural Activity and Optimization Studies of Folate−Tubulysin Conjugates. *Mol. Pharmaceutics* **2009**, 6, 1518-1525.

30. Paulos, C. M.; Reddy, J. A.; Leamon, C. P.; Turk, M. J.; Low, P. S. Ligand Binding and Kinetics of Folate Receptor Recycling in Vivo: Impact on Receptor-Mediated Drug Delivery. *Mol. Pharmcol.* **2004**, 66, 1406-1414.

31. Kamen, B. A.; Wang, M.-T.; Streckfuss, A. J.; Peryea, X.; Anderson, R. G. W. Delivery of Folates to the Cytoplasm of MA104 Cells is Mediated by a Surface Membrane Receptor That Recycles. *J. Biol. Chem*. **1988**, 263, 13602-13609.

32. Rothberg, K. G.; Ying, Y.; Kolhouse, J. F.; Kamen, B. A.; Anderson, R. G. W. The Glycophospholipid-linked Folate Receptor Internalizes Folate without Entering the Clathrin-coated Pit Endocytic Pathway. *J. Cell. Biol*. **1990**, 110, 637-649.

33. Mayor, S.; Sabharanjak, S.; Maxfield, F. R. Cholesterol-dependent retention of GPI-anchored proteins in endosomes. *EMBO J*. **1998**, 17, 4626-4638.

34. Mislick, K. A.; Baldeschwieler, J. D.; Kayyem, J. F.; Meade, T. J. Transfection of Folate-Polylysine DNA Complexes: Evidence for Lysosomal Delivery. *Bioconjugate Chem.* **1995**, 6, 512-515.

35. Lee, R. J.; Low, P. S. Delivery of Liposomes into Cultured KB Cells via Folate Receptor-mediated Endocytosis. *J. Biol. Chem.* **1994**, 269, 3198-3204.

36. Turek, J. J.; Leamon, C. P.; Low, P. S. Endocytosis of folate-protein conjugates: ultrastructural localization in KB cells. *J. Cell Sci*. **1993**, 106, 423-430.

37. Gruenberg, J.; Maxfield, F. R. Membrane Transport in the Endocytic Pathway. *Curr. Opin. Cell Biol*. **1995**, 7:552-563.

38. Marshall, S. Kinetics of Insulin Receptor Internalization and Recycling in Adipocytes. *J. Biol. Chem*. **1985**, 260, 4136-4144.

39. Sorkin, A.; Waters, C. M. Endocytosis of Growth Factor Receptors. *Bio Essays* **1993**, 15, 375-382.

40. Sudimack, J.; Lee, R. J. Targeted Drug Delivery via the Folate Receptor. *Adv. Drug Deliv. Rev*. **2000**, 41, 147–162.

41. Nakashima-Matsushita, N.; Homma, T.; Yu, S.; et al. Selective expression of folate receptor β and its possible role in methotrexate transport in synovial macrophages from patients with rheumatoid arthritis. *Arthritis Rheum*. **1999**, 42, 1609-1616.

42. York, S. J.; Arneson, L. S.; Gregory, W. T.; Dahms, N. M.; Kornfeld, S. The Rate of Internalization of the Mannose 6-Phosphate/Insulin-like Growth Factor II Receptor is Enhanced by Multivalent Ligand Binding. *J. Biol. Chem*. **1999**, 274, 1164-1171.

43. Santoso, S.; Zimmermann, U.; Neppert, J.; Mueller-Eckhardt, C. Receptor patching and capping of platelet membranes induced by monoclonal antibodies. *Blood* **1986**, 67, 343-349.

44. Konner, J. A.; Bell-McGuinn, K. M.; Sebbatini, P. et al. Farletuzumab, a Humanized Monoclonal Antibody against Folate Receptor α, in Epithelial Ovarian Cancer: a Phase I Study. *Clin. Cancer Res*. **2010**, 16, 5288-5295.

45. Press, O. W.; Farr, A. G.; Borroz, K. I.; Anderson, S. K.; Martin, P. J. Endocytosis and Degradation of Monoclonal Antibodies Targeting Human B-Cell Malignancies. *Cancer Res*. **1989**, 49, 4906-4912.

46. Guillemard, V.; Nedev, H. N.; Berezov, A.; Murali, R.; Saragovi, H. U. HER2-Mediated Internalization of a Targeted Produrg Cytotoxic Conjugate Is Dependent on the Valency of the Targeting Ligand. *DNA Cell Biol.* **2005**, 24, 350-358.

47. Zandstra, P. W.; Jervis, E.; Haynes, C. A.; Kilburn, D. G.; Eaves, C. J.; Piret, J. M. Concentration-Dependent Internalization of a Cytokine/Cytokine Receptor Complex in Human Hematopoietic Cells. *Biotechnol. Bioeng.* **1999**, 63, 493-500.

48. Managit, C.; Kawakami, S.; Yamashita, F.; Hashida, M. Effect of Galactose Density on Asialoglycoprotein Receptor-Mediated Uptake of Galactosylated Liposomes. *J. Pharm. Sci.* **2005**, 94, 2266-2275.

49. Finch, A. R.; Caunt, C. J.; Armstrong, S. P.; McArdle, C. A. Agonist-induced internalization and downregulation of gonadotropin-releasing hormone receptors. *Am. J. Physiol.* **2009**, 297, C591-C600.

50. Cescato, R.; Schulz, S.; Waser, B. et al. Internalization of sst_2, sst_3, and sst_5 Receptors: Effects of Somatostatin Agonists and Antagonists. *J. Nucl. Med*. **2006**, 47, 502-511.

51. Roettger, B. F.; Rentsch, R. U.; Pinon, D.; Holicky, E.; Hadac, E.; Larkin, J. M.; Miller, L. J. Dual pathways of internalization of the cholecystokinin receptor. *J. Cell Biol*. **1995**, 128, 1029-1041.

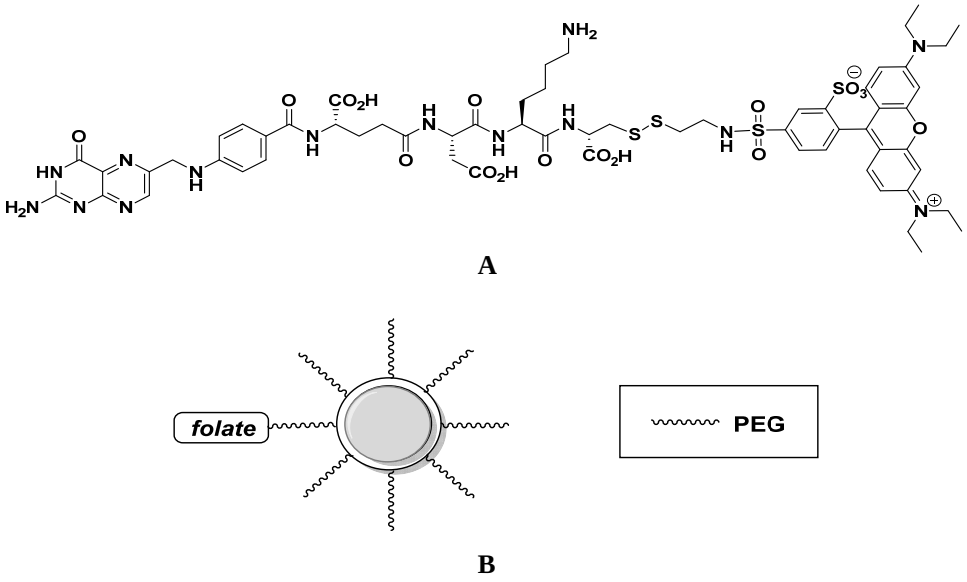

Figure 2.1. General structures of A. Folate-rhodamine conjugate, and B. Folate-PEG liposomes

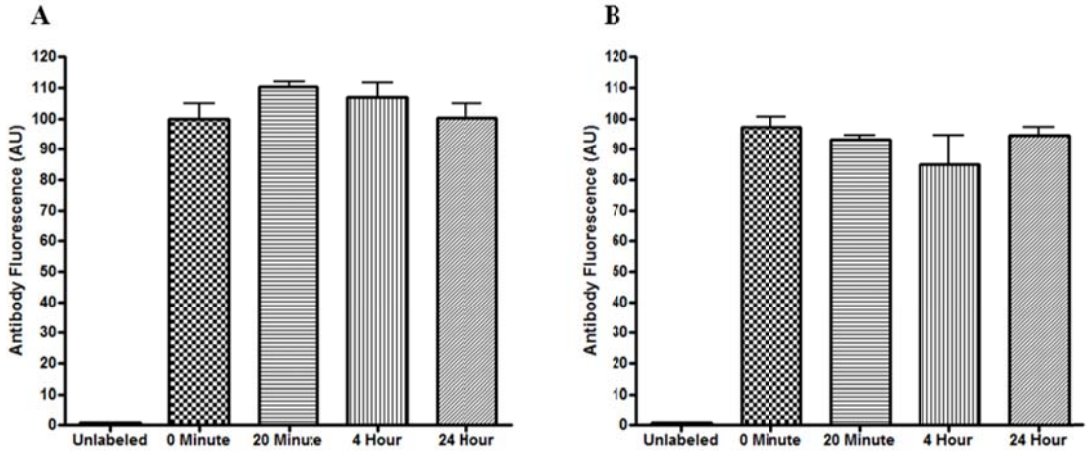

Figure 2.2. Quantitation of cell surface FR-α after incubating KB cells (A) and IGROV cells (B) with a saturating concentration (100 nM) of folic acid for 20 minutes, 4 hours, and 24 hours. Cell surface FR were quantitated by flow cytometry using a noncompeting monoclonal anti-FR-α antibody, as described in the Methods. Mean fluorescent intensities from three samples were averaged and graphed as a percentage of the average fluorescence intensity measured at the 0 minute time point; i.e. before addition of free folic acid.

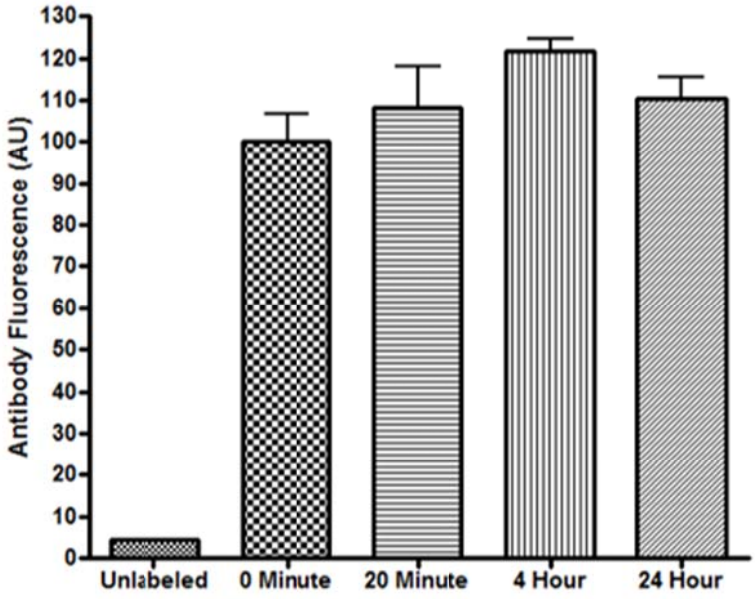

Figure 2.3. Quantitation of cell surface FR-β after incubating CHO-β cells with saturating folic acid for 20 minutes, 4 hours, and 24 hours, as determined by flow cytometry following labeling of extracellular receptors with m909-FITC. Mean fluorescent intensities from three different samples were averaged and graphed as a percentage of the average fluorescence intensity measured at the 0 minute time point; i.e. before addition of free folic acid.

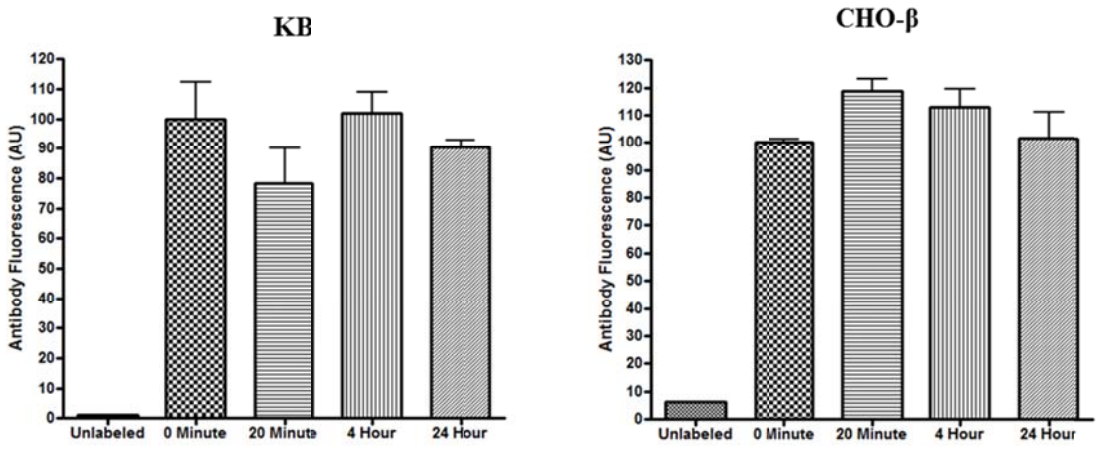

Figure 2.4. Quantitation of cell surface FR-α and FR-β following incubation of cells with folate-rhodamine for the indicated times. As in previous figures, cell surface FR were labeled with mAb343 or m909-FITC and quantitated by flow cytometry. Mean fluorescent intensities from three samples were averaged and graphed as a percentage of the average fluorescence intensity measured at the 0 minute time point; i.e. before addition of free folic acid.

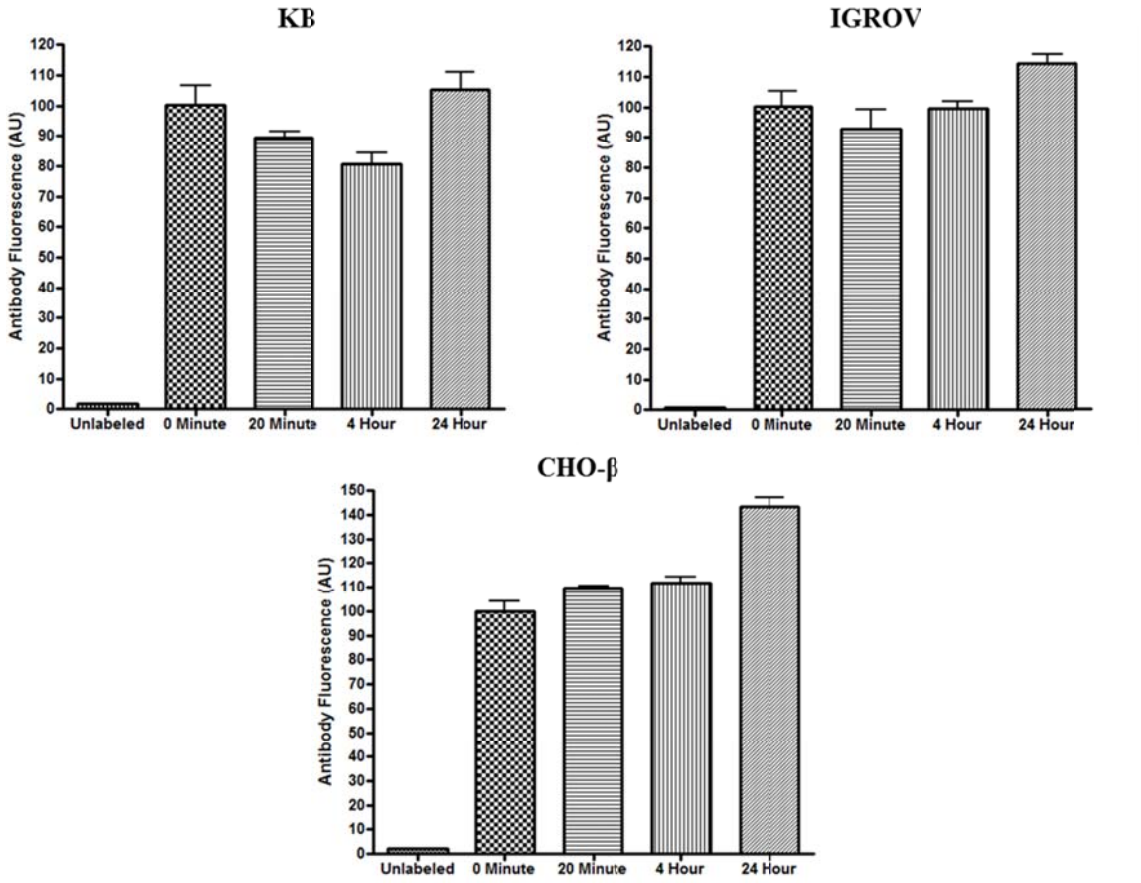

Figure 2.5. Quantitation of cell surface FR-α and FR-β following incubation of cells with folate labeled liposomes for the indicated times. As in previous figures, cell surface FR were labeled with mAb343 or m909-FITC and quantitated by flow cytometry. Mean fluorescent intensities from three samples were averaged and graphed as a percentage of the average fluorescence intensity measured at the 0 minute time point; i.e. before addition of free folic acid.

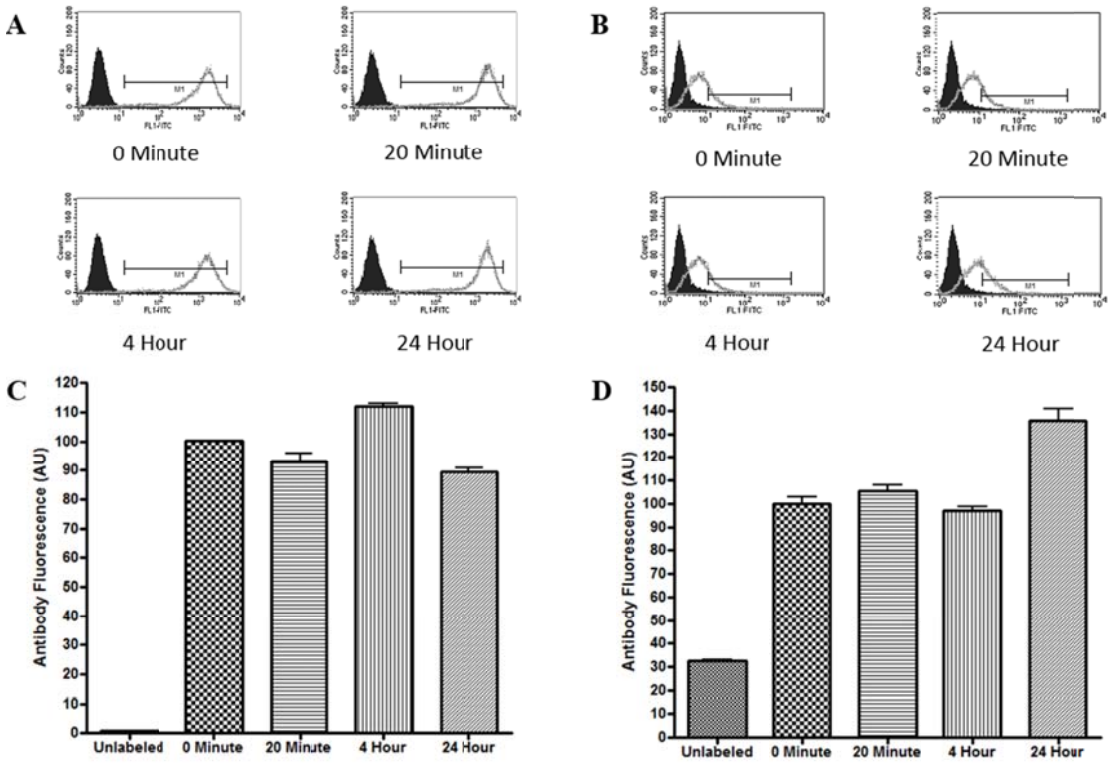

Figure 2.6. Evaluation of cell surface FR after incubation of KB (A, C) and CHO-β (B, D) cells with mAb343 or m909, respectively, for 20 minutes, 4 hours, or 24 hours. Cell surface FR was quantitated by incubation of the cells with saturating folate-fluorescein followed by measurement of FITC fluorescence by flow cytometry. Histograms of representative samples from each incubation time (open histograms) are overlaid with the histograms of unlabeled control cells (filled histograms). The 0 minute incubation plot shows representative histograms from cells not incubated with antibody. C (KB) and D (CHO-β) are graphical representations of the flow cytometry histograms A and B, respectively.

2.6 Copyright Permission

CHAPTER 3:

FOLATE-HAPTEN MEDIATED IMMUNOTHERAPY SYNERGIZES WITH VASCULAR ENDOTHELIAL GROWTH FACTOR RECEPTOR INHIBITORS IN MURINE MODELS OF CANCER

3.1 Introduction

Folic acid, a vitamin required for the synthesis of nucleotide bases, methylation of DNA and the post-translational modification of G proteins, enters cells via either the reduced folate carrier, the proton coupled folate transporter, or a folate receptor (FR).[1-4] While the reduced folate carrier and proton coupled folate transporter are expressed in virtually all cells, FR is present and accessible primarily on activated macrophages, proximal tubule cells of the kidney and certain cancer of epithelial origin, including malignancies of the ovary, endometrium, kidney, lung and breast.[5-8] Because folate-linked imaging and therapeutic agents can only enter cells via the folate receptor, folate has been frequently exploited as a targeting ligand to deliver drugs to cancers and sites of inflammation.[9-13] Over the past two decades, numerous folate-linked therapeutics (e.g. toxic proteins, chemotherapeutic molecules, liposomes, and radionuclides) have been developed and evaluated in murine models of cancer.[9,14] However, the first folate-targeted therapy to enter human clinical trials involved the delivery of an immunotherapeutic to FR over-expressing tumor cells.

This therapy was originally designed using an approach that took advantage of the body's ability to recognize and destroy foreign proteins before they could cause any harm (e.g. immune response to a viral or bacterial infection). Although the immune system consists of very complicated cascades of stimulatory and inhibitory signals, delicate balances of chemokines and cytokines, and a large variety of helper and effector cells, this type of defensive immune response can be simplified into two different categories: cellular and humoral. The humoral response usually occurs first and consists of the recognition of foreign antigens by circulating B cells leading to their activation and proliferation, which in turn induces the production of antibodies against the foreign antigen (Chapter 9, *Immunobiology*, 5th Edition).[15] These antibodies, in turn, can activate the complement system and be recognized by phagocytic macrophages and NK cells, which then mediate the destruction of the foreign substance in a process known as antibody-dependent cellular cytotoxicity or ADCC.[15] The second, cellular defense response involves the presentation of abnormal antigens that are present within the cell membrane by major histocompatibility complexes (MHC-II in the case of an infection and MHC-I in the case of cancer) on the surface of antigen presenting cells (APC) in the body. These MHC-bound antigens are then recognized by circulating T cells leading to their activation and proliferation. Activated cytotoxic T cells subsequently mediate the destruction of any infected cells (Chapter 8, *Immunobiology*, 5th Edition).[15] This MHC-mediated antigen presentation can also facilitate the recruitment of antibody producing B cells to the site of infection.

The immunotherapy method designed for targeting FRs on cancer cells takes advantage of the humoral immune response and anticipates stimulation of a cellular

response in the long term. In short, mice are vaccinated with a foreign protein decorated with a large number of hapten molecules leading to the production of anti-hapten antibodies; these immunized mice are later treated with continual doses of a folate-hapten conjugate that will mediate the recognition of the FR+ tumor by the activated immune system. Haptens are small, non-immunogenic molecules that can elicit an immune response when bound to a large carrier protein.[16] The therapeutic efficacy observed in tumor-bearing mice treated with the folate-hapten conjugate would mainly be a result of ADCC, but a cytotoxic T cell response component could also be involved. However, even though the concept is theoretically sound, folate-hapten mediated immunotherapy alone has been ineffective at controlling tumor progression over longer periods of time and requires supplementation with immunomodulatory cytokines for optimum therapeutic outcome.[17]

Therefore, the earlier preclinical experiments with folate-targeted immunotherapy used the cytokines IL-2 and IFN-α as companion therapies, and the combination was very successful at prolonging overall survival and creating long-term anti-tumor memory in animal models of lung cancer and lymphoma.[17-20] Follow up studies using inhibitory antibodies against each effector cell type have demonstrated that the phagocytic function of NK cells, cytotoxic T cells, and macrophages are essential for the observed therapeutic efficacy, confirming that both arms of the immune system are indeed playing a role in the response.[18,19] Although the murine tumor models were extremely promising,[21,22] the phase 1 clinical data in advanced renal cell carcinoma patients with bulky disease revealed no complete responses and only a few partial responses, with most patients showing either no response or prolonged stable disease.[23] Moreover, the influenza-like

symptoms associated with the cytokine treatments discouraged further clinical testing of the folate-hapten plus cytokine combination therapy. Nevertheless, the strong indication of efficacy in a very difficult-to-treat patient population together with the absence of toxicity associated with the folate-hapten therapy alone motivated further exploration for a less toxic companion therapy that might augment the ability of folate-fluorescein to mark and mediate the removal of FR+ cancer cells.

Recently, several multi-targeted receptor tyrosine kinase (RTK) inhibitors have shown synergy in treating a variety of different cancers when combined with immunotherapy drugs.[24-26] These molecules were initially believed to be effective against cancers due to their ability to inhibit the vascular endothelial growth factor (VEGF) receptors, and thereby impede the growth of new vasculature within the rapidly growing tumors.[27-29] Interestingly, further delving into the mechanism of anti-tumor activity of these drugs have shown that their ability to normalize as opposed to totally downregulate tumor vasculature maybe the cause of tumor-growth inhibition.[30,31] Furthermore, additional studies have demonstrated that their activity may not be limited to an anti-VEGF effect, but may also stem from the molecules' ability to reduce the levels of immunosuppressive myeloid derived suppressor cell (MDSC) populations and T_{reg} activity in tumor-bearing animals.[32,33] A number of VEGF inhibitors are currently approved by the FDA for use in humans. The humanized recombinant monoclonal antibody bevacizumab (Avastin®) is a direct VEGF inhibitor and was the first angiogenesis inhibitor approved for use in the United States. It is approved for use in refractory glioblastomas and in combination with other drugs for the treatment of colorectal cancer, lung cancer, and metastatic renal cell carcinoma. Nexavar®

(hepatocellular carcinoma and kidney cancer), Votrient® (kidney cancer), Afinitor®, and Sutent® (kidney cancer and neuroendocrine tumors) have since been granted permission for use in clinic. In addition to cancer, these drugs are also being used for the treatment of conditions associated with vascular abnormalities, such as macular degeneration.

Although some immunotherapies are administered independently, most are administered in combination or following primary treatment with conventional cancer therapies or other immunotherapeutics. As a result, there is a need for evaluating and describing the types of cancer drugs that combine well with different modes of immunotherapy.[34] Since both VEGF inhibitors and folate-hapten mediated immunotherapies have already been assessed in human kidney cancer patients,[23,35] it was an obvious next step to wonder whether these two therapeutic modalities would synergize in treating FR expressing tumors. Innumerable literature articles report on the successful use of angiogenesis inhibitors in a myriad different cancers including testicular cancer, prostate cancer, colon cancer, melanoma, glioma, sarcoma, and non-Hodgkin's lymphoma showing that their activity is not limited to the few malignancies being treated in clinic by these drugs.[26,27,36,37] In addition, these drugs have already been tested *in vivo* in combination with other drugs such as cisplatin, docetaxel, cyclophosphamide, and dendritic cell vaccines and together have shown significant improvement of therapy over each individual treatment alone.[24-26,36,37]

In this chapter, we describe studies evaluating the effect of combining the VEGF inhibitor sunitinib malate with folate-fluorescein (folate-FITC) therapy in fluorescein immunized mouse models of kidney cancer (Renca), lung cancer (M109), and lymphoma (L1210A). To further confirm the results from these *in vivo* studies, we evaluated the

effect of combining axitinib, a second, more selective VEGF inhibitor, with folate-FITC in mice bearing solid L1210A tumors. We then continued onto examining the potential mechanism behind the therapeutic efficacy observed from these combinations by resecting tumors and spleens from the treated mice and assessing their immune cell and microenvironment components for any differences between the treatment groups. The collected data suggest that VEGF inhibitors play an important role in modulating anti-tumor immunity in tumor-bearing mice when administered in combination with folate-FITC, and could become a potent addition to other ADCC-mediated therapeutic approaches for cancers.

3.2 Materials and Methods

3.2.1 Antibodies and Reagents

Folic acid, keyhole limpet hemocyanin (KLH), SIGMA*FAST*™ OPD substrate tablets, phosphate buffered saline (PBS), carboxymethylcellulose (CMC), Tween 20, collagenase IV, hyaluronidase from bovine testes, deoxyribonuclease I from bovine pancreas, and female Balb/c serum were purchased from Sigma Aldrich (St. Louis, MO). Bovine serum albumin conjugated to fluorescein (BSA-FITC), folate-EDA-fluorescein (Folate-FITC, EC17) and the GPI-0100 adjuvant was kindly provided by Endocyte, Inc. (West Lafayette, IN). Sunitinib malate and axitinib, free base were purchased from LC Laboratories (Woburn, MA). Gelatin was obtained from Bio-Rad Laboratories (Hercules, CA). Disposal PD-10 desalting columns were purchased from GE Healthcare Bio-Sciences (Pittsburgh, PA). The biotin-conjugated goat anti-mouse IgG2a antibody and

streptavidin-HRP conjugate was manufactured by Caltag Laboratories (Burlingame, CA). The Shandon™ Cryomatrix™ resin used for embedding harvested animal tissues during the freezing and sectioning process was purchased from Thermo Scientific (Waltham, MA). All fluorescently labeled antibodies for flow cytometry and confocal microscopy experiments were obtained from either BioLegend (San Diego, CA) or eBioscience, Inc. (San Diego, CA). The special folate-deficient diet on which animals in treatment studies were maintained was purchased from Harlan Laboratories (Indianapolis, IN).

3.2.2 Cell Lines and Culture

All FR positive cell lines were maintained in the Cell Culture Facility of the Purdue University Department of Chemistry or cultured in the Low laboratory at the Drug Discovery Facility. L1210A cells were a generous gift from Dr. Manohar Ratnam, Karmanos Cancer Institute at the Wayne State University (Detroit, MI) and Dr. Gerrit Jansen, Department of Oncology at the University Hospital Vrije Universiteid (Amsterdam, Netherlands). M109 cells expressing FR was kindly provided by Dr. Alberto Gabizon, Sharet Institute of Oncology at the Hadassah-Hebrew University Medical Center (Jerusalem, Israel). Both L1210A (lymphocytic leukemia) and M109 (lung cancer) cells were selected for high folate receptor expression and have been shown to maintain this elevated FR levels through multiple passages. However, both cell lines were monitored for their FR expression by flow cytometry intermittently throughout the duration of the immunotherapy studies. The Renca kidney cancer cell line was a gift from Endocyte, Inc. (West Lafayette, IN) and was selected for high FR expression by extended passage in folate deficient medium followed by multiple cycles of cell sorting to collect

the highest FR expressing fraction. The cell sorting procedures were carried out in the Flow Cytometry and Cell Separation Facility of the Bindley Bioscience Center. All cell lines were maintained in folate-deficient RPMI 1640 medium (Invitrogen, Grand Island, NY) supplemented with 10% heat inactivated fetal bovine serum (Sigma Aldrich, St. Louis, MO), penicillin (100 units/mL) and streptomycin (100μg/mL). Cells were cultured at 37°C in a humidified atmosphere containing 5% CO_2. The adherent M109 and Renca cell lines and were passaged continuously in a monolayer and the L1210A cells, which grow in suspension were passaged in fresh medium every 3-4 days.

3.2.3 Animals and Tumor Models

M109 and Renca tumors were grown in female Balb/c mice which were obtained from Harlan Laboratories (Indianapolis, IN) at 5 to 7 weeks of age. Each mouse weighed approximately 18-20g on arrival. The DBA/2 mice for L1210A tumor studies were purchased from either Harlan Laboratories (Indianapolis, IN) or The Jackson Laboratory (Bar Harbor, ME) also at between 5 to 7 weeks of age. There were no obvious differences in tumor growth, response to therapy, or behavior between mice obtained from the two vendors. The DBA/2 mice weighed approximately 16-18g on arrival. Individual animals were identified during therapy by tail markings. All procedures conducted on animals were carried out in strict accordance with protocols approved by the Purdue Animal Care and Use Committee (protocol # 1310000974, High Affinity Ligand Mediated Immunotherapy of Tumors).

3.2.3.1 Renca Tumors

The Renca renal cell carcinoma cell line was originally developed and characterized by Murphy and Hrushesky at the Roswell Park Memorial Institute (Buffalo, NY). Although these cell naturally express some FR on their cell surfaces, in order to use the cells for FR targeting they needed to be selected for higher FR expression. This enhancement in receptor expression levels was achieved by sorting out the highest FR expressing population by sterile flow cytometry and continually culturing this subset in folate deficient medium. Renca cells grow syngeneic tumors in Balb/c mice when transplanted via a variety of routes, but for the experiments described here solid tumors were implanted by injecting mice s.c. on the left shoulder with 1 x 10^6 cells suspended in serum free medium. Tumors were usually palpable by day 10 and were ready for initiation of therapy (50-75mm^3) by day 14.

3.2.3.2 M109 Tumors

The M109 cell line needs to be passaged in Balb/c mice periodically for the cells to maintain the ability to grow solid tumors. Therefore, in order to have a stock of frozen cells that could be used for tumor implantation, solid M109 tumors from Balb/c mice were processed and directly cryopreserved for future use. Briefly, once a tumor had reached ~500-1000mm^3 it was carefully resected under sterile conditions in order to minimize contamination and washed at least 3 times in sterile PBS. The tumor was then chopped into fine pieces using sterilized dissection scissors and suspended in 10-12 mL of the collagenase digestion cocktail detailed in section 3.2.8. The minced tumors and the cocktail were incubated in a T75 flask at 37°C with gentle agitation for 1-2 hours. The

digestion process was then stopped by the addition of 10% fetal bovine serum (FBS) and the cocktail was passed through a 40 μm cell strainer. Any solid chunks of tumor remaining in the strainer were gently broken down with a pipette tip and washed with complete folate deficient medium to further help loosen up free cells. The collected M109 cells were then spun down at 800rpm for 7-10 minutes and resuspended in complete medium for plating (to remove any debris or unhealthy cells). The folate deficient medium that the cells were cultured in was changed every 24h until each T75 flask become confluent, at which point the adhered cells were detached using a non-enzymatic cell dissociation solution (Sigma Aldrich, St. Louis, MO), counted, and cryopreserved at a density of 1-5 million cells/vial. For tumor implantation, frozen cells were thawed and allowed to grow till confluence at passage zero. Cells were then scraped from the flasks, counted, and suspended in folate-deficient RPMI-1640 medium containing 1% syngeneic female Balb/c serum. Mice were injected with 1 x 10^6 cells s.c. on the left shoulder. Tumors became palpable around day 7-10 and therapy was usually initiated between day 10 and 14.

3.2.3.3 L1210A Tumors

The L1210A tumor cells are syngeneic to the DBA/2 mouse strain and will grow solid tumors when implanted subcutaneously. Female DBA/2 mice were used for all the studies described in this chapter. Cultured L1210A cells were counted and resuspended in serum free sterile PBS and each mouse was injected s.c. with 1 x 10^6 cells on the left shoulder. Tumors were usually palpable by day 5 and measured ~50mm^3 in volume in 7-10 days.

3.2.4 Synthesis and Purification of KLH-FITC

As mentioned in the introduction, animals were vaccinated with a keyhole limpet hemocyanin (KLH) protein labeled with fluorescein molecules in order to elicit an anti-fluorescein antibody response. The KLH-FITC conjugate was synthesized by an overnight reaction between the KLH protein and excess FITC. Briefly, 4mg of FITC was mixed with 10mg potassium carbonate in ~1ml deionized water and slowly added dropwise to 20mg of KLH mixed with 10mg potassium carbonate in ~1ml deionized water under mild stirring. The mixture was then allowed to react in the dark at 37°C. The resulting KLH-FITC conjugate was first purified by running it through a PD-10 desalting column pre-equilibrated with sterile PBS. Protein fractions were collected as they came through the column and the fractions that were determined by absorption measurements (O.D. 280 nm) to have a high concentration of KLH were pooled and further purified by dialyzing in excess PBS at 4°C in order to remove any free FITC molecules (2000-3000 MW dialysis tube). The KLH-FITC solution that was collected following dialysis was analyzed for its protein concentration using a commercially available BCA assay. The FITC to KLH ratio was also calculated using absorbance measurements and the labeling ratio generally measured at >100 fluorescein molecules per KLH protein. KLH-FITC stock solutions were labeled with concentration (g protein/ml) and stored in the dark at -20°C till use in immunization cocktails.

3.2.5 Formulation of Drugs for *in vivo* Administration

3.2.5.1 Sunitinib

Human patients who receive sunitinib or axitinib as a part of their cancer therapy regiment are given the drug in a pill form to be taken orally.[35,38] Therefore, in order to mimic human treatment conditions, the sunitinib malate compound obtained from LC Laboratories was formulated in a CMC solution for administration to mice by oral gavage (p.o). The CMC solution used for dissolving sunitinib was made up of 0.5% carboxymethylcellulose, 1.8% sodium chloride, 0.4% Tween 80, and 0.9% benzyl alcohol in reverse osmosis purified water. The pH of this solution was then adjusted to 6.0. Sunitinib concentration was calculated at 20mg sunitinib per kg of body weight (using an average weight of 18g for DBA/2 mice and 20g for Balb/c mice) in a volume of 100μL CMC solution. Drug formulations for animal administration were prepared freshly every week and stored in the dark at 4°C. The suspension was vortexed or shaken vigorously to ensure even drug distribution before dosing mice.

3.2.5.2 Axitinib

Axitinib was also dosed orally and was formulated in a different CMC solution for administration by oral gavage. CMC was dissolved in reverse osmosis purified water at a 0.5% concentration (w/v) and the solution was then acidified to pH 2-3. Axitinib concentration for treatments was calculated at 15mg per kg of body weight (using an average weight of 18g for DBA/2 mice) in a 100μL volume of the described CMC solution. Axitinib formulations were also prepared once weekly and stored in the dark at

4°C. The somewhat viscous, milky suspension was vortexed or shaken vigorously to ensure even drug distribution before dosing mice.

3.2.5.3 Folate-FITC

Folate-FITC (EC17) provided by Endocyte, Inc. was diluted to the desired concentration in sterile PBS. For the experiments described in this chapter, a 500 nmols/kg folate-FITC concentration was used for dosing animals. Mice in the appropriate treatment groups were injected subcutaneously with 100μL of the conjugate solution. The prepared folate-FITC solutions were divided into daily aliquots and stored in the dark at -20°C. Each aliquot was thawed completely on the day of administration and shaken for even drug distribution before injection into animals.

3.2.6 Evaluation of Antibody Titers

3.2.6.1 Immunization of Mice

Female Balb/c and DBA/2 mice aged 5-7 weeks were allowed to acclimate to the environment in the animal housing facility for one week. Then, mice aged 6-8 weeks were vaccinated with 35μg KLH-FITC in 50 μg GPI-0100 adjuvant formulated in sterile saline. Mice were immunized every two weeks using subcutaneous injections alternating between the base of tail and base of neck for a total of three vaccinations. Blood samples from immunized mice were collected by submandibular puncture with a sterile lancet one week after the 2nd and 3rd vaccinations and pooled by cage. The tubes of pooled blood

were then centrifuged to separate the coagulated red blood cells from the serum, and the serum samples were stored at -20°C pending ELISA analysis (usually performed within 1-2 days).

3.2.6.2 Antibody Titer Assay

The antibody levels in the blood of immunized mice were assayed using a procedure based on one received from Endocyte, Inc. 96-well ELISA plates were coated with 2µg/well of BSA-FITC by incubating each well with 100µL of a 20 µg/ml BSA-FITC solution in PBS (pH 7.4) at 4°C overnight while covered with aluminum foil. The following day, plates were washed 3x with PBS-Tween (0.01 M PBS with 0.05% Tween-20 at pH 7.4) and blotted dry on paper towels before incubating with a freshly prepared 0.2% gelatin solution (0.2g gelatin powder dissolved in 100 mL PBS-Tween by gentle stirring at 37°C) for 1h at 37°C. The gelatin coating step is used to block any uncoated surfaces in the plastic wells to minimize unspecific antibody binding. The gelatin blocked plates were then washed 3x with PBS-Tween. Separately, in different 96-well plates, 2x serial dilutions (in PBS-Tween-Gelatin) of pooled anti-FITC mouse serum and pre-immune mouse serum were performed to make a total of 22 dilutions per sample starting with a 1:100 dilution. 50µL of each of the serial dilutions were then transferred to the gelatin and BSA-FITC coated plates and incubated in the dark for 1h at 37°C followed by washing 4x with PBS-Tween. In order to detect the anti-FITC antibodies from the immunized mice that would have bound to the FITC molecules coated on the wells, the plates were incubated with a biotin-conjugated goat anti-mouse IgG2a primary antibody (1:5000 dilution in PBS-Tween) for 1h at 37°C. Following another 4x PBS-Tween

washing step, the plates were again incubated in the dark for 1h at 37°C with a streptavidin-HRP conjugate (1:5000 dilution in PBS-Tween) before washing 4x with reverse osmosis purified water and exposing to a freshly prepared OPD substrate solution. The substrate-HRP reaction was allowed to continue in the dark for 30 minutes at room temperature and subsequently, was stopped by the addition of 37.5 μL/well of 3N HCl. The plate was then read at 490 nm (O.D.) using a 96-well plate reader and the results were plotted as average O.D. versus log serum dilution factor (e.g. 1:100 dilution is Log_{10} 100 which is 2). Each plate was read twice and each serum sample was run in duplicate in order to obtain an average O.D. for generating the titration curve. A representative graph of the antibody titers obtained from different animal experiments is shown in Figure 3.3.

3.2.7 Combination Therapy Protocol

Preliminary pilot studies had demonstrated that the highest antibody titer in mouse serum was reached 7-10 days following the final KLH-FITC plus GPI-0100 vaccination. These studies had also indicated that L1210A tumors required 7-10 days and M109 tumors required 10-14 days to reach the desired 50-75mm^3 tumor volume for therapy initiation. Therefore, in order to start dosing of the folate-FITC immunotherapy at the peak of antibody titers DBA/2 mice were implanted with s.c. L1210A tumors 1-2 days prior to their 3rd immunization and Balb/c mice were injected with s.c. M109 tumors 3-4 days prior to their 3rd immunization. The day of tumor implantation was designated as day 0 for all experiments. Once tumors had reached the appropriate size, mice were randomized into cages of 5 mice dedicated to each different treatment: PBS control,

folate-FITC immunotherapy, sunitinib or axitinib, and the combination of folate-FITC plus sunitinib or axitinib, and therapy was initiated. Mice in the PBS control group were injected daily (s.c.) with 100μL of sterile PBS and the mice treated with folate-FITC alone were injected s.c. with 100μL of the conjugate appropriately diluted to give a 500 nmol/kg concentration. The immunotherapy was administered on a 5 days on 2 days off schedule. Mice in the sunitinib alone or axitinib alone groups were gavaged daily with 100μL of 20mg/kg sunitinib or 15 mg/kg axitinib respectively. All mice treated with the combination of folate-FITC and sunitinib or axitinib received appropriately timed doses of both treatments described above (i.e. 100μL of 500 nmol/kg folate-FITC s.c. + 100μL of 20mg/kg sunitinib *or* 15 mg/kg axitinib p.o.). Tumor growth was monitored at 48h intervals by measuring each tumor with a pair of calipers and calculating its volume using a standard two-dimensional tumor volume equation; the length of the longest axis of each tumor (L) and the length of the axis perpendicular to it (W) was recorded in millimeters and the corresponding tumor volume in mm^3 was determined by calculating ½ (L x W^2). Treatments were administered continually until the PBS control tumors reached 1000-1500 mm^3 in size at which point mice were euthanized and tumors resected for further analysis. For comparison of tumor growth rates, the calculated tumor volumes were averaged by treatment group and plotted on a graph of tumor size vs. days post tumor implantation. In order to reduce serum folate levels to concentrations comparable with folate levels in humans, all mice in treatment groups were placed on a folate deficient diet one week following the 2^{nd} immunization. Any mice that were not euthanized at the end of the treatment period were returned to regular chow within a week of completing therapy.

3.2.8 Resection and Digestion of Tumors and Spleens

As mentioned in the previous subsection, treatment of tumor-bearing animals was suspended once the control tumors started reaching a size that is considered too large a burden for the animals involved. In the case of M109 cells, the implanted tumors began to ulcerate and scab over as they reached ~750 mm^3 in size and therefore, the therapy needed to be stopped and mice needed to be euthanized at this point. Once it was determined that a study should be ended, all animals in the treatment groups were euthanized within 1-2 days and their tumors and spleens harvested for freezing and analysis by flow cytometry. Briefly, mice were euthanized by CO_2 asphyxiation and their tumors and spleens were removed with the aid of dissection equipment and washed in PBS to remove any excess fur or blood. Both tissues were then weighed in order to obtain a second set of data to corroborate tumor volume measurements and to determine whether tumor cells had metastasized to the spleen. Each tumor was then cut in half and one section was minced into fine pieces. The individual minced tumors were then placed into separately labeled tubes containing ~10ml of a collagenase cocktail. This digestion cocktail, designed in the Low laboratory, was chosen because it causes the least damage to cell-surface proteins. It is composed of 1mg/ml collagenase type IV, 0.1mg/ml of hyaluronidase from bovine testes, and 0.2mg/ml of deoxyribonuclease I from bovine pancreas dissolved in serum free folate deficient (FD)-RPMI1640 medium. Following digestion for 1h at 37°C with mild shaking, the digestion reaction was stopped by the addition of FD-RPMI640 medium containing 10% heat inactivated FBS and the broken down tumors were passed through a 40μm cell strainer to collect individual tumor cells. The isolated cells were then spun down to remove digestion cocktail and resuspended in a

red blood cell lysis buffer (Sigma Aldrich, St. Louis, MO) for 5-10minutes. The lysis buffer was then diluted with an excess of PBS and the red blood cell free tumor cells were collected by centrifugation. The resulting cell pellet was resuspended in PBS containing 1% BSA and used in the flow cytometry experiments described later.

Murine spleen tissue is generally very soft and easily broken apart, and therefore, does not require an extra digestion step for isolation of individual splenocytes. The cleaned spleens collected from treated mice were gently mashed and pressed through a 40μm cell strainer with the aid of a plunger from a small syringe and some PBS. The strainer was carefully washed with a small amount of PBS to remove any attached cells through to the collection tube until only the white connective tissue of the spleen's outer membrane remained in the mesh of the strainer. The collected splenocytes were spun down before subjecting them to the red blood cell lysis procedure detailed earlier. Spleen cells collected from the previous step were subsequently suspended in PBS containing 1% BSA and kept on ice till fluorescent labeling and analysis.

3.2.9 Labeling and Flow Cytometry Analysis of Tumor and Spleen Cells

The tumor and spleen cells that were isolated as described in the previous subsection were labeled with specific antibodies to a variety of immune cell markers. Briefly, 100μl aliquots of the isolated tumor and spleen cells suspended in 1% BSA-PBS-Tween (wash buffer) were transferred to 1.5ml eppendorf tubes for labeling individual cell types. These aliquots were then incubated at 4°C for 5 minutes with a commercially available Fc receptor blocker (BD Biosciences, San Jose, CA). Each different tube was

subsequently incubated for 1h at 4°C with the appropriate antibodies: APC or PE conjugated anti-mouse F4/80 antibody for macrophages; PE conjugated anti-mouse CD3 and FITC conjugated anti-mouse CD4 or FITC conjugated anti-mouse CD8 for CD4+ and CD8+ T cells respectively; APC conjugated anti-mouse CD11b and PE conjugated anti-mouse GR-1 for myeloid derived suppressor cells; and PE conjugated anti-mouse CD3, FITC conjugated anti-mouse CD4, and Alexa Fluor 647 conjugated anti-mouse FR4 (folate receptor δ) for regulatory T cells. Folate receptor expression on tumor cells was detected by staining with a folate-Alexa Fluor 647 conjugate. Following antibody labeling, cells were washed with cold wash buffer and analyzed on a Beckton Dickinson FACS Caliber instrument using CellQuest software. During each experiment, cell samples were also labeled with antibodies of each individual fluorescent label for compensation purposes. At least 100,000 cells were counted from each tumor and spleen sample.

3.2.10 Cryopreservation, Labeling, and Imaging of Tumor and Spleen Tissue

Once a combination therapy study was completed, tumors and spleens were removed and cleaned as described in section 3.2.8. Half of each tumor was embedded in Shandon™ Cryomatrix™ resin and snap frozen by partial submersion in liquid nitrogen. The frozen tissues were then sealed in freezer bags and stored at -80°C till use. When ready, the frozen tumor tissues were sliced into 10μm sections using a cryotome and mounted on to polylysine-coated Superfrost microscopy slides. These tissue mounted slides were also stored at -80°C until they were used for staining and imaging (generally, for no more than 1 week). In order to prepare slides for fluorescent imaging, the slides

were removed from the -80°C freezer and allowed to warm up at room temperature for 30-60 minutes. The tissue sections were subsequently fixed and permeabilized in ice-cold acetone for 10 minutes followed by washing in ice-cold PBS (2x, 5 minutes each). The slides were carefully wiped off with a cotton tip swab and the tissue section was encircled with a Pap pen marker. The marked off tissue containing circles were then incubated in a freshly prepared PBS-Tween solution containing 1% BSA for 30 minutes to block any unspecific binding. After the incubation period, slides were washed 2x for 2 minutes and dried with a cotton swab followed by incubating the marked circles with a 1:50 dilution (in 1% BSA containing PBS-Tween) of Alexa Fluor 647 conjugated rat anti-mouse CD31 antibody (BioLegend, San Diego, CA) in a dark humidified chamber for 1h at room temperature. Thusly labeled tissue slides underwent a final round of washing in PBS (3x, 5 minutes each) before being dried and mounted with cover slips (with one drop of mounting medium). The cover slips were then sealed in place with clear nail polish to prevent drying and movement during imaging. The labeled sections were examined under an Olympus FV1000 inverted confocal laser scanning microscope using a Plan Apo 10X objective. All tissue fluorescence transmission images were obtained under identical conditions. Unlabeled tissue sections that were otherwise treated in the same manner as the anti-CD31 labeled slides were used to ensure that no unspecific background florescence was influencing the observed labeling intensities.

3.2.11 Statistical Analysis

Graphing and certain statistical calculations of the collected data from all the described experiments were performed using GraphPad Prism software. Error bars on tumor volume graphs and all bar graphs represent standard error mean. A simple additivism equation was used to calculate whether the relationship between the two combined drugs were additive or synergistic. E_{add}, the fractional tumor growth inhibition that would be expected if the two drugs combined in an additive manner was calculated as: (E_A x E_B), where E_A and E_B are the fractional tumor growth inhibition accomplished at a particular time point by treating with each individual drug. If the reduction of tumor growth observed at the same time point when animals are administered with both drugs is greater than the projected additive effect, then the treatment is considered synergistic. All flow cytometry data were analyzed on FlowJo software and confocal microscopy data was analyzed on FLUOVIEW Viewer software.

3.3 Results

3.3.1 Anti-FITC Antibody Response in Immunized Mice

As detailed in the Materials and Methods section, for each experiment mice were immunized three times at two week intervals with the KLH-FITC conjugate formulated in a GPI-0100 adjuvant. Mouse blood was collected by submandibular puncture following both the second and third immunizations and antibody titers were assessed to ensure that a robust anti-FITC immune response was generated. The graph shown in Figure 3.3 demonstrates a significant elevation of anti-FITC titers in all groups of

immunized mice (blood was collected from all mice in a cage and pooled for ELISA analysis) when compared to blood serum titers from non-immunized mice (green line). Following the completion of some experiments, blood was again collected and an ELISA titer assays conducted to ensure that antibody levels were maintained during the treatment period. The resulting data demonstrated that only a slight decrease in titers occurs during the 2-3 week treatment period, indicating that KLH-FITC plus GPI-0100 vaccination is capable of inducing a lasting antibody response.

3.3.2 Sunitinib Synergizes with Folate-Hapten Mediated Immunotherapy in the L1210A Tumor Model

As noted in the Introduction, VEGFR inhibitors have been observed not only to downregulate angiogenesis, but also to inhibit the immunosuppressive activities of myeloid derived suppressor cells and regulatory T cells. In order to test whether these immunodulatory properties of VEGFR inhibitors might augment the anti-tumor activities of receptor-targeted hapten immunotherapies, it was necessary to grow folate receptor-expressing tumors in immunocompetent mice. For this purpose, L1210A tumors were implanted in DBA/2 mice and Renca and M109 cancers were grown in Balb/c mice as described previously. The first experiment to evaluate the desired combination therapy was conducted in Balb/c mice implanted with Renca tumors, but even though the therapy originally seemed to work as anticipated (Figure 3.4), flow cytometry analysis of the tumor cells following completion of the study indicated that they were losing FR while proliferating *in vivo*. As a result, any further immunotherapy studies in Renca tumors

were discontinued since folate-FITC would not be able to mediate a tumor-targeted immune response against FR negative tumors.

The next study to evaluate the combination of sunitinib plus folate-hapten mediated immunotherapy was conducted in L1210A tumor-bearing mice previously immunized against fluorescein. As seen in Figure 3.6, DBA/2 mice implanted with L1210A cancer cells grew tumors that expanded to 1000 mm^3 in <3 weeks. Surprisingly, neither sunitinib nor the folate-targeted immunotherapy alone exerted any impact on this rapid tumor growth, at least when exposed to the dosing regimen explored in this study. In contrast, the combination of sunitinib plus folate-targeted immunotherapy caused a significant reduction in tumor growth (Figures 3.6 and 3.8 A), suggesting that the combination therapy is better than the sum of the two single agent therapies. These data imply that some type of synergy between the tumor-targeted hapten immunotherapy and the VEGFR inhibitor therapy exists.

Because L1210A cells derive from a murine B cell lymphocytic leukemia, it was also instructive to examine the weights of each animal's spleen, since malignant cells from the tumor metastasize to the spleen in this animal model. As shown in Figures 3.7 and 3.8 B, spleens became similarly enlarged in the PBS-, sunitinib- and folate-FITC-treated animals, but remained essentially normal in the combination therapy animals. These data suggest that either metastasis of malignant cells to the spleen is strongly suppressed by the combination therapy or that malignant cells that spread to the spleen are rapidly eliminated in this therapy.

3.3.3 Sunitinib Synergizes with Folate-Hapten Mediated Immunotherapy in the M109 Tumor Model

Folate receptors are overexpressed by a number of different human cancers. Therefore, in order to develop drugs that can treat these FR expressing tumors, successful therapeutic efficacy needs to be demonstrated in more than one murine tumor model. The M109 lung cancer cell line was selected as a follow-up to the L1210A tumor model because of its ability to grow syngeneic solid tumors in immunocompetent mice and its highly immunogenic nature. These tumors have also demonstrated an ability to respond well to folate-FITC immunotherapy in the past and some treated animals even generated a lasting anti-tumor memory (curative folate-FITC + IL-2 + IFN- α treatment).[17] For the purposes of the experiments described in this chapter, female Balb/c mice were implanted s.c. with solid M109 tumors and divided into 4 groups: PBS control, folate-FITC alone, sunitinib alone, and folate-FITC + sunitinib. As shown in Figure 3.9, the groups of mice treated with either sunitinib or folate-FITC alone responds better to individual therapy than the L1210A tumor bearing mice treated with the same drug. However, the mice in the group administered with a combination of both folate-FITC and sunitinib continued to maintain a slower growth rate and smaller tumor volumes than either treatment alone (purple diamond ♦). Moreover, calculating the E_{add} of the two independent drug therapies yields a projected tumor volume reduction of 46% (assuming average tumor volume of the PBS group to be 100%), which is approximately two folds less efficacious than the 23% attained by the combination therapy. These results endorse the original hypothesis that combining folate-hapten mediated immunotherapy with angiogenesis inhibitor therapy would likely result in a potently augmentation of each drug's therapeutic

efficacy. Figure 3.10 visually represents the differences in tumor and spleen sizes harvested from mice following completion of the study. In contrast to the L1210A tumors, no significant metastasis of cancer cells to the spleen was apparent in this tumor model.

3.3.4 Axitinib Synergizes with Folate-Hapten Mediated Immunotherapy in the L1210A Tumor Model

It is generally imprudent to assume that multiple drugs with the same mechanism of action would behave identically in a certain tumor type. Therefore, any claim suggesting that all angiogenesis inhibitors synergize with folate-hapten mediated immunotherapy against FR expressing cancers simply based on studies using one angiogenesis inhibitor would be an extrapolative statement. In fact, as demonstrated in previously described experiments, the same angiogenesis inhibitor (sunitinib) could have better anti-tumor effects in one murine model (M109) than in a different one (L1210A).

Given these possibilities, we wanted to ensure that sunitinib was not the only VEGFR inhibitor that would synergize with folate-FITC immunotherapy. Following a thorough search of the literature, we chose axitinib as a second angiogenesis inhibitor to evaluate in FR+ cancers because it is a more selective inhibitor of VEGF receptors and therefore, displays slightly different characteristics from sunitinib while maintaining the same fundamental mechanism of anti-tumor efficacy. We elected to test the new drug in the L1210A tumor model because it was clearly the more aggressive and less immunogenic of the two available tumor types and therefore, would be more likely to answer the question of whether this drug combination would succeed in other FR+ tumor

models. Immunized DBA/2 females were implanted s.c. with solid L1210A tumors and administered with PBS, folate-FITC, axitinib (15mg/kg) or a combination of axitinib and folate-FITC once their tumors reached 50-75mm^3 in volume. As shown in Figure 3.11 axitinib combines with folate-FITC immunotherapy to slow tumor growth and prolong survival of treated mice. In this particular tumor model, axitinib alone performed better than sunitinib alone, but was unable to slow tumor progression significantly. The average tumor volume in the axitinib treated group at the end of the study (day 20) was 53% of the tumor volumes measured in the PBS treated mice. The mice treated with the axitinib + folate-FITC combination, however, demonstrated considerably smaller tumor volumes (23% at 20 days post tumor implantation) which is also an approximately two fold improvement from the projected additive therapeutic efficacy (43%). Following completion of the *in vivo* treatment studies, mice from each group were euthanized and their tumors and spleens were harvested for further analysis. Figure 3.12 visually represents the differences in tumor sizes resected from mice in the four treatment groups, and Figure 3.13 shows average tumor and spleen weights measured from the harvested tissues.

3.3.5 Immune Effector Cell and Suppressor Cell Levels are Augmented in Combination Treated Mice

A significant amount of effort has been poured into studying the mechanisms underlying the anti-cancer effects caused by angiogenesis inhibitors. Studies reported in the literature propose a number of other mechanisms beyond the basic inhibition of tumor vasculature leading to tumor necrosis. These include the down-regulation of MDSCs and

T_{regs}, and inhibition of stat3 activity.[29,32,33] Since previous studies have already determined that in order for folate-FITC immunotherapy to be successful, a full recruitment of immune effector cells to the tumor site was necessary, we were interested in determining which of these effector cell functions could be augmented by the addition of an angiogenesis inhibitor. In order to answer this question, tumors and spleens from treated mice in all studies were resected, digested, and labeled with a range of immune cell-specific antibodies for analysis by flow cytometry. As shown in Figure 3.14, the collected data indicate that CD4+ and CD8+ T cell levels are elevated in the spleens of the combination treated mice in both the L1210A and the M109 tumor models. The data also show that the MDSC levels are suppressed in the spleens of M109 tumor-bearing mice treated with the sunitinib plus folate-FITC combination (Figure 3.15). Interestingly, although MDSC suppression in VEGF inhibitor treated animals is widely reported in the literature, it was only observed in the M109 tumor model. Therefore, these results indicate that with this particular combination therapy, T cells are the most effectively modulated immune cell type, possibly due to the combined effect of T_{reg} downregulation and stimulation of antigen presentation stemming from hapten-mediated destruction of tumor cells.

3.3.6. Significant Inhibition of Tumor Vascular Growth is Observed in Combination Treated Mice

Since the primary mechanism of anti-tumor activity of angiogenesis inhibitors is the retardation of neovascularization, it is natural to expect that a reduction in blood vessel density would be observable within the tumors of any animal treated with sunitnib

or axitinib. However, recent studies by Prof. Rakesh Jain at the Harvard Medical School has shown that contrary to prevailing belief, the use of low dose vascular endothelial growth factor (VEGF) inhibitors in tumor treatment leads to the normalization of the otherwise disorganized and extremely leaky blood vessels of the tumor and results in the formation of a somewhat more organized and uniformly distributed vascular system.[31] Since both sunitinib and axitinib strongly inhibit the activity of multiple VEGF receptors,[27,33] this vascular normalization theory may represent one mechanism that contributes to the significant retardation of tumor growth observed following the administration of the combination therapies described in this chapter.

We isolated and cryopreserved a portion of the solid tumors from all treated mice for analysis of tumor vasculature by immunofluorescence. The surprising observation from the confocal microscopy imaging of tumor sections stained for CD31 expression was that, contrary to expectations, the angiogenesis inhibitors alone had little effect in inhibiting vasculature within the tumors of treated mice, whereas the combination treated tumors demonstrated a dramatic reduction in CD31 staining. As shown by Figures 3.16, 3.18, and 3.19, this observation was consistent for all three different combination studies described in this chapter, indicating that at least at the administered doses, the combination of folate-hapten mediated immunotherapy with VEGF inhibitors leads to the down regulation of neovascularization within FR positive tumors. The most likely reason for this potent synergy is twofold; first, the sunitinib and axitinib perform their primary function of inhibiting the VEGF receptors on the surface of endothelial cells which make them inaccessible to the VEGF proteins in the surrounding environment and second, the folate-FITC therapy mediates the destruction of FR expressing MDSCs, which are known

secretors of VEGF, leading to an overall lower concentration of VEGF in the tumor microenvironment.[39] An alternate possibility is that the reduction in tumor growth rate caused by the dual-drug therapy maintains tumors at a small enough volume to prevent the necessity for rapid neovascularization.

3.4 Discussion

The mammalian immune system is an intricate, complex, and highly efficient machine that has evolved over many millennia to recognize each and every healthy protein of the host as a 'self' component that is permitted to reside in the body.[15] Along the same token, this sentinel system is constantly on alert to recognize and block foreign antigens that are not in its repertoire of acceptable self-sequences from infecting or residing in the body. Cancer has proved to be an incredibly difficult and daunting disease to treat partly because tumor cells have evolved the ability avoid detection by one of the most scrupulous security systems known to science.[40] Therefore, it is only natural to conclude that in order to successfully eradicate a cancerous malignancy, an immune component should to be incorporated into the treatment regimen. However, most cancer immunotherapies that were developed over the past century have had to deal with not only waking up the unresponsive immune system against the cancer, but also with the cancer's remarkable ability to suppress anti-tumor immunity.[40] So, a successful immunotherapeutic needs to consistently recruit a robust immune response to the tumor site whilst meticulously blocking the cancer's immunosuppressive activities.[18] Since it would be rather difficult to incorporate two such functionalities into a single therapeutic drug that does not cause unpleasant toxicities, it has become apparent that, at least for the

time being, an effective immunotherapy approach would need to be composed of more than one anti-tumor agent.

Folate receptor targeted cancer therapeutics have attained exceptional success in both preclinical and clinical studies.[9] Moreover, the folate-hapten mediated immunotherapy that was evaluated in clinical trials against late-stage renal cell carcinomas resulted in negligible (if any) toxicities associated with the folate-hapten therapy.[23] Therefore, we were highly motivated to explore alternate therapeutic options that would combine well and improve the anti-tumor activity of folate-hapten immunotherapy. Previous preclinical studies using folate-fluorescein immunotherapy in murine models of cancer had shown that the therapy was ineffective at slowing cancer progression once solid tumors had reached a certain size (~200mm^3) and the cancer's rate of proliferation exceeded the immunotherapy's ability to mediate cancer cell death.[41] Concurrent studies had also demonstrated that localized tumor irradiation and the use of folate-CpG to mediate attraction of toll-like receptor expressing immune cells to the tumor-site synergized with folate-hapten mediated immunotherapy to decrease tumor burden and prolong animal survival.[41] However, neither of these therapies could easily be taken into clinic as companions to folate-hapten mediated immunotherapy because 1) most tumors are very difficult to treat with localized tumor irradiation since they are not easily accessible without surgical exposure, and 2) two new exploratory therapies (folate-hapten and folate-CpG) would be challenging to obtain approval for through the FDA. Fortunately, having such extensive amounts of information regarding folate-hapten mediated immunotherapy was helpful in determining the desirable characteristics of a novel companion therapy for our immunotherapy. Inhibitors of the vascular endothelial

growth factor receptors held the most appeal for us because a number of VEGFR inhibitors were already approved for use in human cancers,[28,38,42] they were continually showing efficacy against a variety of different cancers in murine models,[24,25,36,37] and they had both direct tumor inhibition activity (which would help keep the tumors from proliferating faster than folate-hapten therapy could keep up with) and immunomodulating properties (which would aid the folate-hapten to better recruit immune effector cells to the site of tumor).[29,31]

Following a number of small pilot studies to evaluate whether the VEGFR inhibitors, sunitinib and axitinib, had any effect on two high FR expressing cancers that were syngeneic to mouse strains, and also to determine the range of doses that showed efficacy against these tumors, suboptimal doses of both the angiogenesis inhibitors and folate-fluorescein were used in the combination therapy studies in order to clearly determine whether the two therapies would work better in concert than as individual drugs. Sunitinib and axitinib were most effective as single therapies against M109 and L1210A tumors at doses higher than 20mg/kg and 15mg/kg respectively, and therefore, those concentrations were chosen for the purposes of the studies described in this chapter. With any receptor targeted, antibody-dependent immunotherapy care must be taken to ensure that the administered dose is not so saturating that both tumor cell receptors and the circulating antibodies are occupied by the therapeutic conjugate such that no tumor-antibody interaction could occur.[19] Past studied had shown that this saturation occurs at doses above 1500-1800 nmols/kg of folate-fluorescein.[19] Thus, it was decided that a 500 nmol/kg folate-fluorescein dose would be suboptimal yet effective.

As shown in Figures 3.6 and 3.9, supplementation with sunitinib significantly augments folate-fluorescein immunotherapy in both L1210A and M109 tumor models. These results are particularly encouraging because L1210A is known to be an extremely aggressive tumor that has proven very difficult to impede once it has taken hold. In fact, even some extremely potent folate-cytotoxic agent conjugates have failed to slow L1210A tumor growth (Endocyte, Inc., personal communication). This tumor's aggressive nature is further corroborated by the essential inactivity of both sunitinib and folate-fluorescein alone against the tumor in the studies described in this chapter. In contrast, both individual therapies have some therapeutic efficacy against the highly immunogenic M109 lung cancer model. The combination therapy, however, is markedly better than either treatment alone as demonstrated by both the tumor volume graph and the average weight of tumors resected from the different treatment groups (Figure 3.10). Furthermore, a clear increase in spleen size is observed in the DBA/2 animals treated with PBS, sunitinib or folate-fluorescein (Figure 3.7) indicating that L1210A tumor cells escape the original subcutaneous site of tumor implantation and metastasize to the spleen at some point during tumor progression. Healthy DBA mouse spleens average ~100mg (personal measurements) and the mice treated with the combination of folate-fluorescein plus sunitinib display spleen sizes that are only slightly heavier than normal tumors, leading to the most likely conclusion that the retardation of tumor growth caused by this therapy either prevents or slows tumor cells from escaping the solid tumor and lodging on other tissues. Alternatively, the less likely conclusion is that tumors metastasize at similar rates in each tumor treatment group, but the combination therapy is better able to destroy

any circulating L1210A tumor cells and metastatic nodules than any of the individually administered treatments.

An *in vitro* IC_{50} study of sunitinib with L1210A cells in culture showed that the compound had very low cytotoxicity against these cells. The data plotted on the graph shown in Figure 3.5 reveals that micromolar concentrations of sunitinib is necessary to kill 50% of the cells in the culture plate following a continuous 72h incubation. In contrast, some folate-cytotoxic drug conjugates display IC_{50} values in the single digit nanomolar range following only 2h incubations.[12] This data raises the question of which mechanisms are playing a role in creating the synergy that exists between folate-mediated immunotherapy and VEGFR inhibitors if these inhibitors are not exerting their anti-tumor properties by killing tumor cells directly. Further mechanistic studies aimed towards better understanding this impressive synergy showed that cytotoxic T cell as well as CD4+ T cell levels compose a higher percentage of the total viable cell population in the spleens of combination treated DBA/2 and Balb/c mice than in any other treatment group. It was also interesting to observe that a significant reduction in MDSC populations, consistent with data reported in the literature that VEGFR inhibitors downregulate MDSC activity,[31,32] is apparent in the spleens of M109 tumor-bearing mice dosed with the folate-fluoresceing plus sunitinib therapy. The fact that this difference was only clearly visible in the M109 tumor model is not to say that a similar mechanism is not underway in the L1210A tumor model, but that the large numbers of metastasized tumor cells may make it difficult to differentiate marked differences in % MDSC levels among the different treatment groups. The most surprising data collected during the search for a therapeutic mechanism were the confocal microscopy images of CD31-stained frozen

tumor sections, which showed that the dual therapy dramatically suppressed neovascularization of tumors. Although it was expected that a reduction of tumor vasculature would be observed in the two treatment groups dosed with the angiogenesis inhibitors, we did not anticipate finding a significantly lower blood vessel density in the combination treated tumors. As displayed by the images in Figures 3.16, 3.18, and 3.19, the reported observation is consistent among the three different experiments (sunitinib + folate-fluoresceing in L1210A and M109 tumors, and axitinib + folate-fluorescein in L1210A tumors), and a clear suppression of the tumor vasculature is apparent in the tumors treated with combination therapy. As mentioned in the Results section, studied by professor Rakesh Jain have concluded that VEGFR inhibitors, when administered consistently over a period of time at low doses, is capable of normalizing the abnormal and erratic tumor vasculature to reflect those more commonly found within healthy tissues.[31] But, it is apparent that if a tumor grows too fast for these drugs to exert any effect, then the vascular normalization does not occur even if the animals are dosed consistently with the VEGFR inhibitor. So, if a tumor is treated with a low dose of an angiogenesis inhibitor and its progression is slowed by the addition of a different therapeutic drug, then the blood vessel normalization effects should become apparent within these tumors. Moreover, an alternate reason for why this inhibition of neovascularization is occurring could be that the sunitinib and axitinib are blocking the VEGFR-VEGF recognition that is critical for growth of new blood vessels while the folate-fluorescein is simultaneously mediating the opsonization of VEGF-releasing MDSCs and tumor-associated anti-inflammatory macrophages. An experiment that

examines the aforementioned hypothesis would be an interesting addition to the available results and would strengthen the argument being made.

In short, the results collected from the studies described in this chapter leads to the conclusion that vascular endothelial growth factor receptor inhibitors are potent additions to the folate-hapten mediated antibody-dependent cellular cytotoxicity therapy described in this chapter. We have shown that two different angiogenesis inhibitors show synergy when combined with folate-hapten immunotherapy against both lung cancer (M109) and lymphocytic leukemia (L1210A) models of folate receptor expressing cancers. Furthermore, we have shown that this synergy occurs by improving the function of immune effector cells, reducing populations of immunosuppressive cells, and inhibiting tumor neovascularization.

3.5 References

1 Antony, A. The biological chemistry of folate receptors. *Blood* **79**, 2807-2820 (1992).

2 Lucock, M. Folic acid: nutritional biochemistry, molecular biology, and role in disease processes. *Molecular genetics and metabolism* **71**, 121-138 (2000).

3 Kim, Y.-I. Nutritional epigenetics: impact of folate deficiency on DNA methylation and colon cancer susceptibility. *The Journal of nutrition* **135**, 2703-2709 (2005).

4 Matherly, L. H. & Goldman, I. D. Membrane transport of folates. *Vitamins & Hormones* **66**, 403-456 (2003).

5 Parker, N. *et al.* Folate receptor expression in carcinomas and normal tissues determined by a quantitative radioligand binding assay. *Analytical biochemistry* **338**, 284-293 (2005).

6 Weitman, S. D. *et al.* Distribution of the folate receptor GP38 in normal and malignant cell lines and tissues. *Cancer research* **52**, 3396-3401 (1992).

7 Weitman, S. D. *et al.* Cellular localization of the folate receptor: potential role in drug toxicity and folate homeostasis. *Cancer research* **52**, 6708-6711 (1992).

8 Elnakat, H. & Ratnam, M. Distribution, functionality and gene regulation of folate receptor isoforms: implications in targeted therapy. *Advanced drug delivery reviews* **56**, 1067-1084 (2004).

9 Reddy, J. A. & Low, P. S. Folate-mediated targeting of therapeutic and imaging agents to cancers. *Critical Reviews™ in Therapeutic Drug Carrier Systems* **15** (1998).

10 Ayala-López, W., Xia, W., Varghese, B. & Low, P. S. Imaging of atherosclerosis in apoliprotein e knockout mice: targeting of a folate-conjugated radiopharmaceutical to activated macrophages. *Journal of Nuclear Medicine* **51**, 768-774 (2010).

11 Turk, M. J. *et al.* Folate-targeted imaging of activated macrophages in rats with adjuvant-induced arthritis. *Arthritis & Rheumatism* **46**, 1947-1955 (2002).

12 Reddy, J. A. *et al.* In Vivo Structural Activity and Optimization Studies of Folate−Tubulysin Conjugates. *Molecular pharmaceutics* **6**, 1518-1525 (2009).

13 Wang, S. *et al.* Design and synthesis of [111In] DTPA-folate for use as a tumor-targeted radiopharmaceutical. *Bioconjugate chemistry* **8**, 673-679 (1997).

14 Low, P. S., Henne, W. A. & Doorneweerd, D. D. Discovery and development of folic-acid-based receptor targeting for imaging and therapy of cancer and inflammatory diseases. *Accounts of chemical research* **41**, 120-129 (2007).

15 Janeway, C. A., Travers, P., Walport, M. & Shlomchik, M. J. Immunobiology. (2001).

16 Erkes, D. A. & Selvan, S. R. Hapten-Induced Contact Hypersensitivity, Autoimmune Reactions, and Tumor Regression: Plausibility of Mediating Antitumor Immunity. *Journal of Immunology Research* **2014** (2014).

17 Lu, Y. & Low, P. S. Folate targeting of haptens to cancer cell surfaces mediates immunotherapy of syngeneic murine tumors. *Cancer Immunology, Immunotherapy* **51**, 153-162 (2002).

18 Lu, Y., Sega, E., Leamon, C. P. & Low, P. S. Folate receptor-targeted immunotherapy of cancer: mechanism and therapeutic potential. *Advanced drug delivery reviews* **56**, 1161-1176 (2004).

19 Lu, Y., Sega, E. & Low, P. S. Folate receptor-targeted immunotherapy: Induction of humoral and cellular immunity against hapten-decorated cancer cells. *International Journal of Cancer* **116**, 710-719 (2005).

20 Lu, Y. & Low, P. S. Immunotherapy of folate receptor-expressing tumors: review of recent advances and future prospects. *Journal of Controlled Release* **91**, 17-29 (2003).

21 Paulos, C. M. *et al.* Folate-targeted immunotherapy effectively treats established adjuvant and collagen-induced arthritis. *Arthritis research & therapy* **8**, R77 (2006).

22 Lu, Y. *et al.* Preclinical pharmacokinetics, tissue distribution, and antitumor activity of a folate-hapten conjugate–targeted immunotherapy in hapten-immunized mice. *Molecular cancer therapeutics* **5**, 3258-3267, doi:10.1158/1535-7163.mct-06-0439 (2006).

23 Amato, R. J., Shetty, A., Lu, Y., Ellis, R. & Low, P. S. A phase I study of folate immune therapy (EC90 vaccine administered with GPI-0100 adjuvant followed by EC17) in patients with renal cell carcinoma. *Journal of Immunotherapy* **36**, 268-275 (2013).

24 Bose, A., Lowe, D. B., Rao, A. & Storkus, W. J. Combined vaccine+ axitinib therapy yields superior anti-tumor efficacy in a murine melanoma model. *Melanoma research* **22**, 236 (2012).

25 Bose, A. *et al.* Sunitinib facilitates the activation and recruitment of therapeutic anti-tumor immunity in concert with specific vaccination. *International Journal of Cancer* **129**, 2158-2170 (2011).

26 Ma, J. & Waxman, D. J. Modulation of the antitumor activity of metronomic cyclophosphamide by the angiogenesis inhibitor axitinib. *Molecular cancer therapeutics* **7**, 79-89 (2008).

27 Hu-Lowe, D. D. *et al.* Nonclinical antiangiogenesis and antitumor activities of axitinib (AG-013736), an oral, potent, and selective inhibitor of vascular endothelial growth factor receptor tyrosine kinases 1, 2, 3. *Clinical Cancer Research* **14**, 7272-7283 (2008).

28 Goodman, V. L. *et al.* Approval summary: sunitinib for the treatment of imatinib refractory or intolerant gastrointestinal stromal tumors and advanced renal cell carcinoma. *Clinical Cancer Research* **13**, 1367-1373 (2007).

29 Ellis, L. M. & Hicklin, D. J. VEGF-targeted therapy: mechanisms of anti-tumour activity. *Nature reviews cancer* **8**, 579-591 (2008).

30 Chauhan, V. P. *et al.* Normalization of tumour blood vessels improves the delivery of nanomedicines in a size-dependent manner. *Nature nanotechnology* **7**, 383-388 (2012).

31 Huang, Y. *et al.* Vascular normalizing doses of antiangiogenic treatment reprogram the immunosuppressive tumor microenvironment and enhance immunotherapy. *Proceedings of the National Academy of Sciences* **109**, 17561-17566 (2012).

32 Xin, H. *et al.* Sunitinib inhibition of Stat3 induces renal cell carcinoma tumor cell apoptosis and reduces immunosuppressive cells. *Cancer research* **69**, 2506-2513 (2009).

33 Ozao-Choy, J. *et al.* The novel role of tyrosine kinase inhibitor in the reversal of immune suppression and modulation of tumor microenvironment for immune-based cancer therapies. *Cancer research* **69**, 2514-2522 (2009).

34 Vanneman, M. & Dranoff, G. Combining immunotherapy and targeted therapies in cancer treatment. *Nature reviews cancer* **12**, 237-251 (2012).

35 Motzer, R. J. *et al.* Sunitinib in patients with metastatic renal cell carcinoma. *Jama* **295**, 2516-2524 (2006).

36 Guerin, O. *et al.* Supra-additive antitumor effect of sunitinib malate (SU11248, Sutent®) combined with docetaxel. A new therapeutic perspective in hormone refractory prostate cancer. *Journal of cancer research and clinical oncology* **134**, 51-57 (2008).

37 Castillo-Ávila, W. *et al.* Sunitinib inhibits tumor growth and synergizes with cisplatin in orthotopic models of cisplatin-sensitive and cisplatin-resistant human testicular germ cell tumors. *Clinical Cancer Research* **15**, 3384-3395 (2009).

38 Rini, B. I. *et al.* Phase II study of axitinib in sorafenib-refractory metastatic renal cell carcinoma. *Journal of Clinical Oncology* **27**, 4462-4468 (2009).

39 Murdoch, C., Muthana, M., Coffelt, S. B. & Lewis, C. E. The role of myeloid cells in the promotion of tumour angiogenesis. *Nature reviews cancer* **8**, 618-631 (2008).

40 Hanahan, D. & Weinberg, R. A. Hallmarks of cancer: the next generation. *Cell* **144**, 646-674 (2011).

41 Sega, E. I. *Folate Receptor Targeted immunotherapy of Cancer: Mechanism of Action and Augmentation of Therapeutic Efficacy* Doctor of Philosophy thesis, Purdue University, (2006).

42 *AngiogenesisInhibitors*, <http://www.cancer.gov/cancertopics/factsheet/Therapy/angiogenesis-inhibitors> (2011).

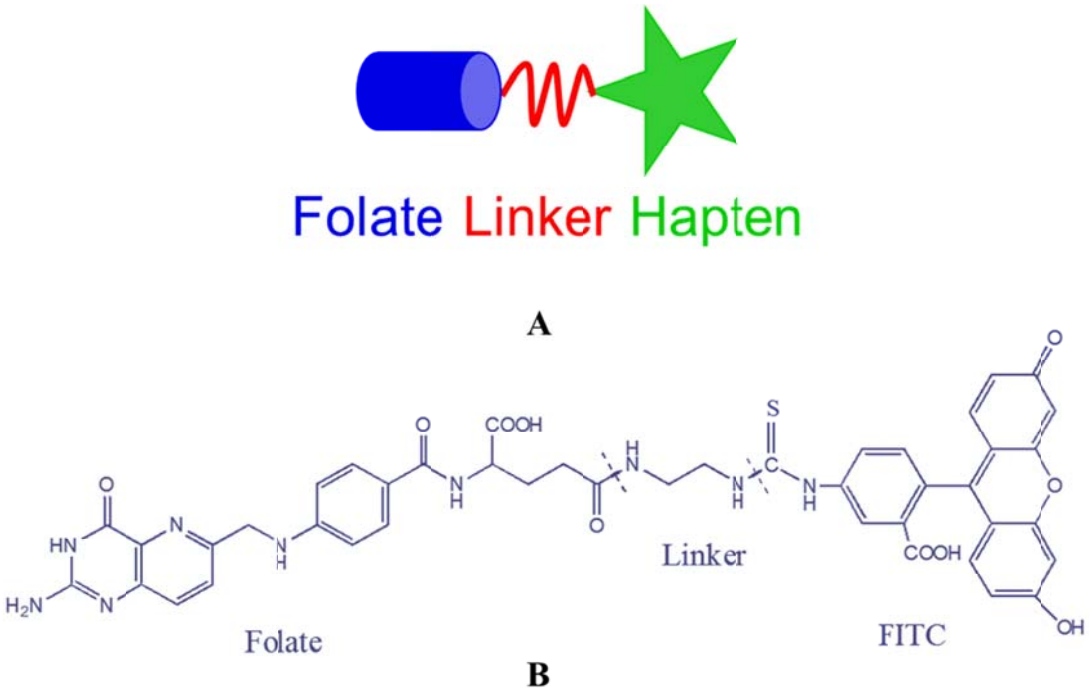

Figure 3.1. Common structural components of folate-hapten conjugates (A) and the Folate-FITC conjugate used in the described immunotherapy experiments (B).

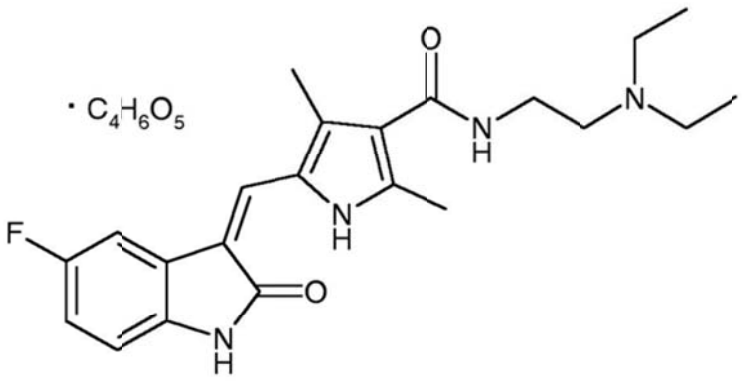

A

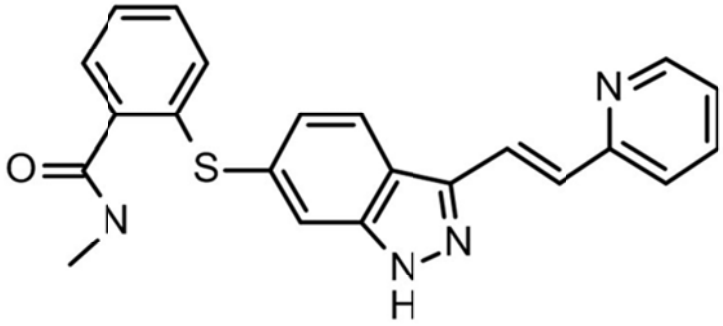

B

Figure 3.2. Chemical structures of the VEGF inhibitors used in the described combination therapy studies, (A) sunitinib, malate salt (Sutent®) and (B) axitinib, free base (Inlyta®).

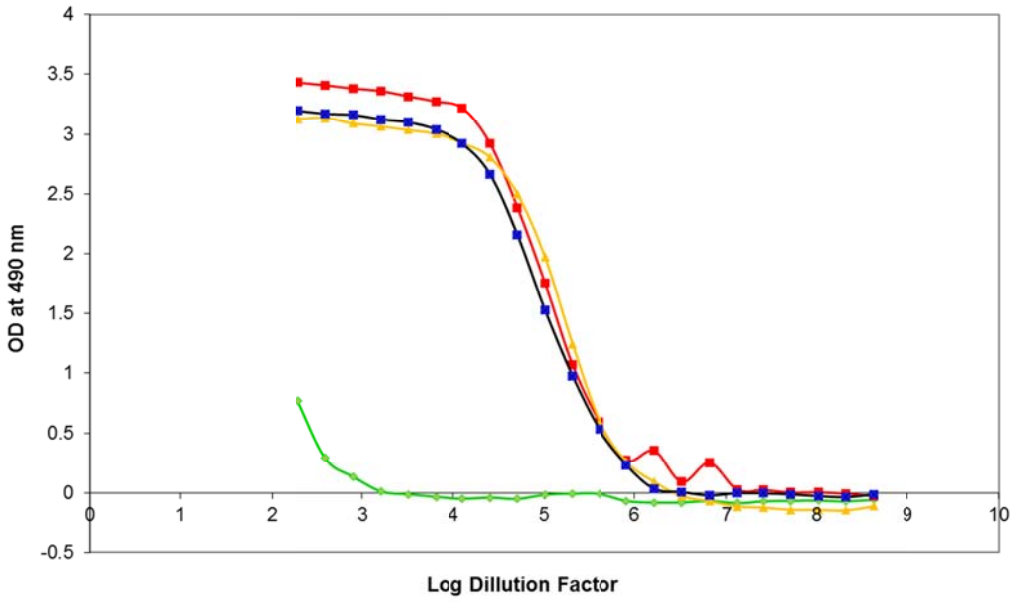

Figure 3.3. Anti-FITC antibody titers determined for KLH-FITC + GPI-0100 immunized DBA/2 mice following the 2nd immunization. Blood was collected from mice in individual cages and pooled together for analysis. The red, blue, and orange lines represent titers determined with pooled blood from 3 different cages of immunized mice and the green line represents the anti-FITC antibody titer in blood collected from non-immunized mice. The titers shown here are graphed using optical density measurements obtained at 490nm vs. Log_{10} of the dilution factor.

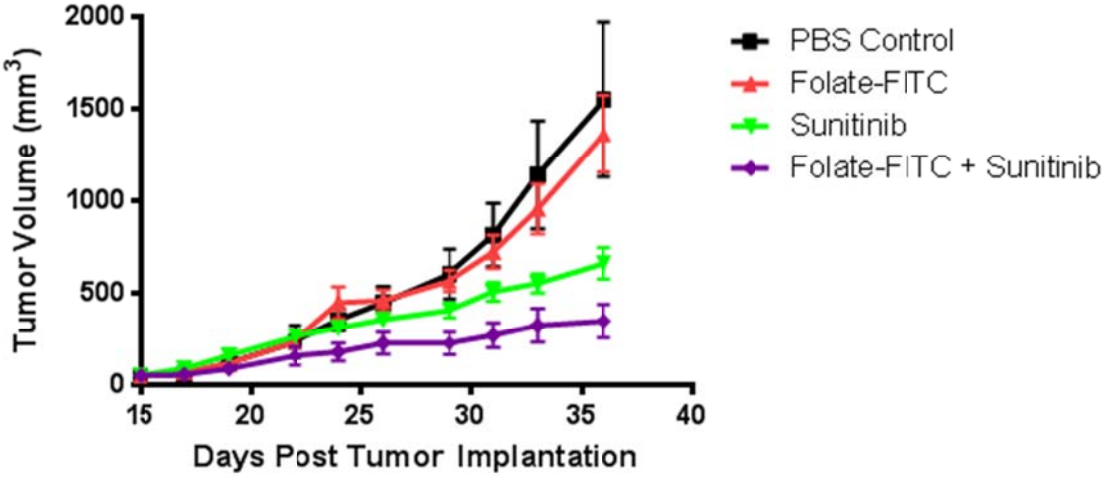

Figure 3.4. Tumor volume graph showing the growth of solid Renca cell tumors treated with PBS, folate-FITC immunotherapy (500nmol/kg), sunitinib (20mg/kg), or a combination of folate-FITC and sunitinib. Mice were randomized into groups following tumor implantation and treatment was initiated when tumor sizes averaged 50-75mm^3. Each treatment group contained at least 5 mice. Error bars represent SEM.

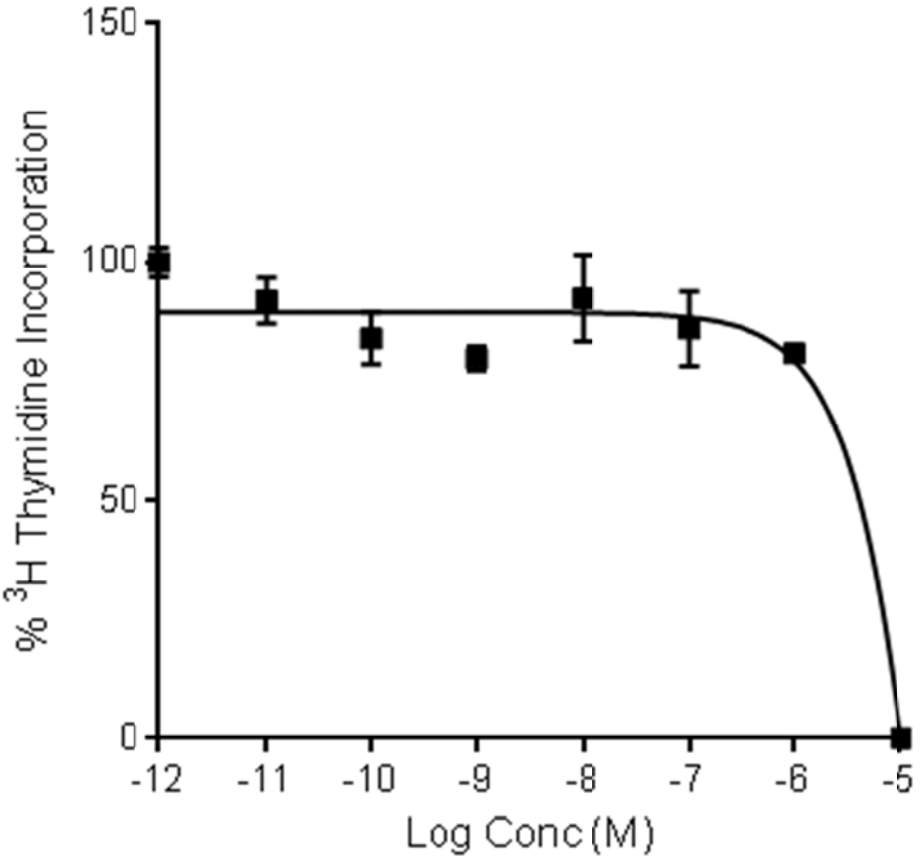

Figure 3.5. Graph showing the effect of incubating with different concentrations of sunitinib malate on the survival of L1210A cells *in vitro.* The data shows that sunitinib only has a weak cytotoxic effect on L1210A cells in culture. Therefore, the majority of the therapeutic effect *in vivo* must come from sunitinib's ability to modulate the tumor microenvironment.

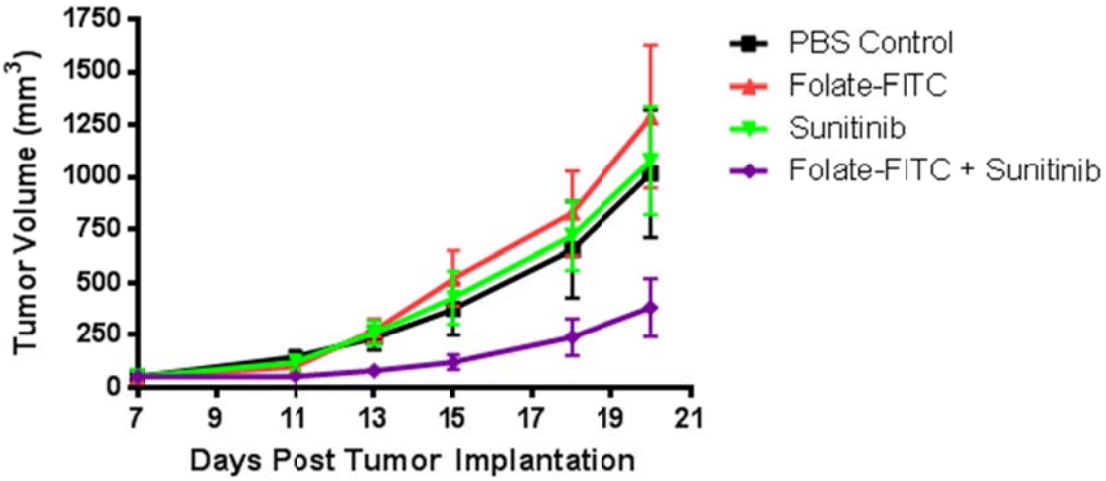

Figure 3.6. Tumor volume graph showing the growth of solid L1210A tumors treated with PBS, folate-FITC immunotherapy (500nmol/kg), sunitinib (20mg/kg), or a combination of folate-FITC and sunitinib. Mice were randomized into groups following tumor implantation and treatment was initiated when tumor sizes averaged 50-75mm^3. Each treatment group contained at least 5 mice. Error bars represent SEM.

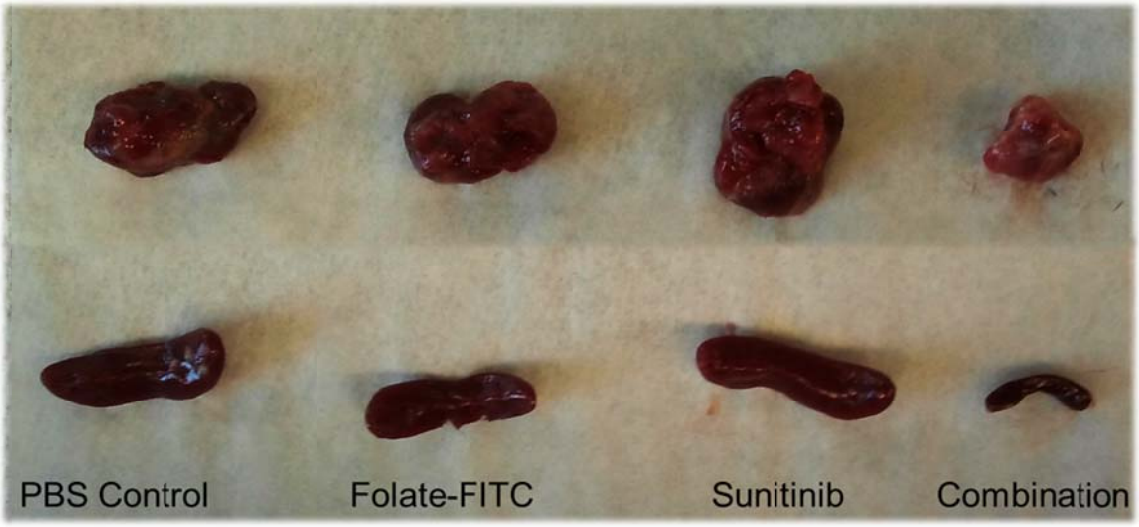

Figure 3.7. Resected tumors (top panel) and spleens (bottom panel) from L1210A tumor-bearing DBA/2 mice dosed with the indicated treatments. As the image shows, mice treated with the combination of folate-FITC and sunitinib have significantly smaller tumors and have dramatically smaller spleens, which indicates that the treatment can prevent or slow tumor cell metastasis to the spleen.

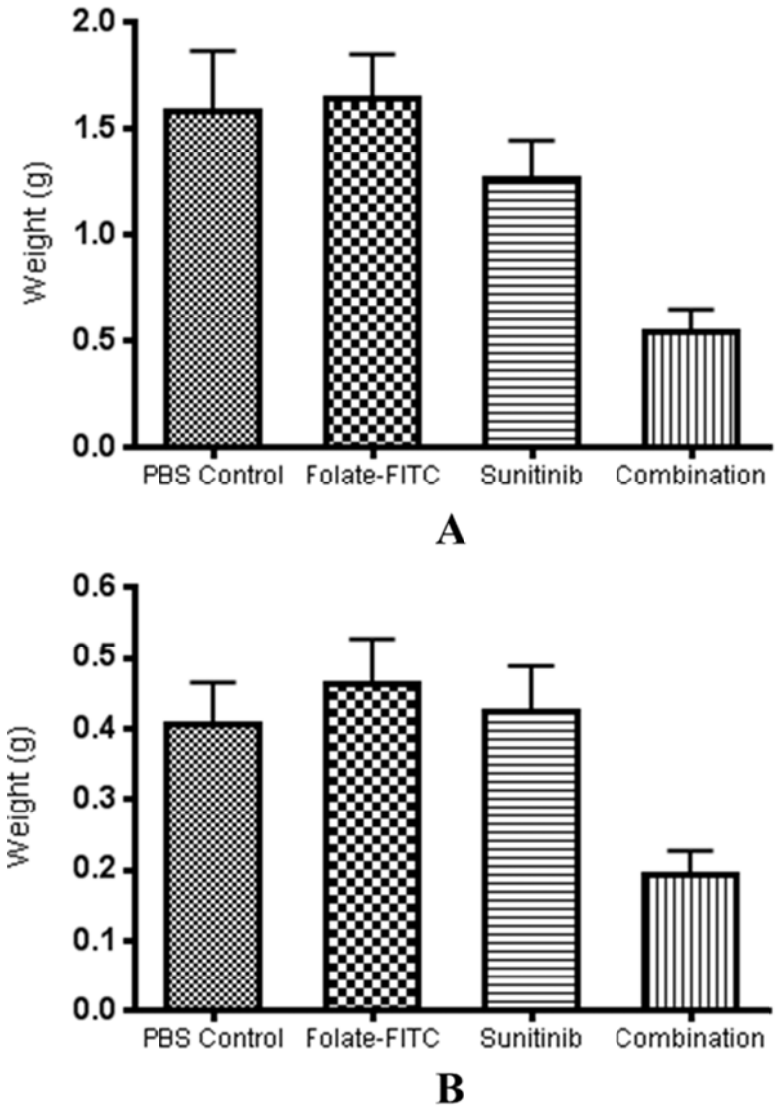

Figure 3.8. Average weights of excised tumors (A) and spleens (B) from L1210A tumor-bearing DBA/2 mice dosed with the indicated therapies. Tumors and spleens were harvested from at least five mice in each treatment group and weighed on a countertop balance. Error bars represent SEM.

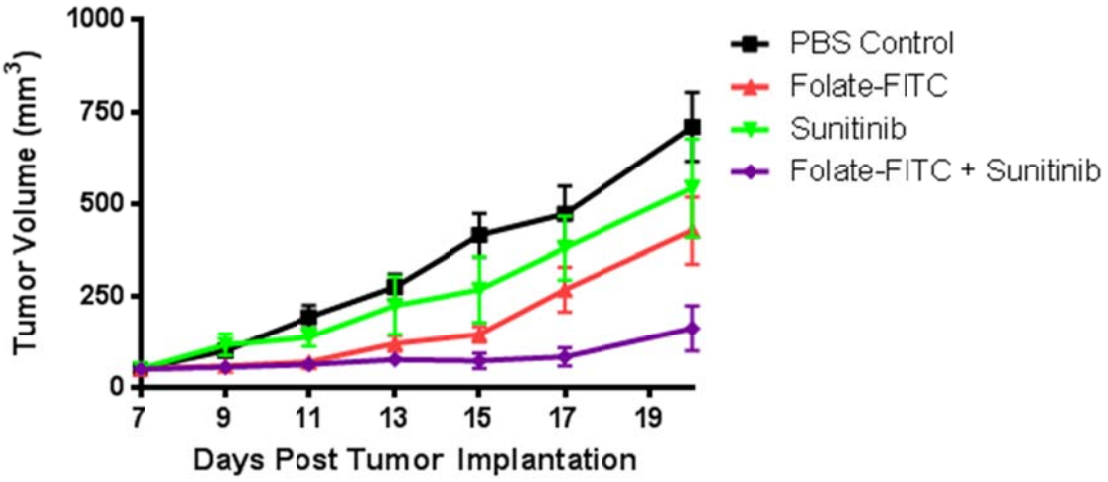

Figure 3.9. Tumor volume graph showing the growth of solid M109 tumors treated with PBS, folate-FITC immunotherapy (500nmol/kg), sunitinib (20mg/kg), or a combination of folate-FITC and sunitinib. Mice were randomized into groups following tumor implantation and treatment was initiated when tumor sizes averaged 50-75mm^3. Each treatment group contained at least 5 mice. Error bars represent SEM.

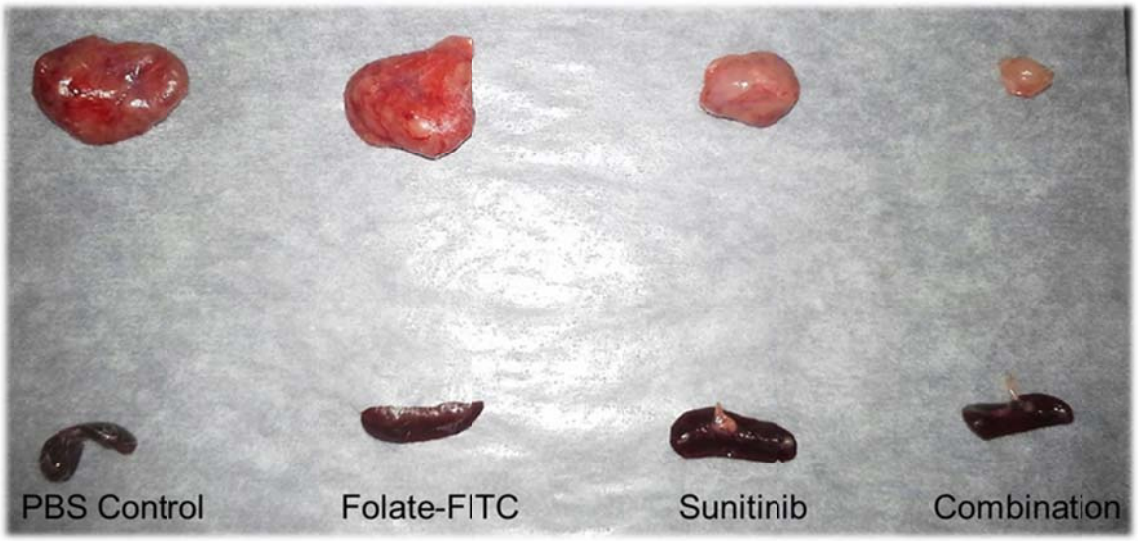

A

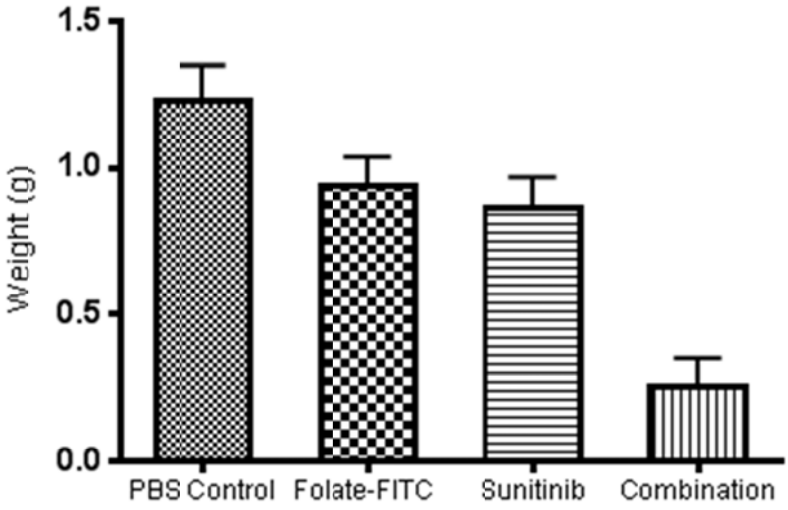

B

Figure 3.10. (A) Resected tumors (top panel) and spleens (bottom panel) from M109 tumor-bearing Balb/c mice dosed with the indicated treatments. As the image shows, mice treated with the combination of folate-FITC and sunitinib have significantly smaller tumors. However, the spleens show little if any variation in size and therefore, indicate that the M109 cells are not as prone to early metastasis as the L1210A cells. (B) Average weights of excised tumors from M109 tumor-bearing Balb/c mice dosed with the indicated therapies. Tumors were harvested from at least five mice in each treatment group and weighed on a countertop balance. Error bars represent SEM.

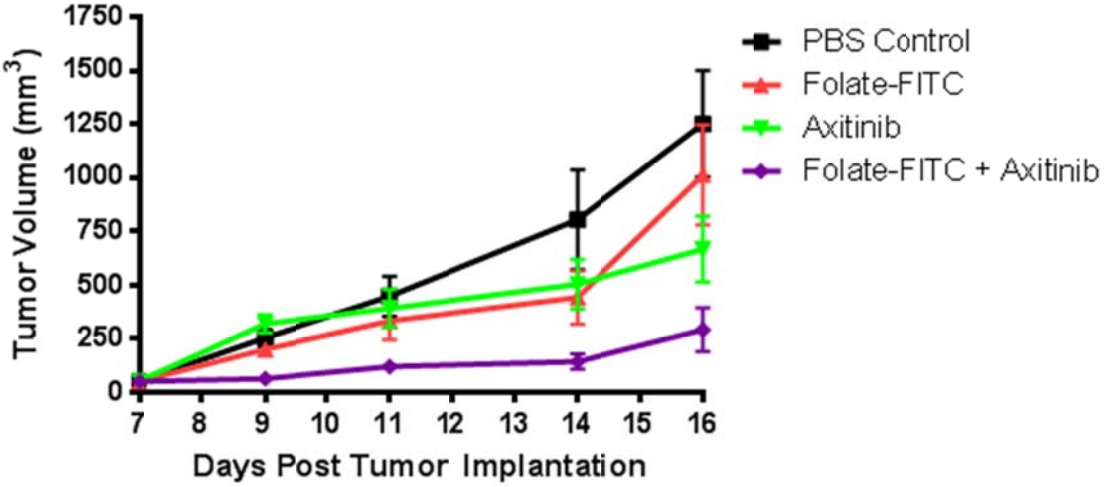

Figure 3.11. Tumor volume graph showing the growth of solid L1210A tumors treated with PBS, folate-FITC immunotherapy (500nmol/kg), axitinib (15mg/kg), or a combination of folate-FITC and axitinib. Mice were randomized into groups following tumor implantation and treatment was initiated when tumor sizes averaged 50-75mm^3. Each treatment group contained at least 5 mice. Error bars represent SEM.

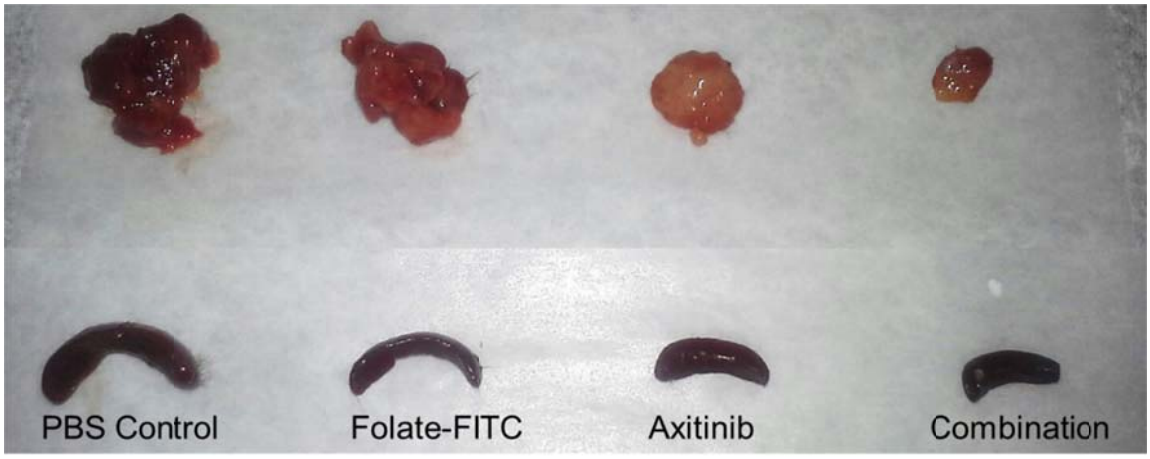

Figure 3.12. Resected tumors (top panel) and spleens (bottom panel) from L1210A tumor-bearing DBA/2 mice dosed with the indicated treatments. As the image shows, mice treated with the combination of folate-FITC and axitinib have significantly smaller tumors. However, the spleens show only a small difference in size between the axitinib and the combination group indicating that axitinib alone is efficient at preventing/slowing metastasis of tumor cells to the spleen.

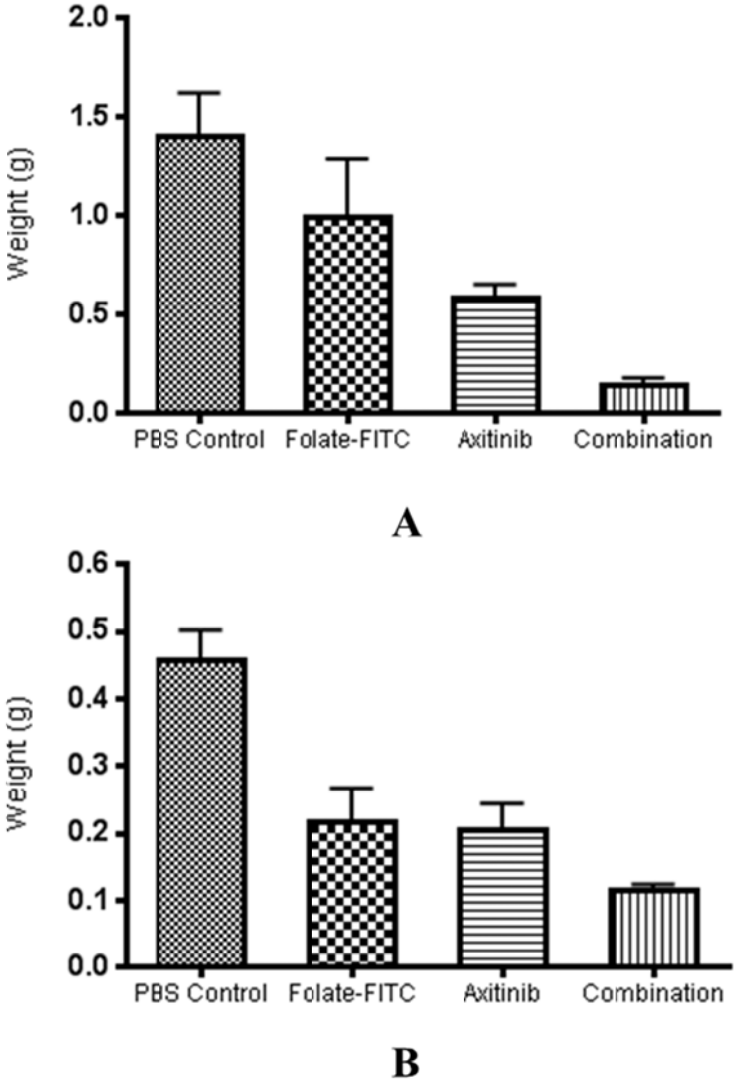

Figure 3.13. Average weights of excised tumors (A) and spleens (B) from L1210A tumor-bearing DBA/2 mice dosed with the indicated therapies. Tumors and spleens were harvested from at least five mice in each treatment group and weighed on a countertop balance. Error bars represent SEM.

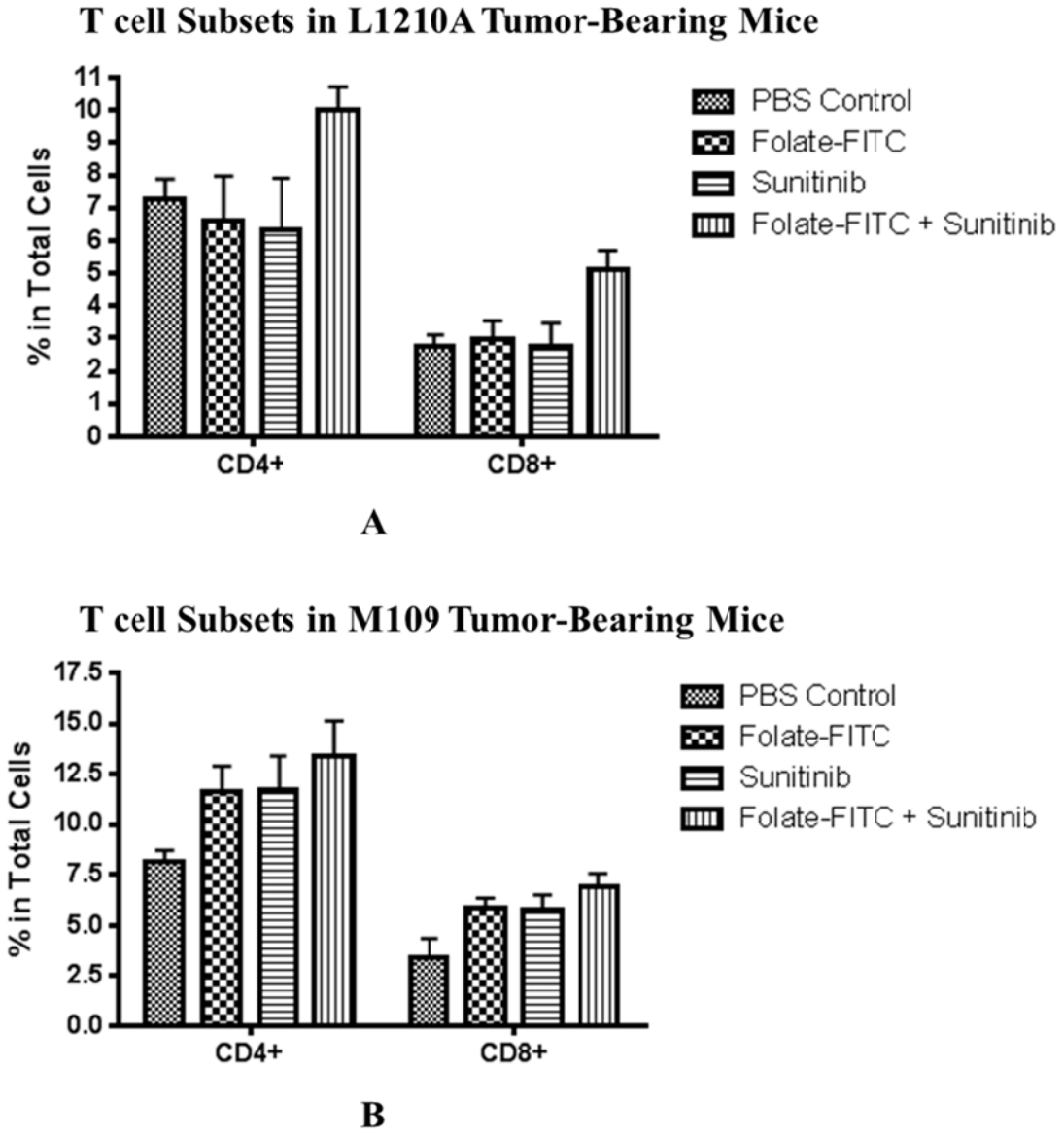

Figure 3.14. CD4+ and CD8+ T cell populations in the spleens of L1210A tumor-bearing DBA/2 mice (A) and M109 tumor-bearing Balb/c mice (B). Spleens were harvested and splenocytes were isolated from different mice in each treatment group followed by staining with appropriate combinations of fluorescently labeled antibodies against CD3, CD4, and CD8. The antibody-labeled cell samples were then analyzed by flow cytometry. 100,000 cells were counted from each sample.

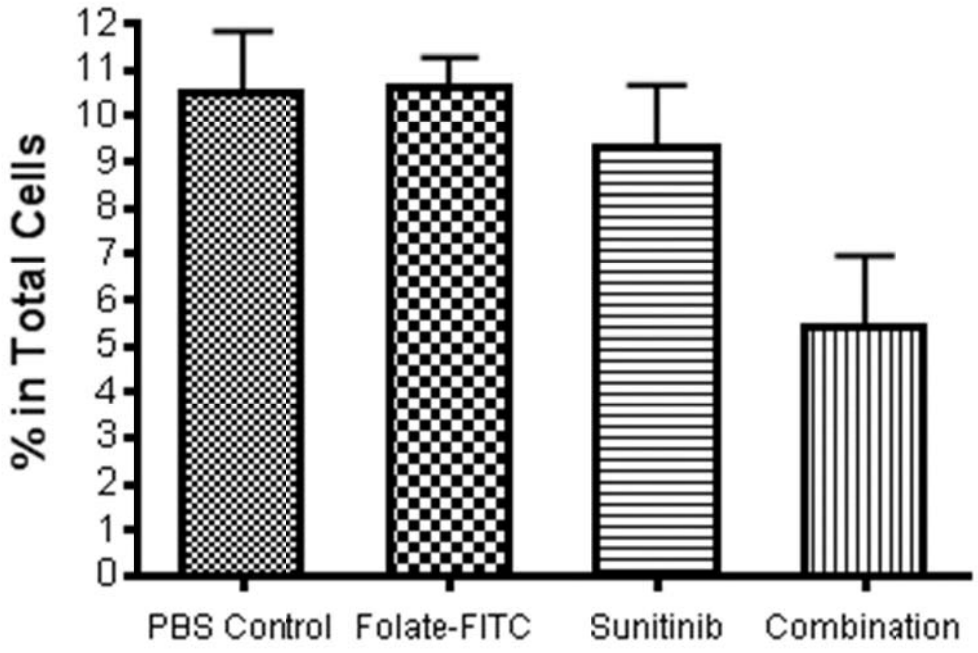

Figure 3.15. Myeloid derived suppressor cell (MDSC) populations in the spleens of M109 tumor-bearing mice dosed with the indicated therapies. Spleens were harvested and splenocytes were isolated from different mice in each treatment group followed by staining with fluorescently labeled antibodies against CD11b and GR-1. The antibody-labeled cell samples were analyzed by flow cytometry. 100,000 cells were counted from each sample.

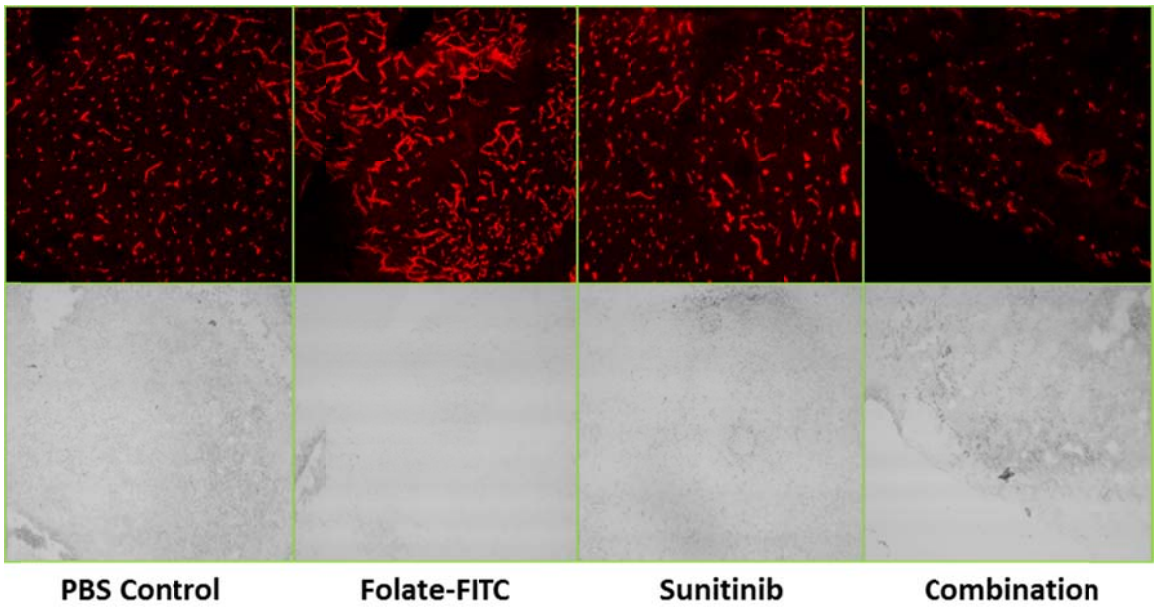

Figure 3.16. Fluorescent staining and imaging of the vasculature within L1210A tumors harvested from DBA/2 mice treated with PBS, folate-FITC, sunitinib, or a combination of folate-FITC and sunitinib. Frozen tissue sections were stained with an anti-CD31 antibody labeled with AlexaFluor 647 and imaged under an Olympus FV1000 confocal microscope using a 10X objective.

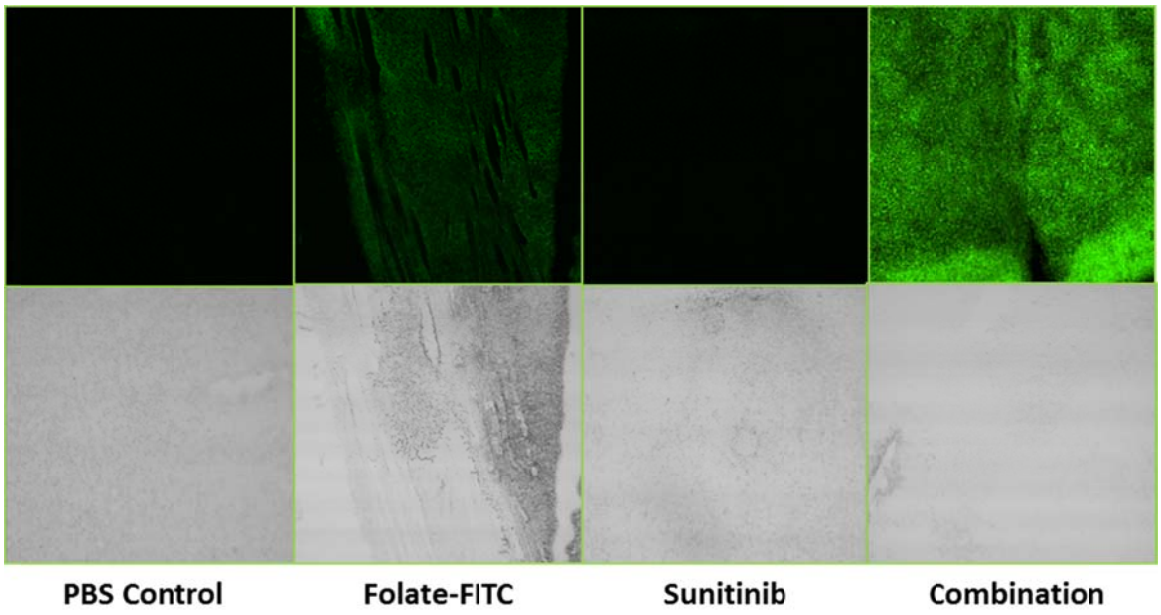

Figure 3.17. Imaging of residual fluorescein labeling due to *in vivo* treatment with folate-FITC within L1210A tumor tissues harvested from mice treated with the indicated therapies. Since only the immunotherapy alone and combination treatment groups were dosed with folate-FITC, only those two groups display tumor-bound fluorescein intensities. Frozen tissue sections from each treatment group were imaged under an Olympus FV1000 confocal microscope using a 10X objective.

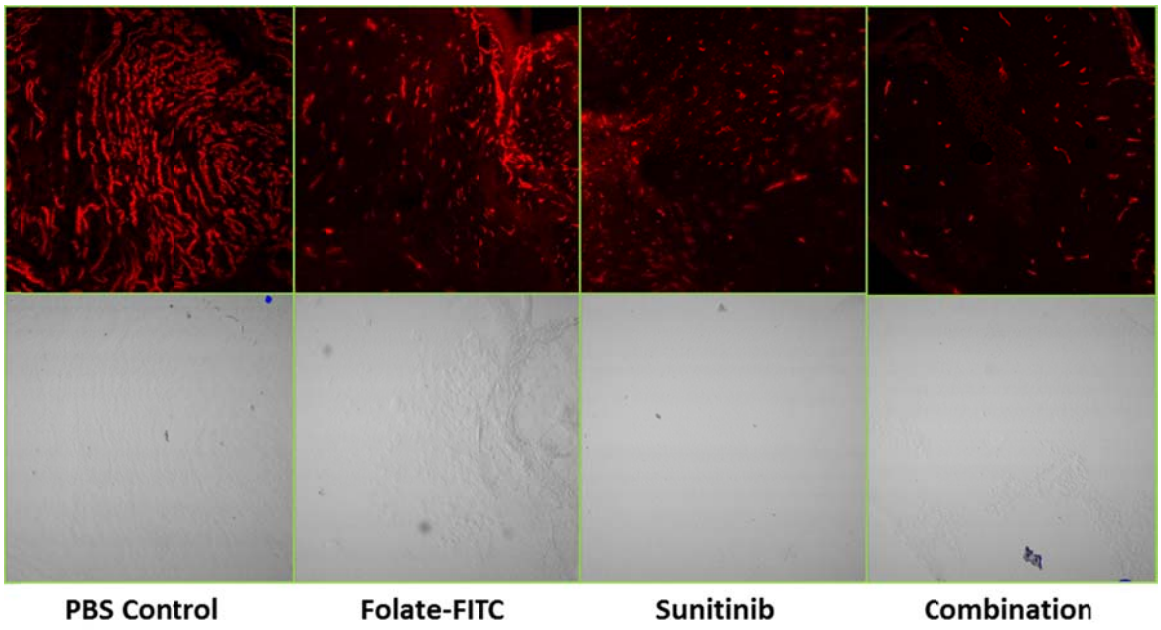

Figure 3.18. Staining and imaging of the vasculature within M109 tumors harvested from Balb/c mice treated with PBS, folate-FITC, sunitinib, or a combination of folate-FITC and sunitinib. Frozen tissue sections were stained with an anti-CD31 antibody labeled with AlexaFluor 647 and imaged under an Olympus FV1000 confocal microscope using a 10X objective.

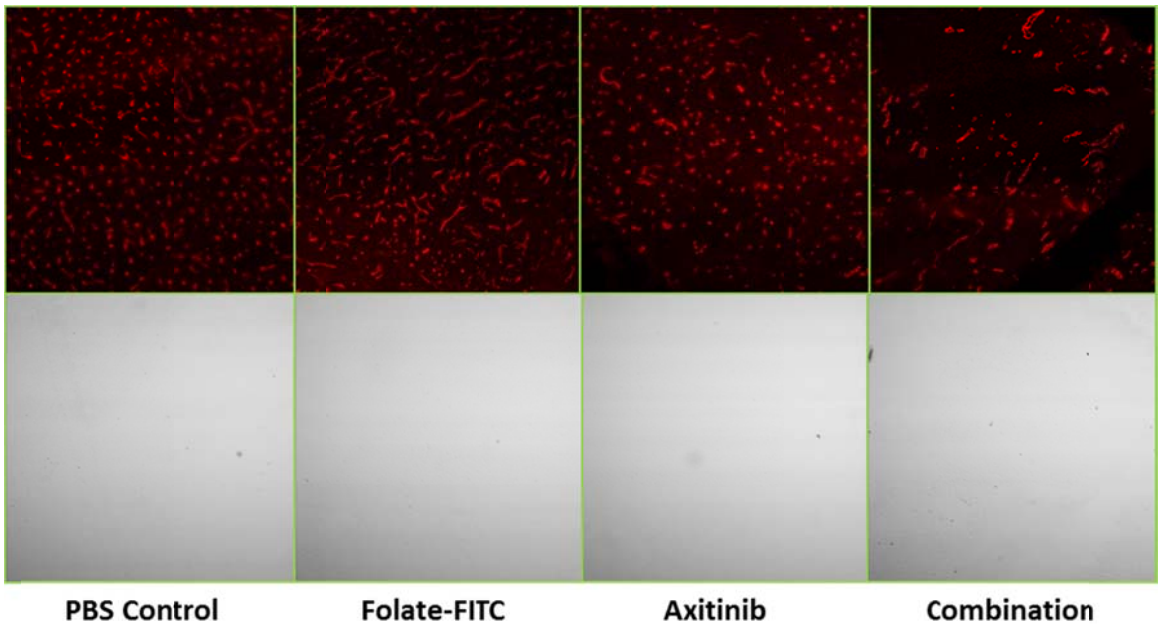

3.19. Fluorescent staining and imaging of the vasculature within L1210A tumors harvested from DBA/2 mice treated with PBS, folate-FITC, axitinib, or a combination of folate-FITC and axitinib. Frozen tissue sections were stained with an anti-CD31 antibody labeled with AlexaFluor 647 and imaged under an Olympus FV1000 confocal microscope using a 10X objective.

CHAPTER 4:

FOLATE-HAPTEN MEDIATED IMMUNOTHERAPY SYNERGIZES WITH ANTIBODY INHIBITORS OF THE T CELL CHECKPOINTS, PD-1 AND CTLA-4, IN MURINE MODELS OF CANCER

4.1 Introduction

The past two decades have marked the dawn of an age of renaissance for cancer immunotherapy. More and more research efforts are being poured into the study and understanding of tumor-associated immunity each year, and consequently, increasing numbers of immunotherapies are regularly entering clinical trials.[1] At this time alone, there are over 600 immunotherapy based clinical trials in the United States and over 1000 globally (ClinicaTrials.gov, NIH). Part of the reason for cancer immunotherapy receiving such serious attention in recent years is the publication of several high-impact articles that have demonstrated the important role that cancer cells play in modulating the body's immune system. In fact, a 2011 sequel to an article originally published in 2000 in *Cell* by Douglas Hanahan and Robert Weinberg lists the ability to evade immune-mediated destruction as an emerging hallmark of cancers.[2] Malignant tumors manage to evade the immune system through a multitude of different mechanisms, the most important of which are: 1) thwarting of cancer antigen processing and presentation, 2) downregulation of immune cell engaging co-receptors, 3) secretion of immune inhibitory factors and chemokines (e.g., IL-10), 4) stimulation of inhibitory receptor expression on immune

cells, and 5) promoting tolerance and apoptosis in host immune cells.[2] Many immunotherapy drugs are, therefore, aimed at combatting one of these immunosuppressive mechanisms. However, because cancers employ a range of techniques to hide from the immune system, most immunotherapies have low success rates when administered as a single therapy and need to be prescribed in combination with another cancer therapeutic.[3,4]

Two of the most recent drugs to receive approval by the US Food and Drug Administration, Yervoy® (2011) and Keytruda® (2014), are inhibitors of immune cell checkpoints and were designed to counteract the immune evasion mechanism 4 listed above. Immune checkpoints play a vital role in the regulation of immune effector cell function by activating negative feedback loops.[5] These two particular drugs target the T cell checkpoint proteins CTLA-4 and PD-1, respectively. Generally, T cells are activated by the interaction between the T cell receptor (TCR) and major histocompatibility complexes (MHCs) on antigen presenting cells (APCs).[6] In order to signal a complete activation of the T cell response, stimulation of CD28 co-receptors on T cells by B7 proteins (CD80/CD86) on APCs is required.[6] Without a co-receptor recognition signal, any T cell activated sorely through a TCR-MHC interaction will become anergic. T cell anergy causes the cell to be functionally inactive even though it has encountered a foreign antigen, but allows the cell to remain alive for a prolonged period in this activated-but-incapacitated state.[7] Since co-receptor signaling is so imperative in T cell activation, the body also utilizes co-receptors as regulators of prolonged activation. Once a T cell has been fully activated against an antigen and begins proliferating, other co-receptors that can downregulate this activation are produced and expressed on their cell surface.[8]

Cytotoxic T-lymphocyte associated protein-4 (CTLA-4) and programmed cell death protein-1 (PD-1) are two such inhibitory co-receptor proteins. CTLA-4 has a higher binding affinity to the B7 complex than CD28 and therefore, competes with CD28 for B7 binding.[8] Once a CTLA-4-B7 interaction has taken place, the T cell receives internal signals to stop proliferating and producing immune-activating cytokines. PD-L1 and PD-L2 are ligands expressed by APCs that interact with the PD-1 receptors newly produced by activated T cells to mediate anergy, cell exhaustion, and apoptosis.[9,10] In healthy animals, these intricate layers of immune regulation are imperative in maintaining a controlled immune response that does not lead to dangerous autoimmune conditions.

Cancer cells display a remarkable ability to recognize the roles that different immune cells play in disease surveillance. They understand the value of inhibitory co-receptors for immune regulation, and therefore, elevate the expression of PD-L1 and PD-L2 on their cell membranes.[11-13] This upregulation makes it difficult to recruit a persistent immune response to the site of tumor since most cytotoxic T cells become inactivated once they encounter a cancer cell expressing ligands to PD-1.[13,14] Therefore, although it would be imprudent to interfere with these regulatory mechanisms in a healthy human, inhibiting the T cell checkpoint interactions has led to promising levels of immune stimulation in cancer patients.[5] Studies in both murine models and humans patients have shown that the administration of monoclonal antibody inhibitors of PD-1 and CTLA-4 lead to an elevated, prolonged, and highly effective anti-tumor response mediated by T cells.[15-20] Checkpoint inhibitor therapies in clinic are approved for the treatment of melanomas and are undergoing clinical trials in lung, bladder, and prostate cancers among several others.[19]

One of the biggest disadvantages to checkpoint inhibitor antibodies is their lack of a tumor-targeting modality. Although the treatment is successful at increasing T cell activation and causing cancer cell death as a result of normal T cell accumulation at disease sites, it is conceivable that the therapy would work well in cohort with a drug that enhances immune cell attraction to the tumor microenvironment. Since folate receptor (FR)-mediated immunotherapy recruits anti-tumor immunity with selectivity and specificity, it was natural to wonder whether these two therapies would synergize in treating FR positive cancers. Folate receptors are known to be overexpressed in a number of important chancers including ovarian, renal, lung, and breast cancers.[21] The receptor is also expressed on some healthy tissues,[21,22] but is inaccessible to FR-targeted drugs in the blood stream due to its expression on the apical, non-blood-facing surface of healthy cells.[23] Therefore, since folic acid binds FR with extremely high affinity (picomolar) and conjugation of folic acid to other chemical and biological compounds only slightly lowers its binding affinity, a large number of folate-conjugates have been developed for cancer imaging and therapy purposes.[24-28]

Folate receptor-mediated immunotherapy works by taking advantage of the body's natural defense mechanisms against infection by pathogens. In this approach, a patient is first immunized against a hapten molecule leading to the development of anti-hapten antibodies, and subsequently treated with a folate-hapten conjugate to mediate tumor recognition by the previously induced antibodies.[29-31] Haptens are generally small, non-toxic molecules that when administered in conjunction with a large carrier protein leads to the stimulation of an immune response.[32] Once an animal has been vaccinated against a hapten, the animal's immune system recognizes any hapten-bound cell as a

danger to self health and mediates its destruction via antibody dependent cellular cytotoxicity (ADCC). Previous experiments with folate-hapten mediated immunotherapy have demonstrated that a strong effector cell response by activated macrophages, NK cells, and cytotoxic T cells is necessary for the successful elimination of FR+ tumor cells.[31,33] Since CTLA-4 and PD-1 checkpoint inhibitors can facilitate an extended activation of cytotoxic T cells that are recruited to the tumor site by folate-hapten mediated immunotherapy and previous studies have shown that FR-targeted immunotherapy is ineffective at eradicating tumors when administered alone,[29] we conducted several experiments to evaluate the therapeutic efficacy of combining these two immunotherapy techniques in FR+ cancer models.

In this chapter, we describe studies focused on evaluating the effect of combining monoclonal antibody inhibitors of CTLA-4 and PD-1 with folate-fluorescein (folate-FITC) immunotherapy in fluorescein vaccinated mice implanted with tumors of two aggressive FR expressing cancer cell lines, M109 and L1210A. The collected data show that T cell checkpoint inhibitors work together with folate-FITC to reduce tumor burden, slow tumor progression, and significantly prolong animal survival.

4.2 Materials and Methods

4.2.1 Antibodies and Reagents

Keyhole limpet hemocyanin (KLH), fluorescein isothiocyanate, SIGMA*FAST*™ OPD substrate tablets, sterile phosphate buffered saline (PBS), and female Balb/c serum were purchased from Sigma Aldrich (St. Louis, MO). Bovine serum albumin conjugated to fluorescein (BSA-FITC), folate-EDA-fluorescein (Folate-FITC, EC17) and the GPI-0100 adjuvant were generously provided by Endocyte, Inc. (West Lafayette, IN). Monoclonal antibodies to mouse CTLA-4/CD152 (clone 9H10) and PD-1 (clone RMP1-14) were obtained from BioXcell (West Lebanon, NH). Gelatin was purchased from Bio-Rad Laboratories (Hercules, CA). The biotin-conjugated goat anti-mouse IgG2a antibody and streptavidin-HRP conjugate was manufactured by Caltag Laboratories (Burlingame, CA). The special folate-deficient diet on which animals in treatment studies were maintained was purchased from Harlan Laboratories (Indianapolis, IN).

4.2.2 Cell Lines and Culture

The folate receptor expressing L1210A cell line was a gift from Dr. Manohar Ratnam, Karmanos Cancer Institute at Wayne State University (Detroit, MI) and Dr. Gerrit Jansen, Department of Oncology at the University Hospital Vrije Universiteid (Amsterdam, Netherlands). M109 cells selected for high FR expression were a generous gift from Dr. Alberto Gabizon, Sharet Institute of Oncology at the Hadassah-Hebrew University Medical Center (Jerusalem, Israel). Both L1210A (lymphocytic leukemia) and M109 (lung cancer) cells were maintained in folate-deficient RPMI 1640 medium

(Invitrogen, Grand Island, NY) supplemented with 10% heat inactivated fetal bovine serum (Sigma Aldrich, St. Louis, MO), penicillin (100 units/mL) and streptomycin (100μg/mL) to ensure maintenance of high FR levels on their cell surface. All cells were cultured at 37°C in a humidified atmosphere containing 5% CO_2. The adherent M109 cells were passaged continuously in a monolayer and the L1210A cells, which grow in suspension were passaged in fresh medium every 3-4 days.

4.2.3 Animals and Tumor Models

M109 tumors were grown in female Balb/c mice which were obtained from Harlan Laboratories (Indianapolis, IN) at 5 to 7 weeks of age. Each mouse weighed approximately 18-20g on arrival. The DBA/2 mice used for L1210A tumor implantation were purchased at 5 to 7 weeks old from either Harlan Laboratories (Indianapolis, IN) or The Jackson Laboratory (Bar Harbor, ME). The DBA/2 mice weighed approximately 16-18g on arrival. Individual animals were identified during therapy by tail markings. All procedures conducted on animals were carried out in strict accordance with protocols approved by the Purdue Animal Care and Use Committee (protocol # 1310000974, High Affinity Ligand Mediated Immunotherapy of Tumors).

4.2.3.1 M109 Tumors

M109 cells grow optimal tumors when implanted into animals at early passage (P0 or P1) and need to be maintained in Balb/c mice periodically in order for the cell line to maintain ability to grow tumors. Therefore, a stock of cryopreserved M109 cells at passage zero was continually kept available for tumor implantation purposes. The cells

were collected directly from solid tumors grown in mice as described in the previous chapter. When preparing to inject tumors, vials of frozen cells were thawed and allowed to grow till confluence in T75 or T150 flasks. Cells were then scraped from the flasks, counted, and suspended in folate-deficient RPMI-1640 medium containing 1% syngeneic female Balb/c serum. Mice were injected in their peritoneal cavity (i.p.) with 5 x 10^5 cells in 100-200µl of total medium. These ascites tumors grow more rapidly than solid tumors injected subcutaneously and untreated mice usually become moribund within 19-23 days of injecting cancer cells. Treatments were started on day 7 following tumor implantation.

4.2.3.2 L1210A Tumors

The original L1210 cell line was derived from a tumor that occurred in a female DBA (subline 212) mouse following skin exposure to 0.2% methylcholanthrene in ether. The L1210A cells used in these experiments were selected for high FR expression by the donors. For tumor implantation, cultured cells were counted and resuspended in serum free sterile PBS and each mouse was injected intraperitoneally with 3 x 10^4 cells. L1210A cells are extremely aggressive and poorly immunogenic, and therefore, proliferate rapidly in this ascetic tumor model. Untreated mice bearing peritoneal L1210A tumors generally do not survive longer than 18-20 days. Treatment was initiated on day 7 following tumor implantation.

4.2.4 Formulation of Therapeutic Antibodies for *in vivo* Administration

In the clinic, melanoma patients receive up to 4 intravenous infusions of the checkpoint antibodies at 3 week intervals. In the published literature describing

evaluation of the antibodies in murine models of cancer, the antibodies are simply diluted in PBS and administered by i.p. injection from whence they are absorbed into circulation. Therefore, for the animal studies conducted to evaluate the checkpoint inhibitor plus folate-FITC immunotherapy, the αCTLA-1 antibody stock received from BioXcell was diluted in sterile PBS to give a final concentration of 100µg in 100µl of solution and the αPD-1 antibody was diluted to give a concentration of either 100µg or 200µg in 100µl of liquid. The stock antibodies were stored in the dark at 4°C and treatment dilutions were prepared fresh on the day of administration. Each mouse was dosed i.p. with 100µl of the appropriate antibody solution.

The folate-FITC (EC17) provided by Endocyte, Inc. was diluted to the desired concentration in sterile PBS. For the survival studies described in this chapter, a 1000 nmols/kg folate-FITC concentration was used to treat animals in the folate-FITC and combination therapy groups. Mice were injected i.p. with 100µL of the conjugate solution. The folate-FITC solutions prepared for animal dosing were divided into daily aliquots and stored in the dark at -20°C. Each aliquot was thawed completely on the day of administration and shaken for even drug distribution before injection into animals.

4.2.5 Induction of Anti-FITC Antibodies and Measurement of Titers

Female Balb/c and DBA/2 mice aged 5-8 weeks (following a week of acclimatization to their new environment) were vaccinated with 35µg KLH-FITC in 50 µg GPI-0100 adjuvant formulated in sterile saline. All mice to be used in treatment studies were immunized every two weeks for a total of three vaccinations. The mice were injected s.c. at sites close to the neck or tail. Blood samples from immunized mice were

collected by submandibular puncture one week after the 2nd and 3rd vaccinations and pooled by cage. Serum was isolated from the collected pooled blood samples by centrifugation and antibody titers were measured by ELISA.

As mentioned in the previous chapter, antibody titers in immunized mouse blood were measured by an established ELISA procedure. Briefly, 96-well ELISA plates were coated with 2μg/well of BSA-FITC by overnight incubation. The plates were then washed and incubated with a freshly prepared 0.2% gelatin solution to block non-specific binding. Following a wash step to remove excess gelatin, the plates were again incubated with a total of 22 2x serial dilutions of pooled anti-FITC mouse serum and pre-immune mouse serum. The serum anti-FITC antibodies that were bound to the BSA coated FITC molecules on the 96-well plate were recognized by incubation with a biotin-conjugated goat anti-mouse IgG2a primary antibody which was subsequently quantified with a streptavidin-HRP conjugate. The assay was completed by exposing the HRP conjugate to a freshly prepared OPD substrate solution. Finally, the plate was read at 490 nm (to measure O.D.) using a 96-well plate reader and the results were plotted as average O.D. versus log serum dilution factor. Each plate was read twice and each serum sample was run in duplicate in order to obtain an average optical density. A representative graph of the antibody titers obtained from one of the mouse studies is shown in figure 4.1.

4.2.6 Combination Therapy Protocols

Since the peak antibody titer in mouse serum is reached approximately 7-10 days following the final immunization, in order to initiate antibody treatment close to this date mice were implanted with peritoneal M109 or L1210A tumors 1-2 days following inoculation with the 3rd vaccination. The day of tumor implantation was designated day 0 for all conducted animal studies. On day 7, mice were randomly distributed among cages and treatment was initiated. At least 5 animals were allocated to each treatment group designated as PBS control, folate-FITC immunotherapy, αCTLA-4 antibody alone, αPD-1 antibody alone, combination of folate-FITC plus αCTLA-4 antibody, or combination of folate-FITC plus αPD-1 antibody. Mice in the PBS control group were injected with 100μL (i.p.) of sterile PBS 5 days per week. Mice treated with folate-FITC alone were injected with 100μL (i.p.) of thawed 1000 nmol/kg folate-FITC solution. The immunotherapy was administered on a 5 days on 2 days off schedule. The two groups of mice treated with each individual checkpoint inhibitor alone were injected with 100μL volumes of the appropriate antibody concentration on days 7, 10, and 13. Each L1210A or M109 tumor-bearing mouse in the αCTLA-4 antibody group received 100μg of the antibody per injected dose. However, L1210A tumor-bearing DBA/2 mice in the αPD-1 antibody group received 200μg of the antibody per injected dose whereas the M109 tumor-bearing Balb/c mice in the same group received only 100μg of the antibody. All treatments were administered according to the designated schedule until the mice showed clear signs of terminal disease burden. Mice fed on regular chow are known to have extremely high serum folate concentration, so in order to reduce folate levels to those

comparable with healthy humans, all mice in treatment studies were placed on a folate deficient diet three weeks prior to initiation of therapy.

4.2.7 Measurement of Treatment Group Survival

All treated mice were closely monitored on a daily basis for signs of distress associated with the ascetic tumors. The two strains of mice displayed very different signs of morbidity. Balb/c mice injected with M109 tumors were considered moribund when they had lost ~20% of their starting body weight or had extremely scruffy fur, were lethargic, and had loose stool. In contrast, L1210A tumor-bearing DBA/2 mice were considered terminal when their peritoneum became swollen due to extensive fluid buildup and the mice showed signs of scruffiness and extreme lethargy by hunching in a corner of the cage. Once a mouse was determined moribund, it was euthanized immediately by CO_2 asphyxiation. The number of days from tumor implantation to euthanasia or death for each mouse was recorded and plotted on a survival graph.

4.2.8 Data Analysis

Graphing and certain statistical calculations of the collected data from all the animal experiments were performed using the survival measurement tool in GraphPad Prism software.

4.3 Results

4.3.1 Anti-FITC Antibody Response in Immunized Mice

A robust antibody response is critical for the success of folate-hapten mediated immunotherapy. Therefore, before implantation of tumors, mice in each experiment were immunized three times at two week intervals with a KLH-FITC plus GPI-0100 (adjuvant) cocktail. Following the second immunization in all cases and sometimes also the third immunization, blood was collected from each mouse by a small submandibular puncture and anti-FITC antibody titers were assessed by ELISA. For comparison purposes, blood was also collected from a mouse that had never been immunized with the KLH-FITC cocktail and assayed for anti-FITC titer levels. The graph shown in figure 4.1 shows that a significantly elevated anti-FITC titer is present in all groups of immunized mice (blood was collected from all mice in a cage and pooled for ELISA analysis). These results reconfirm previous studies that established KLH-FITC plus GPI-0100 vaccination as a combination capable of inducing a strong and lasting antibody response.

4.3.2 Antibody Inhibitors of PD-1 Synergize with Folate-Hapten Mediated Immunotherapy in the Ascitic L1210A Tumor Model

Previous publications from the lab have described the requirement of a cytotoxic T cell component for the mediation of a successful therapeutic response by folate-hapten immunotherapy.[31,33] As mentioned in the Introduction, some of the T cells recruited to the tumor site by folate-hapten immunotherapy are likely being inactivated by immunosuppressive receptors expressed by the cancer cells. Therefore, in order to

evaluate whether antibodies that inhibit the interaction between these receptors and the checkpoint proteins on activated T cells would augment the therapeutic efficacy of FR-mediated immunotherapy, syngeneic tumors were grown in mice with an intact immune system capable of responding to modulation of its components. The L1210A lymphocytic leukemia cell line was selected for initial studies because it is known to be a highly aggressive tumor model that is difficult to treat with most folate-conjugates and therefore, an indication of success in this cell line would encourage further evaluation of the combination in other tumors. Ascitic L1210A tumors were implanted in female DBA/2 mice as described in the Materials and Methods section and treated with either folate-FITC or αPD-1 antibody alone or a combination of both. As shown in figure 4.2A, DBA/2 mice injected i.p. with L1210A cancer cells and treated with only PBS rapidly developed symptoms of terminal illness and had to be euthanized (median survival ~20 days). Interestingly, neither folate-FITC nor the αPD-1 antibody managed to slow the progression of disease at the administered doses and the mice in those treatment groups were also euthanized within a few days of the mice in the PBS group. In contrast, the group of mice that were treated with both folate-FITC and αPD-1 antibody (indicated by ▲ on the graph) lived, on average, 10 days longer than the mice in the other treatment groups with survival extending beyond 40 days for two of the mice. This remarkable synergy observed in a difficult to treat tumor model was indicative of a combination therapy that would be potent against FR+ cancers in human patients.

4.3.3 Antibody Inhibitors of CTLA-4 Synergize with Folate-Hapten Mediated Immunotherapy in the Ascitic L1210A Tumor Model

In addition to PD-1, activated T cells express another protein, the cytotoxic T lymphocyte associated antigen 4, which also mediates the regulation of their activity.[8] These proteins compete for recognition of the co-stimulatory receptors on APCs and once bound, signal the T cell to shut down production of cytokines and become anergic. Since combination with an αPD-1 antibody enhanced the therapeutic efficacy of folate-FITC immunotherapy so dramatically, it was possible that an antibody inhibitor of the CTLA-4 protein would also yield similar therapeutic results. As seen in figure 4.2B, the αCTLA-4 antibody behaved very similar to αPD-1 antibody when administered alone and only prolonged life in the treated mice by a few days. As anticipated, the combination of folate-FITC therapy plus αCTLA-4 antibody significantly extended survival of L1210A tumor-bearing DBA/2 mice, but was not as successful as the earlier described combination with the αPD-1 antibody (figure 4.3). However, the results from this experiment, together with the previous study, confirm the original hypothesis that T cell checkpoint inhibitors would be potent companion therapies to folate-hapten mediated immunotherapy.

4.3.4 Antibody Inhibitors of PD-1 Only Slightly Augment Animal Survival when Combined with Folate-Hapten Immunotherapy in the Ascitic M109 Tumor Model

Since folate receptors are upregulated by a number of different cancers in humans, in order to conclude that any drug combination would be a good candidate for treating these FR+ tumors the therapeutic efficacy needs to be established in more than one *in vivo* model. Therefore, M109 ascites were grown in female Balb/c mice as

previously described and the animals were allocated randomly to groups that were treated with PBS, folate-FITC, αPD-1 antibody, or both folate-FITC and αPD-1 antibody. As demonstrated by the survival graph in figure 4.4A, the Balb/c mice treated with PBS (⊥) and folate-FITC alone (▼) start to become moribund around day 20 and are euthanized within days of each other. The surprising results from the other two treatment groups show that that even though the αPD-1 antibody enhances survival of these M109 tumor-bearing mice, the combination of folate-FITC with αPD-1 antibody does little to improve upon that survival. The mice treated with the combination therapy (▲) display symptoms of terminal illness within 2-3 days of the mice treated with the checkpoint inhibitor antibody alone (●). These data contradict the findings of the study conducted with L1210A tumor-carrying DDA/2 mice which responded with synergistic survival rates when dosed with the same two therapies and could indicate a mouse strain-specific reason for the diminished therapeutic synergy.

4.3.5 Antibody Inhibitors of CTLA-4 Synergize with Folate-Hapten Mediated Immunotherapy in the Ascitic M109 Tumor Model

As the experiment to evaluate the combination of folate-FITC immunotherapy with αPD-1 antibody therapy on M109 tumors were still underway, different groups of mice were concurrently treated with either αCTLA-4 antibody alone or in addition to folate-FITC treatments. Since the αPD-1 antibody component did not appear to be positively augmenting the folate-FITC immunotherapy in the combination treated mice, it was anticipated that similar results would be observed in mice dosed with the αCTLA-4 antibody plus folate-FITC co-therapy. However, the unexpected results from this

experiment indicate that although the antibody therapy alone has an effect in enhancing survival, the combination therapy is emphatically more potent at controlling tumor growth and extending animal survival than either of the two individual therapies (figure 4.4B). Moreover, as shown in figure 4.4, the individually administered αCTLA-4 antibody is no better at slowing tumor progression than the individually dosed αPD-1 antibody suggesting that the dramatic synergy observed during the folate-FITC plus αCTLA-4 antibody therapy must result from variations in the immune cell composition and the specific make-up of the T cells in this particular strain of mice carrying this particular type of tumor.

4.4 Discussion

In an ideal situation, abnormal proteins from established tumors would be recognized and processed by infiltrating antigen presenting cells in the body early in the tumor's development. These proteins would then be displayed on MHC proteins for recognition by circulating T cells, which would become activated, proliferate, and release immune-stimulatory cytokines.[6] However, such normal pro-inflammatory functions are dramatically suppressed in tumors and the cancer cells evade recognition and destruction by immune effector cells.[2] Cytotoxic T cells play an imperative role in the elimination of malignant cells in the body by promoting recruitment of other immune cells to the site of disease and by the calcium-dependent release of cell lytic granules that mediate the death of unhealthy cells.[6] In order to avoid immune-mediated cell death, cancer cells express receptors that inactivate T cells before they can unleash their apoptosis mechanisms.

In FR-mediated immunotherapy, cancer cells are decorated with hapten-bound autologous antibodies which can be recognized by F_c receptors on phagocytic macrophages and NK cells. The cytotoxic T cell response associated with folate-hapten immunotherapy is mediated by the presentation of antigens derived from the cells that were destroyed by the aforementioned macrophages and NK cells. Therefore, since the tumor microenvironment's ability to suppress recruitment of macrophages and NK cells to the site of tumor is directly counteracted by folate-hapten immunotherapy, a therapy that enhances anti-tumor T cell activity is likely to be a potent companion to folate-hapten immunotherapy.

Although checkpoint inhibitor antibodies are currently showing therapeutic efficacy during clinical trials in a range of solid tumors,[19,34] in murine models of solid tumors the drugs have little impact in slowing tumor growth. Therefore, in order to evaluate whether these antibody inhibitors of CTLA-4 and PD-1 would combine well with folate-fluorescein immunotherapy, the therapies were evaluated in ascites models of syngeneic murine cancers. As demonstrated by L1210A tumor studies, the mice treated with a combination of either checkpoint inhibitor with folate-fluorescein display significantly prolonged survival than those dosed with only a single drug. These results confirm the hypothesis that blocking the interaction between CTLA-4 and CD28 and PD-1 and PD-L1/PD-L2 results in a rather potent cytotoxic T cell response that aids the tumor infiltrating macrophages and NK cells to further mediate cell death. We then attempted to reproduce these results in a different FR+ tumor model, and evaluated the folate-fluorescein plus checkpoint inhibitor combination in ascitic M109 tumors. Even though these tumors are known to be more immunogenic than L1210A tumors, the

collected data surprisingly indicated that only the anti-CTLA-4 antibody synergizes with folate-fluorescein immunotherapy. However, both the anti-CTLA-4 and the anti-PD-1 therapies were able to prolong survival when administered alone better than folate-fluorescein alone. These unexpected results are difficult to explain without further exploration into the differences in nature of *in vivo* tumor growth between L1210A and M109 cells. It could be the case that M109 cells express less PD-L1 and PD-L2 than L1210A tumors, and therefore, blocking of PD-1 receptors has only a small effect on overall T cell activation against this particular tumor model. The minor therapeutic success demonstrated by anti-PD-1 antibody single therapy on M109 tumors does not appear to be enough to enhance the folate-hapten mediated ADCC response in the combination therapy. Alternatively, the discrepancy could be explained by a difference between the mouse strains; T cells derived from Balb/c mice may express lower PD-1 levels than T cells from DBA/2 mice.

In summary, further delving into the makeup of the tumor microenvironment in animals treated with the different drugs and combination will be necessary to better answer the questions arising from these results. We can, nevertheless, conclude that certain T cell checkpoint inhibitors synergize with folate-hapten mediated immunotherapy to decrease tumor burden, delay tumor progression, and prolong survival in treated FR+ tumor-bearing animals.

4.5 References

1 Mellman, I., Coukos, G. & Dranoff, G. Cancer immunotherapy comes of age. *Nature* **480**, 480-489 (2011).

2 Hanahan, D. & Weinberg, R. A. Hallmarks of cancer: the next generation. *Cell* **144**, 646-674 (2011).

3 Melero, I., Grimaldi, A. M., Perez-Gracia, J. L. & Ascierto, P. A. Clinical development of immunostimulatory monoclonal antibodies and opportunities for combination. *Clinical Cancer Research* **19**, 997-1008 (2013).

4 Vanneman, M. & Dranoff, G. Combining immunotherapy and targeted therapies in cancer treatment. *Nature reviews cancer* **12**, 237-251 (2012).

5 Pardoll, D. M. The blockade of immune checkpoints in cancer immunotherapy. *Nature reviews cancer* **12**, 252-264 (2012).

6 Janeway, C. A., Travers, P., Walport, M. & Shlomchik, M. J. Immunobiology. (2001).

7 Schwartz, R. H. T Cell Anergy*. *Annual review of immunology* **21**, 305-334 (2003).

8 Alegre, M.-L., Frauwirth, K. A. & Thompson, C. B. T-cell regulation by CD28 and CTLA-4. *Nature Reviews Immunology* **1**, 220-228 (2001).

9 Latchman, Y. *et al.* PD-L2 is a second ligand for PD-1 and inhibits T cell activation. *Nature immunology* **2**, 261-268 (2001).

10 Francisco, L. M. *et al.* PD-L1 regulates the development, maintenance, and function of induced regulatory T cells. *The Journal of experimental medicine* **206**, 3015-3029 (2009).

11 Blank, C. & Mackensen, A. Contribution of the PD-L1/PD-1 pathway to T-cell exhaustion: an update on implications for chronic infections and tumor evasion. *Cancer Immunology, Immunotherapy* **56**, 739-745 (2007).

12 Konishi, J. *et al.* B7-H1 expression on non-small cell lung cancer cells and its relationship with tumor-infiltrating lymphocytes and their PD-1 expression. *Clinical Cancer Research* **10**, 5094-5100 (2004).

13 Blank, C., Gajewski, T. F. & Mackensen, A. Interaction of PD-L1 on tumor cells with PD-1 on tumor-specific T cells as a mechanism of immune evasion: implications for tumor immunotherapy. *Cancer Immunology, Immunotherapy* **54**, 307-314 (2005).

14 Ahmadzadeh, M. *et al.* Tumor antigen–specific CD8 T cells infiltrating the tumor express high levels of PD-1 and are functionally impaired. *Blood* **114**, 1537-1544 (2009).

15 Curran, M. A., Montalvo, W., Yagita, H. & Allison, J. P. PD-1 and CTLA-4 combination blockade expands infiltrating T cells and reduces regulatory T and myeloid cells within B16 melanoma tumors. *Proceedings of the National Academy of Sciences* **107**, 4275-4280 (2010).

16 Duraiswamy, J., Kaluza, K. M., Freeman, G. J. & Coukos, G. Dual blockade of PD-1 and CTLA-4 combined with tumor vaccine effectively restores T-cell rejection function in tumors. *Cancer research* **73**, 3591-3603 (2013).

17 Hurwitz, A. A. *et al.* Combination immunotherapy of primary prostate cancer in a transgenic mouse model using CTLA-4 blockade. *Cancer research* **60**, 2444-2448 (2000).

18 Peggs, K. S., Quezada, S. A., Chambers, C. A., Korman, A. J. & Allison, J. P. Blockade of CTLA-4 on both effector and regulatory T cell compartments contributes to the antitumor activity of anti–CTLA-4 antibodies. *The Journal of experimental medicine* **206**, 1717-1725 (2009).

19 Topalian, S. L. *et al.* Safety, activity, and immune correlates of anti–PD-1 antibody in cancer. *New England Journal of Medicine* **366**, 2443-2454 (2012).

20 Van Elsas, A., Hurwitz, A. A. & Allison, J. P. Combination immunotherapy of B16 melanoma using anti–cytotoxic T lymphocyte–associated antigen 4 (Ctla-4) and granulocyte/macrophage colony-stimulating factor (Gm-Csf)-producing vaccines induces rejection of subcutaneous and metastatic tumors accompanied by autoimmune depigmentation. *The Journal of experimental medicine* **190**, 355-366 (1999).

21 Parker, N. *et al.* Folate receptor expression in carcinomas and normal tissues determined by a quantitative radioligand binding assay. *Analytical biochemistry* **338**, 284-293 (2005).

22 Elnakat, H. & Ratnam, M. Distribution, functionality and gene regulation of folate receptor isoforms: implications in targeted therapy. *Advanced drug delivery reviews* **56**, 1067-1084 (2004).

23 Low, P. S., Henne, W. A. & Doorneweerd, D. D. Discovery and development of folic-acid-based receptor targeting for imaging and therapy of cancer and inflammatory diseases. *Accounts of chemical research* **41**, 120-129 (2007).

24 Ayala-López, W., Xia, W., Varghese, B. & Low, P. S. Imaging of atherosclerosis in apoliprotein e knockout mice: targeting of a folate-conjugated radiopharmaceutical to activated macrophages. *Journal of Nuclear Medicine* **51**, 768-774 (2010).

25 Reddy, J. A. *et al.* In Vivo Structural Activity and Optimization Studies of Folate−Tubulysin Conjugates. *Molecular pharmaceutics* **6**, 1518-1525 (2009).

26 Reddy, J. A. & Low, P. S. Folate-mediated targeting of therapeutic and imaging agents to cancers. *Critical Reviews™ in Therapeutic Drug Carrier Systems* **15** (1998).

27 Turk, M. J. *et al.* Folate-targeted imaging of activated macrophages in rats with adjuvant-induced arthritis. *Arthritis & Rheumatism* **46**, 1947-1955 (2002).

28 Wang, S. *et al.* Design and synthesis of [111In] DTPA-folate for use as a tumor-targeted radiopharmaceutical. *Bioconjugate chemistry* **8**, 673-679 (1997).

29 Lu, Y. & Low, P. S. Folate targeting of haptens to cancer cell surfaces mediates immunotherapy of syngeneic murine tumors. *Cancer Immunology, Immunotherapy* **51**, 153-162 (2002).

30 Lu, Y. & Low, P. S. Immunotherapy of folate receptor-expressing tumors: review of recent advances and future prospects. *Journal of Controlled Release* **91**, 17-29 (2003).

31 Lu, Y., Sega, E., Leamon, C. P. & Low, P. S. Folate receptor-targeted immunotherapy of cancer: mechanism and therapeutic potential. *Advanced drug delivery reviews* **56**, 1161-1176 (2004).

32 Erkes, D. A. & Selvan, S. R. Hapten-Induced Contact Hypersensitivity, Autoimmune Reactions, and Tumor Regression: Plausibility of Mediating Antitumor Immunity. *Journal of Immunology Research* **2014** (2014).

33 Sega, E. I. *Folate Receptor Targeted immunotherapy of Cancer: Mechanism of Action and Augmentation of Therapeutic Efficacy* Doctor of Philosophy thesis, Purdue University, (2006).

34 Callahan, M. K. & Wolchok, J. D. At the Bedside: CTLA-4- and PD-1-blocking antibodies in cancer immunotherapy. *Journal of Leukocyte Biology* **94**, 41-53, doi:10.1189/jlb.1212631 (2013).

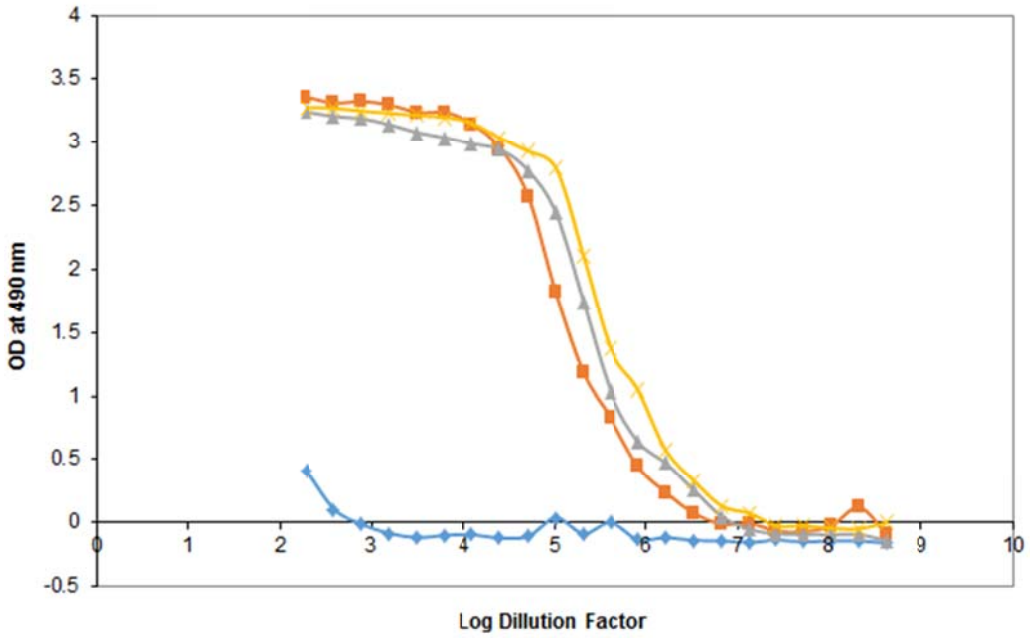

Figure 4.1. Anti-FITC antibody titers determined for KLH-FITC + GPI-0100 immunized Balb/c mice following the 2nd immunization. Blood was collected from mice in individual cages and pooled together for analysis. The orange, grey, and yellow lines represent titers determined with pooled blood from 3 different cages of immunized mice and the blue line represents the anti-FITC antibody titer in blood collected from non-immunized mice. The titers shown here are graphed using optical density measurements obtained at 490nm vs. Log_{10} of the dilution factor.

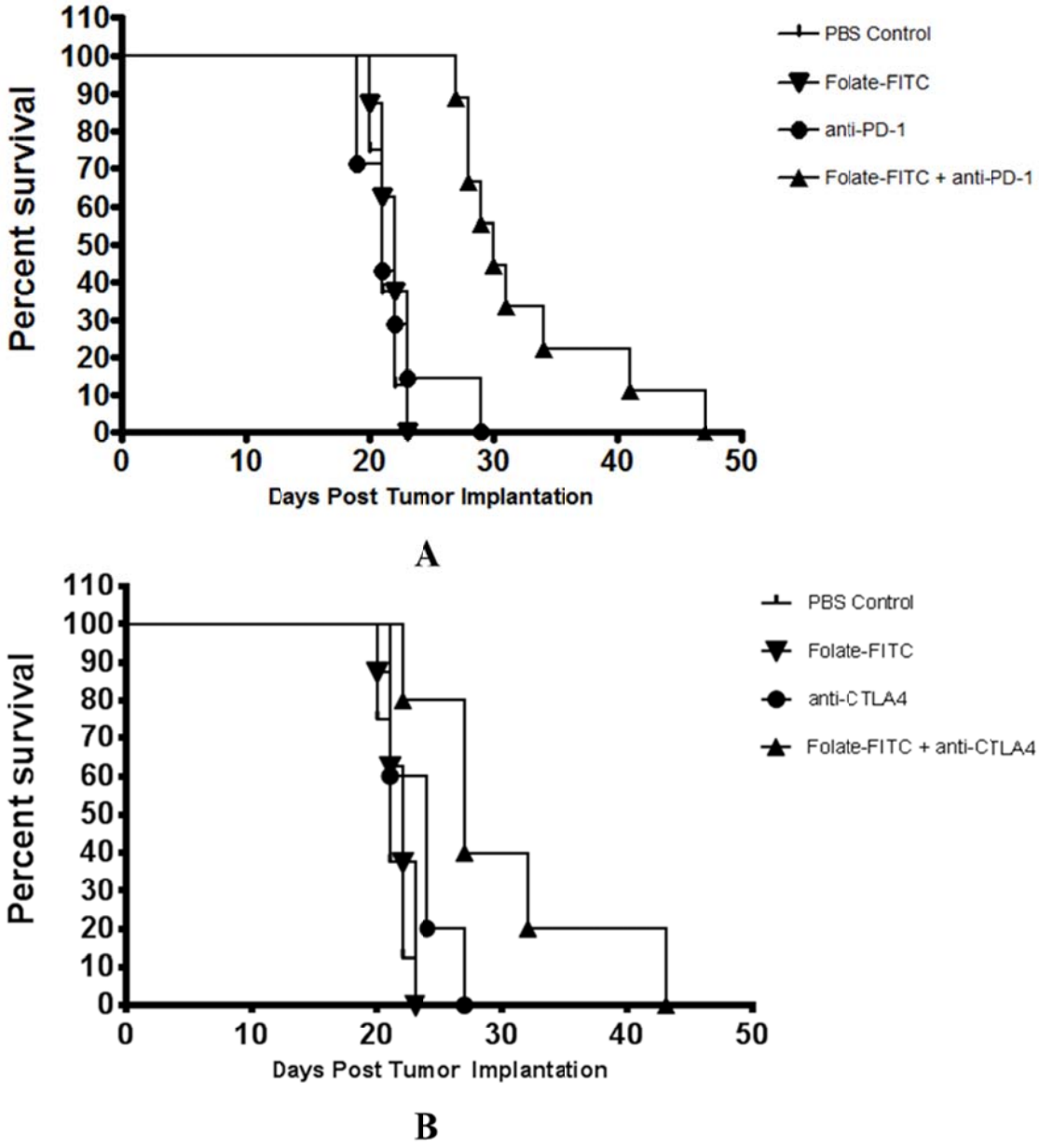

Figure 4.2. Survival measurements of mice bearing intraperitoneal L1210A tumors treated with PBS, folate-FITC immunotherapy (1000nmol/kg), anti-PD-1 antibody (200μg), or a combination of folate-FITC + anti-PD-1 antibody (A) and mice treated with PBS, folate-FITC (1000nmol/kg), anti-CTLA-4 antibody (100μg) or a combination of folate-FITC + anti-CTLA-4 antibody (B).

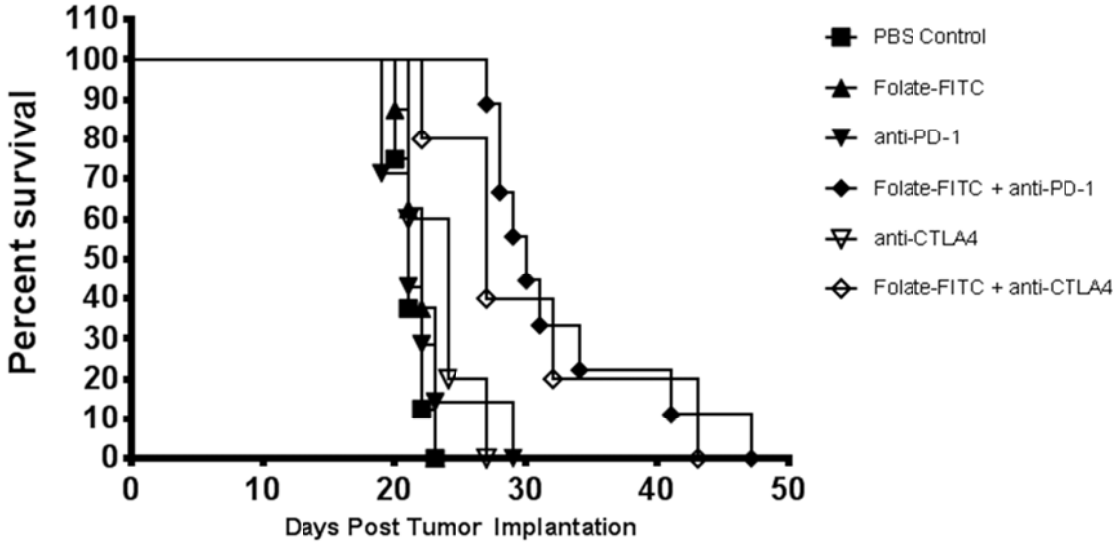

Figure 4.3. Graph of survival data comparing the differences in therapeutic efficacy of combining either anti-PD-1 antibody or anti-CTLA-4 antibody with folate-FITC mediated immunotherapy in the ascitic L1210A tumor model.

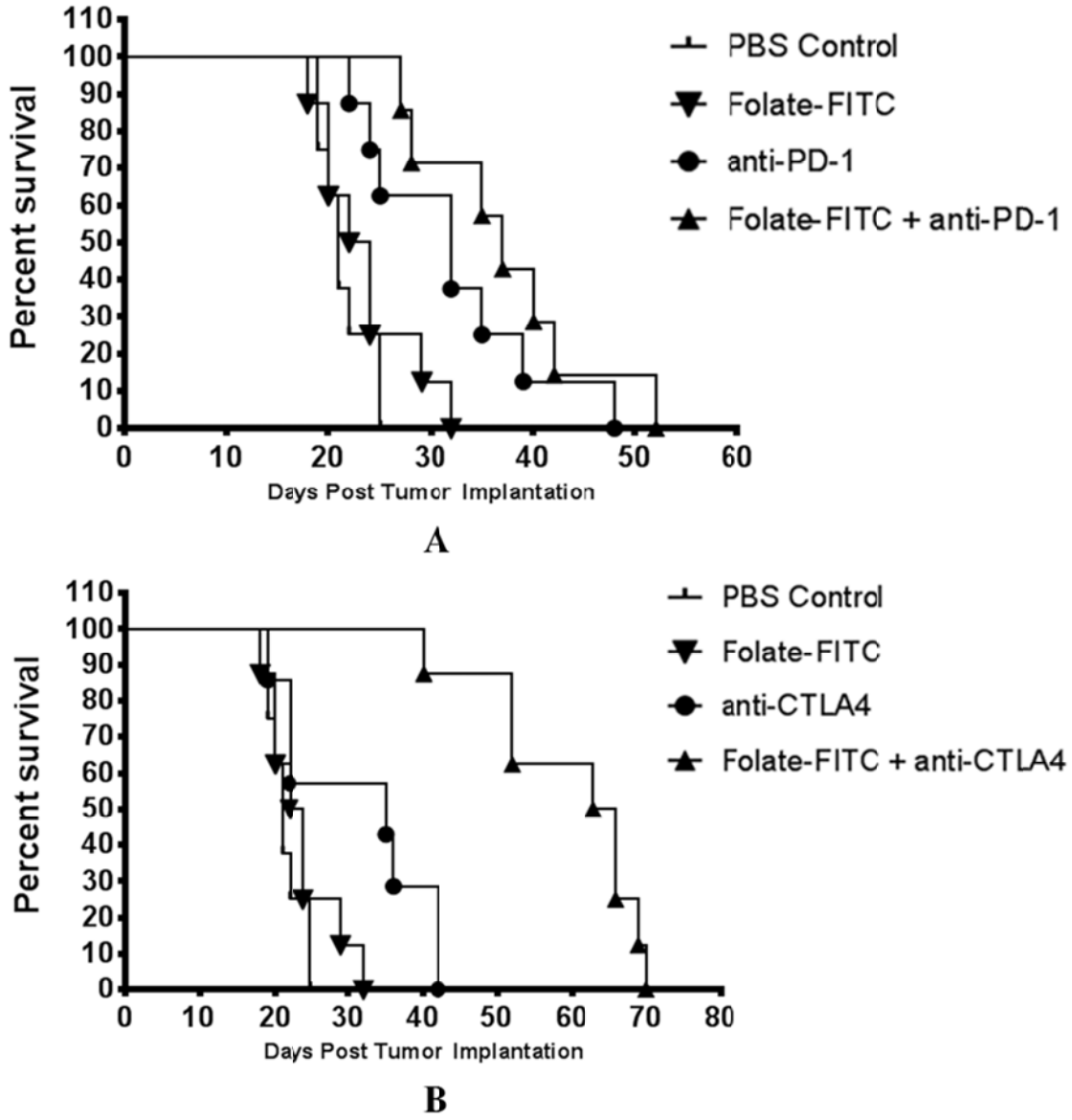

Figure 4.4. Survival measurements of Balb/c mice bearing intraperitoneal M109 tumors treated with PBS, folate-FITC immunotherapy (1000nmol/kg), anti-PD-1 antibody (100μg), or a combination of folate-FITC + anti-PD-1 antibody (A) and mice treated with PBS, folate-FITC (1000nmol/kg), anti-CTLA-4 antibody (100μg) or a combination of folate-FITC + anti-CTLA-4 antibody (B).

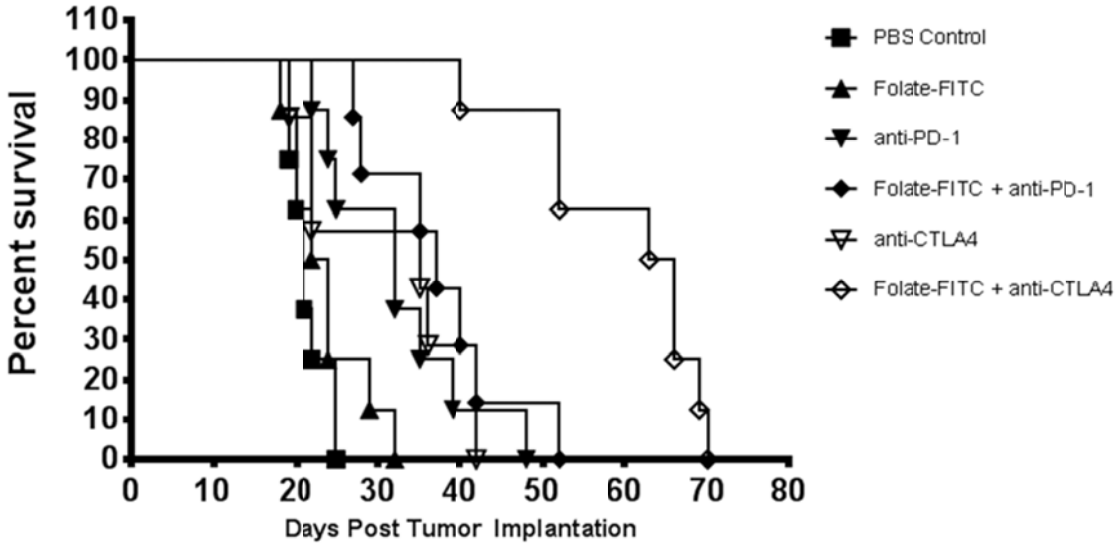

Figure 4.5. Graph of survival data comparing the differences in therapeutic efficacy of combining either anti-PD-1 antibody or anti-CTLA-4 antibody with folate-FITC mediated immunotherapy in the ascitic M109 tumor model. The graph demonstrates the clear superiority of the anti-CTLA-4 antibody in modulating T cell activation against this tumor model.

CHAPTER 5:

TARGETING THE SOMATOSTATIN AND CCR5 RECEPTORS FOR CANCER IMAGING AND THERAPY

5.1 Introduction

A number of cell surface receptors expressed on healthy organs and tissues are upregulated by the malignant cells of certain tumors.[1-2] This overexpression facilitates the higher-than-normal rate of signal transduction and nutrient uptake required for the uncontrolled proliferation of cancer cells.[2] Researchers can take advantage of this marked upregulation by designing small molecules that bind to such receptors with high affinity and use these molecules to selectively deliver therapeutics to malignant clusters of cells while avoiding toxicity to the surrounding healthy tissue.[3] High affinity targeting ligands can also be linked to imaging agents in order to aid diagnosis and surgical procedures.[4] Cell surface receptor imaging with radio or fluorescently labeled ligands allows for the detection and visualization of both primary tumor and metastatic lesions allowing physicians to determine how far a tumor has already progressed at the time of diagnosis and also evaluate how much tissue needs to be removed during surgical resection.[5] Therefore, the discovery of novel tumor associated antigens that can selectively be targeted for delivery of drugs and imaging agents is an important contribution to the field of cancer research.

The somatostatin receptor and chemokine receptor 5 (CCR5) are two such receptors that are overexpressed by cancer cells.[6-7] Somatostatin is an endocrine regulatory hormone that inhibits the release of growth hormone from the anterior pituitary gland.[8] The natural hormone is found in the body in two active forms: as cyclic peptides of either 14 or 28 amino acid units resulting from alternative cleavage processes.[8] Somatostatin receptors are expressed throughout the central nervous system (CNS), including the hypothalamus, the cerebral cortex and the brain stem, as well as anterior pituitary, neuroendocrine, and gastrointestinal cells.[8] While playing a neurotransmitter role in the CNS, somatostatin's hormonal activities throughout the rest of the body include the inhibition of growth hormone, insulin, glucagon, and gastrin release.[8-9] Somatostatin receptors belong to the G protein-coupled receptor (GPCR) family and their general structure comprises of seven transmembrane peptide domains. The extracellular portion of the receptor binds somatostatin hormones leading to signal transduction by the intracellular segment of the receptor.[8] The human somatostatin receptor family is composed of five different receptor subtypes, named $sst_{1\text{-}5}$, according to chronological order of discovery.[10-12] These receptor subtypes arise from individual genes located on different chromosomes, which allows for a tissue-specific regulation of each isoform's expression.[10-12] Although all five receptor subtypes bind the natural somatostatin peptides, their affinities for somatostatin analogues vary widely.[11,13] Therefore, each individual receptor subtype can be specifically targeted by the development of ligands that have a high affinity for that particular isoform but not the others. Due to the important role that these hormones play in the regulation of growth signals, the expression of somatostatin receptors are augmented by certain cancers and

rare diseases. The receptor is reported to be overexpressed by numerous neuroendocrine tumors and adenocarcinomas as well as cancers of the breast, kidneys, and pituitary.[14-17] Somatostatin is also implicated in acromegaly, Cushing's disease, gigantism, and carcinoid syndrome.[18-20]

The natural somatostatin hormone itself has proven unsuitable for therapeutic purposes (partially due it its extremely low plasma half-life owing to rapid enzymatic degradation), and therefore, extensive research efforts have been focused on the development of peptide mimetics of somatostatin.[21] Several of these peptide analogs (Octreotide, Lanreotide, etc.) have been studied in animal models of cancer for their potential as imaging and therapeutic agents.[17] Although the FDA has already granted approval to a few analogs for use in clinic against certain conditions, e.g. Sandostatin® (acromegaly, gigantism, thyrotropinoma, carcinoid syndrome, and vasoactive intestinal peptide-secreting tumors), Signifor® (Cushing's disease), and Somatuline® (acromegaly and carcinoid syndrome associated with neuroendocrine tumors), approval for applying any of these somatostatin ligands as anti-cancer therapeutics is still pending.

Small molecules generally tend to be significantly better cancer therapeutics than peptide ligands due to their ability to penetrate deeper into solid tumors.[22-23] Therefore, in order to use the somatostatin receptor as a cancer target, we perused the literature for reports describing high affinity, small molecule analogs of the somatostatin hormone. Sections of this chapter describes the synthesis and functionalization of a somatostatin receptor subtype 2 and 5 specific small molecule agonist. This particular molecule is reported to bind sst_2 and sst_5 with an affinity of approximately 2 nM and 0.38 nM, respectively.[24-25]

A portion of this chapter also focuses on the development of an imaging agent to visualize CCR5 positive tumors. CCR5 is a chemokine receptor belonging to the rhodopsin-like G-protein coupled receptor family. The CCR5 protein has seven transmembrane segments, three intracellular loops, three extracellular loops, and is coded by a gene located on 3p21.[27-28] The receptor is primarily expressed on helper T cells, macrophages, monocytes, and dendritic cells. It also serves as one of the co-receptors for human immunodeficiency virus (HIV) entry into T cells.[27-28]

In healthy animals and humans chemokine receptors on circulating white blood cells selectively bind small soluble chemokine molecules that can activate and attract these immune cells to sites of inflammation.[29] CCR5 can selectively bind CCL5 (RANTES), MIP-1α (CCL3), and MIP-1β (CCL4).[30] Physiological CCL5 is a 91 amino acid chemokine usually expressed by T cells due to their role in the basic immune response against viral infections.[27,31] Since modulation of inflammation is a major characteristic of cancer,[32] chemokines and chemokine receptors are thought to play an important role in the development of the tumor microenvironment, helping set a foundation for cancer progression. Substrate binding by chemokine receptors initiates a cascade of downstream signaling events impacting certain cellular functions that are essential for cancer cell survival.[33-34] The interaction between CCL5 and CCR5 leads to the activation of ERK, MAPK, and AKT pathways, which, in the case of tumors, help sustain an environment of cancer-promoting chronic inflammation.[28] CCR5 is specifically believed to play a role in cancer progression by promoting angiogenesis, aiding tumor growth and survival, and most importantly, by supporting invasive metastasis.[33-34]

In the field of drug design, CCR5 is most attractive to researchers due to the critical role it plays in HIV infection. Therefore, great efforts have been made to design and synthesize antagonist of the CCR5 receptor with strong affinity to the receptor (sub-nanomolar IC_{50} values).[35-37] One of the receptor analogs discovered via a high-throughput medicinal chemistry screening was maraviroc (K_D for CCR5 = ~5 nM), a small-molecule antagonist of the CCR5 receptor with potent anti-HIV-1 activity.[35] The molecule was originally developed by Pfizer and is currently marketed under the trade name Selzentry®. Since CCR5 is believed to be important for the growth, metastasis, and survival of certain cancers including those of the breast, colon, prostate, and ovary,[33] it was conceivable that maraviroc could be used as a 'Trojan horse' drug carrier molecule for tumor imaging and treatment purposes. Certain sections of this chapter detail our efforts aimed towards functionalizing and subsequently conjugating maraviroc to a fluorescent dye for imaging of CCR5 expressing cancer cells.

5.2 Materials and Methods

5.2.1 Reagents

Maraviroc was obtained through the AIDS Research and Reference Reagent Program, Division of AIDS, NIAID, NIH (Bethesda, MD). All organic solvents were obtained from either Sigma Aldrich (St. Louis, MO) or the Purdue University Stores. The starting materials and reaction reagents for the synthesis of the described small molecule

somatostatin agonist were obtained from either Sigma Aldrich (St. Louis, MO) or TCI America (Portland, OR).

5.2.2 Cell Lines and Culture

LNCaP, a prostate adenocarcinoma cell line, and MCF-7, a breast cancer cell line, are reported to express elevated levels of CCR5. Both cell lines are commercially available and originated from human cancer patients. Neither cell line has undergone any modification or enhancement of receptor expression. All cells were maintained in the Cell Culture Facility of the Purdue University Department of Chemistry. LNCaP cells were cultured in RPMI 1640 medium (Invitrogen, Grand Island, NY) supplemented with 10% heat inactivated fetal bovine serum (Atlanta Biologicals, Flowery Branch, GA), 1% sodium pyruvate, penicillin (100 units/mL) and streptomycin (100µg/mL). MCF-7 cells were cultured in RPMI 1640 medium (Invitrogen, Grand Island, NY) containing 10% heat inactivated fetal bovine serum (Atlanta Biologicals, Flowery Branch, GA), 1% glutamine, penicillin (100 units/mL) and streptomycin (100µg/mL). Cells were passaged continuously in a monolayer at 37°C in a humidified atmosphere containing 5% CO_2.

5.2.3 Synthesis of the Somatostatin Receptor-Targeted Small Molecule Ligand

The synthesis of several small molecule, triazole derivative somatostatin analogs similar to the one that was chosen for the purposes of the studies described in this chapter (shown in figure 5.1) are described in some detail in a patent granted to Contour-Galcera, et al. (US Patent# 2005154039A1).[25] A modified synthetic scheme derived from this

patent and other procedures reported in literature was used in the synthesis of the desired sst_2/sst_5 agonist. Briefly, a 3-Thio-1,2,4-triazole derivative (**V**) was prepared according to the synthesis scheme detailed in figure 5.2. The starting molecules necessary for the synthesis of compound **V** and the final desired molecule, **VI**, were synthesized according to the steps summarized in figure 5.3 from commercially available materials. Condensation of isothiocyanate **I** with the acyl hydrazide **II** afforded the hydrazinecarbothioamide **IV**. The 1,2,4-triazole derivative **V** is obtained by base-catalyzed cyclization, allowing for the introduction of the third and final substituent, **III**, by subsequent S-alkylation, using polymer-supported BEMP as a deprotonating agent.[24-25] The 3-Bromo-1-(indol-3-yl)propan-1-one, **III**, was synthesized using a standard Grignard activated addition reaction.[26] All purified synthetic products used in the preparation of the final sst_2/sst_5 agonist were verified by NMR and MS.

5.2.4 Synthesis of the CCR5-Targeted Maraviroc-Rhodamine Conjugate

The purified maraviroc compound generously provided by the AIDS Research and Reference Reagent Program was functionalized for the purposes of linking a fluorescent imaging agent using standard synthetic methods reported in the literature. The initial step involved the addition of a bromine functional group to the methyl group located on the triazole ring of maraviroc. This step was accomplished by an AIBN catalyzed reaction between maraviroc and *N*-Bromosuccinimide. Due to the small amounts of maraviroc made available by the NIH, the initial bromination reactions were run on a very small scale (2-10mg) to optimize reaction conditions before moving onto larger starting material amounts (20-50mg). This reaction process is outlined in figure

5.4. Following the initial bromination step, the bromide product was subsequently reacted with the alcohol group of *N*-Fmoc-ethanolamine in order to introduce a terminal amine group that, once deprotected, was allowed to react with the NHS group of NHS-rhodamine. This final step (detailed in figure 5.5) yielded the fluorescently conjugated maraviroc, **III**, as the desired product. An alternate conjugation was also attempted to evaluate whether differences in position of linkage would alter binding affinity of the ligand to the receptor. A rather simplified flow chart detailing the synthesis of this alternate conjugate is shown in figure 5.8. Although the confocal analysis of this second molecule also showed similar results, all experiments describes henceforth will relate to conjugate **III**.

5.2.5 Confocal Microscopy Evaluation of the Maraviroc-Rhodamine Conjugate

In order to determine whether the newly synthesized maraviroc-rhodamine conjugate can recognize and bind CCR5 on the surface of LNCaP and MCF7 cells, these cells were plated on separate 4-well glass-bottomed confocal microscopy plates till ~80% confluent. The media in the wells were then removed and replaced with the appropriate unmodified complete medium (well 1), medium with a 50nM maraviroc-rhodamine concentration (well 2), medium with a 100nM maraviroc-rhodamine concentration (well 3), or the 100nM maraviroc-rhodamine solution along with a 100 fold excess of free maraviroc as competition (well 4). The cells were allowed to incubate with the fluorescent agents for 1 hour, washed 3 times with PBS to remove any unbound maraviroc-rhodamine, and the wells were replenished with complete medium before examination under an Olympus FV1000 Confocal Laser Scanning Microscope using a

60X oil-immersion objective. All fluorescence transmission images were obtained under identical conditions.

5.3 Results and Discussion

5.3.1 Functionalization of the Somatostatin Receptor-Targeted Small Molecule Ligand

Although a remarkable amount of resources and time have been dedicated to the development of novel therapeutics against cancer surgery, chemotherapy, and radiation therapy continue to be the main treatment modalities used in the clinic.[38] Surgical resection of tumor masses leading to complete cures would be an ideal scenario, but since this is rarely the case, follow-up administration of chemotherapeutic drugs with undesirable side effects is a necessity for most patients.[38-39] The unpleasant toxicities associated with chemotherapy and radiation therapy (e.g. hair loss, weight loss, nausea, anemia, reproductive issues) are a result of the non-selective manner in which these drugs treat cancer.[39] Therefore, in order to minimize damage to healthy tissues and maximize elimination of tumor cells, drugs that target cancerous tissue with high affinity and selectivity need to be developed. One way to accomplish this therapeutic goal is by designing molecules that target cancer-associated antigens. These antigens need to be either inaccessible or only expressed at low levels on healthy tissues. Generally, a 5-10 fold elevation in expression level from normal expression is regarded appropriate for targeting an antigen for cancer treatment.[40]

Following a thorough examination of the literature, it was determined that the somatostin receptor was an antigen appropriate for targeting a number of important cancers including neuroendocrine tumors and adenocarcinomas.[17] Although studies have indicated that the receptor could be present on some important healthy tissues (e.g. liver, spleen), its expression on cancer cells was expected to be significantly higher and we hoped that any negative side effects would be overshadowed by a potent therapeutic efficacy against malignant cells.[11] As described earlier in the chapter, the small molecule we selected for targeting the somatostatin receptor has extremely high affinities for the 2nd and 5th isoforms of the receptor, both of which are overexpressed by certain cancer cells.[11-12,24] The synthetic scheme outlined in the original publication that reported the molecule's discovery was reproducible for the most part with only minor modifications in regard to reaction length or temperature being necessary to obtain the desired product. However, after several failed attempts and explorations into alternate approaches, it was decided that a Grignard reaction was the most effective technique for synthesizing product **III** shown in figure 5.3.

Having completed the somewhat challenging synthesis of the molecule, the most daunting hurdle was faced while attempting to functionalize the molecule for attachment of a water soluble linker and a fluorescent imaging agent. We carefully analyzed any available literature reports that described structure activity studies and, based on these findings, were inclined to believe that the lysine-based (primary amine) and tryptophan-based side groups of the triazole ring were critical for receptor recognition and binding. Therefore, a reaction to functionalize the molecule through a quaternary ammonium bond at the aromatic ring group on the triazole was attempted. However, the product of this

reaction was deemed unstable since no mass peak of the desired molecular weight could be observed during LCMS analysis. The reaction was attempted several times under a number of different reaction conditions, but was ultimately abandoned due to the unlikely possibility of finding a location on the molecule whence to attach a therapeutic or imaging cargo without serious altering its binding affinity to the somatostatin receptor. Any significant decline in binding affinity would render the molecule useless for cancer targeting due to the fear of off-side toxicity caused by non-specific binding.

5.3.2 Conjugation of Maraviroc Interferes with its CRR5 Binding Ability

As described in the Materials and Methods, our goal for maraviroc was to functionalize the molecule at its single methyl side group by the addition of a bromine group which would then be used as a site of linkage for a fluorescent dye. This synthesis proved rather difficult because we were unable to exercise much control over the site of reaction and it was possible that bromine groups were also being added at the isopropyl group on the opposite carbon of the triazole ring. However, following many persistent trials, a conjugate with the desired molecular weight (by LCMS) was synthesized and purified. It is conceivable that the final product was a mixture of two conjugates derived from different linkage sites that both have the same molecular weight. Nevertheless, it was decided that regardless of the site of conjugation, determining whether any modifications of the molecule affected its binding affinity to the receptor was important.

We had maintained two cell lines that have been reported in the literature to express CCR5, LNCaP and MCF-7, for the evaluation of any successfully synthesized fluorescent conjugates of maraviroc. Therefore, since the affinity of naked maraviroc to

CCR5 is reported to be in the low nanomolar range and any reduction in affinity beyond 100nM would make the conjugate undesirable for further development, the two cell lines were incubated with 50 and 100nM concentrations of the maraviroc-rhodamine conjugate. Receptor-specific binding of the conjugate was measured by competition with free maraviroc. The labeled cell samples were examined under a confocal laser scanning microscope. Much to our great disappointment, as shown in figure 5.6, no uptake of fluorescent conjugate was visible in either cell line at the tested concentrations. These results could most likely be explained by two factors: 1) LNCaP and MCF-7 cells do not express any CCR5 or 2) modifications to the molecule leads to the loss of affinity for the receptor. In order to eliminate the possibility that the cell lines do not express CCR5, the maraviroc-rhodamine conjugate was incubated in wells containing human white blood cells (separated from whole blood using a ficoll gradient). Several types of immune cells, particularly T cells, are reported to express CCR5. Much to our chagrin, the data from this experiment also showed no ligand binding to cancer cells (figure 5.7) leading to the conclusion that this receptor-binding inactivity is most likely a result of the conjugation of a new compound (rhodamine) to the otherwise highly specific maraviroc molecule. Since these experiments did not eliminating CCR5 as a promising cancer antigen, it still remains a very desirable candidate for cancer targeting due to its clear implication in a number of important cancers. Other CCR5-binding small molecules should continue to be explored as targeting ligands for cancers that over-express this receptor.

5.4 References

1. Hastings, B. M.; Hecht, T. T.; Mellman, I.; Prindiville, S. A.; et al. The Prioritization of Cancer Antigens: A National Cancer Institute Pilot Project for the Acceleration of Translational Research. *Clin. Cancer Res*. **2009,** 15: 5323-5337.

2. Hanahan, D.; Weinberg, R. A. The Hallmarks of Cancer. *Cell* **2000**, 100: 57-70.

3. Low P.; Henne W.; Doorneweerd D. Discovery and development of folic-acid-based receptor targeting for imaging and therapy of cancer and inflammatory diseases. *Acc. Chem. Res.* **2008**, 41: 120-129.

4. Kelderhouse, L. E.; Chelvam, V.; Wayua, C.; Mahalingam, S.; Poh, S.; Kularathne, S. A.; Low, P. S. Development of Tumor-Targeted Near Infrared Probes for Fluorescence Guided Surgery. *Bioconjug. Chem*. **2013**, 24: 1075-1080.

5. Van Dam, G. M.; Themelis, G.; Crane, L. M.; Harlaar, N. J.; et al. Intraoperative tumor-specific fluorescence imaging in ovarian cancer by folate receptor-α targeting: first in-human results. *Nat. Med.* **2011**, 17: 1315-1319.

6. Kwekkeboom, D. J.; Kam, B. L.; Essen, M. V.; et al. Somatostatin receptor-based imaging and therapy of gastroenteropancreatic neuroendocrine tumors. *Endocr-Relat Cancer* **2010,** 17: R53-R73.

7. Vaday, G. G.; Peehl, D. M.; Kadam, P. A.; Lawrence, D. M. Expression of CCL5 (RANTES) and CCR5 in Prostate Cancer. *Prostate* **2006,** 66: 124-134.

8. Patel, Y. C. General Aspects of the Biology and Function of Somatostatin. *Basic and Clinical Aspects of Neuroscience: Somatostatin* **1992,** 4: 1-16.

9. Breeman, W. A. P.; de Jong, M.; Kwekkeboom, D. J. et al. Somatostatin receptor-mediated imaging and therapy: basic science, current knowledge, limitations and future perspectives. *Eur J Nucl. Med.* **2001,** 28: 1421-1429.

10. Patel, Y. C.; Greenwood, M. T.; Panetta, R.; Demchyshyn, L.; et al. The somatostatin receptor family. *Life Sci.* **1995**, 57: 1249-1265.

11. Reubi, J. C.; Waser, B.; Schaer, J.-C.; Laissue, J. A. Somatostatin receptor sst1-sst5 expression in normal and neoplastic human tissues using receptor autoradiography with subtype-selective ligands. *Eur. J. Nucl. Med.* **2001**, 28: 836-846.

12. Reubi, J. C.; Schaer, J.-C.; Laissue, J. A.; Waser, B. Somatostatin receptors and their subtypes in human tumors and in peritumoral vessels. *Metabolism* **1996**, 45: 39–41.

13. Cescato, R.; Schulz, S.; Waseri, B.; et al. Internalization of sst2, sst3, and sst5 receptors: effects of somatostatin agonists and antagonists. *J. Nuc. Med.* **2006,** 47: 502-511.

14. Prasad, V.; Baum, R. P. Biodistribution of the Ga-68 labeled somatostatin analogue DOTA-NOC in patients with neuroendocrine tumors: characterization of uptake in normal organs and tumor lesions. *Q. J. Nucl. Med. Mol. Imaging* **2010**, 54: 61-67.

15. Khuroo, M. S.; Khuroo, M. S.; Khuroo, N. S. Treatment of type I gastric neuroendocrine tumors with somatostatin analogs. *J. Gastroen. Hepatol.* **2010,** 25: 548-554.

16. Fottner, C.; Mettler, E.; Goetz, E.; et al. In vivo molecular imaging of somatostatin receptors in pancreatic islet cells and neuroendocine tumors by miniaturized confocal laser-scanning fluorescence microscopy. *Endocrinology* **2010**, 151: 2179-2188.

17. Lamberts, S. W. J.; de Herder, W. W.; Hofland, L. J. Somatostatin analogs in the diagnosis and treatment of cancer. *TRENDS Endocrin. Met.* **2002**, 13: 451-457.

18. Freda, P. U. Somatostatin Analogs in Acromegaly. *J. Clin. Endocrinol. Metab*. **2002**, 87: 3013-3016.

19. Lamberts, S. W. Jl; Uitterlinden, P.; Klijn, J. M. G. The effect of the long-acting somatostatin analogue SMS 201–995 on ACTH secretion in Nelson's syndrome and Cushing's disease. *Acta Endocrinol*. **1989**, 120: 760-766.

20. Vinik, A.; Moattari, A. R. Use of somatostatin analog in management of carcinoid syndrome. *Digest. Dis. Sci*. **1989**, 34: S14-S27.

21. Wolkenberg, S.; Thut, C. J. Recent progress in the discovery of selective, non-peptide ligands of somatostatin receptors. *Curr. Opin. Drug Disc.* **2008**, 11: 446-457.

22. Dreher, M. R.; Liu, W.; Michelich, C. R.; Dewhirst, M. W.; Yuan, F.; Chilkoti, A. Tumor vascular permeability, accumulation and penetration of macromolecular drug carriers. *J. Natl. Cancer Inst*. **2006**, 98: 335-344.

23. Lu, Y.; Yang, J.; Sega, E. Issues related to targeted delivery of proteins and peptides. *AAPS J*. **2006**, 8: E466-E478.

24. Contour-Galcera, M.-O.; Sidhu, A.; Plas, P.; Roubert, P. 3-thio-1,2,4-triazoles, novel somatostatin sst_2/sst_5 agonists. *Bioorg. Medchem. Lett.* **2005** (5): 3555-3559.

25. Contour-Galcera, M.-O.; Sidhu, A.; Roubert, P.; Thurieau, C. 5-Sulphanyl-4H-1,2,4-triazole derivatives and their use as medicine. **2005,** US Patent: 2005154039A1.

26. Bergman, J.; Venemaim, V. Acylation of the zinc salt of indole. *Tetrahedron* **1990** (46): 6061-6066.

27. Tasrif, A. Discovery of a Novel CCR5 Antagonist as an Effective Therapeutic Agent for Prostate Cancer. **2010**. M.S. Thesis: Virginia Commonwealth University.

28. Oppermann, M. Chemokine receptor CCR5: insights into structure, function, and regulation. *Cell. Signal*. **2004**, 16: 1201–1210.

29. Sallusto, F. The role of chemokine receptors in primary, effector and memory immune response. *Exp Dermatol*. **2002**, 11: 476-478.

30. Qin, S.; Rottman, J. B.; Myers, P.; Kassam, N. The Chemokine Receptors CXCR3 and CCR5 Mark Subsets of T Cells Associated with Certain Inflammatory Reactions. *J. Clin. Invest*. **1998**, 101: 746–754.

31. Wang, X.; Watson, C.; Sharp, J. S.; Handel, T. M.; Prestegard, J. H. Oligomeric Structure of the Chemokine CCL5/RANTES from NMR, MS, and SAXS Data. *Structure* **2011**, 19: 1138–1148.

32. Hanahan, D.; Weinberg, R. A. Hallmarks of Cancer: The Next Generation. *Cell* **2011**, 144: 646-674.

33. Aldinucci, D.; Colombatti, A. The Inflammatory Chemokine CCL4 and Cancer Progression. *Mediators Inflamm.* **2014**, Article ID 292376, 12 pages.

34. Lazennec, G.; Richmond, A. Chemokines and chemokine receptors: new insights into cancer-related inflammation. *Trends Mol. Med*. **2010**, 16: 133-144.

35. Dorr, P.; Westby, M.; Dobbs, S. et al. Maraviroc (UK-427,857), a Potent, Orally Bioavailable, and Selective Small-Molecule Inhibitor of Chemokine Receptor CCR5 with Broad-Spectrum Anti-Human Immunodeficiency Virus Type 1 Activity. *Antimicrob. Agents Ch.* **2005**, 4721-4732.

36. Li, G.; Haney, K. M.; Kellogg, G. E.; Zhang, Y. Comparative Docking Study of Anibamine as the First Natural Product CCR5 Antagonis in CCR5 Homology Models. *J. Chem. Inf. Model.* **2009,** 49: 120-132.

37. Zhang, X.; Haney, K. M.; Richardson, A. C. et al. Anibamine, a natural product CCR5 antagonist, as a novel lead for the development of anti-prostate cancer agents. *Bioorg. Med. Chem. Let.* **2010**, 20: 4627-4630.

38. Siegel, R.; DeSantis, C.; Virgo, K.; Stein, K.; et al. Cancer treatment and survivorship statistics, *CA Cancer J. Clin*. **2012**, 62:220-241.

39. Coates, A.; Abraham, S.; Kaye, S. B.; Sowerbutts, T.; Frewin, C.; et al. On the receiving end—patient perception of the side-effects of cancer chemotherapy. *Eur. J. Cancer Clin. Oncol*. **1983**, 19: 203-208.

40. Srinivasarao, M.; Galliford, C. V.; Low, P. S. Principles in the design of ligand-targeted cancer therapeutics. *Nature Rev. Drug Disc.* **2015**, manuscript in press.

41. Deady, L. W.; Devine, S. M. Synthesis and reactivity of some Imidazo-, Triazolo- and Tetrazolo-Isoquinoline derivatives. *J Heterocyclic Chem.* **2004**, 41: 549-555.

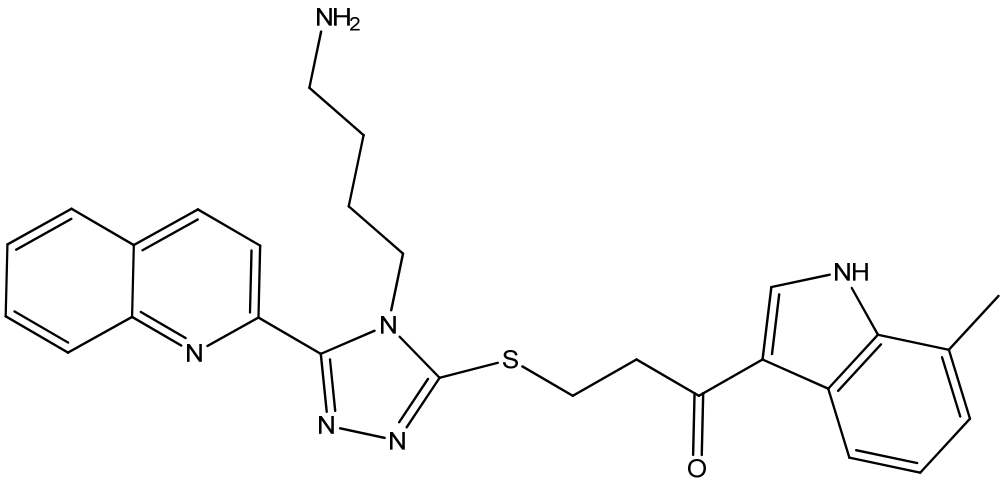

Figure 5.1. The high affinity small molecule ligand synthesized for the purposes of imaging and treating somatostatin receptor subtype 2 and 5 over-expressing cancers. The molecule is reported to be an agonist of the receptor and binds sst_2 with an affinity of ~2 nM and sst_5 with an affinity of ~0.38 nM.

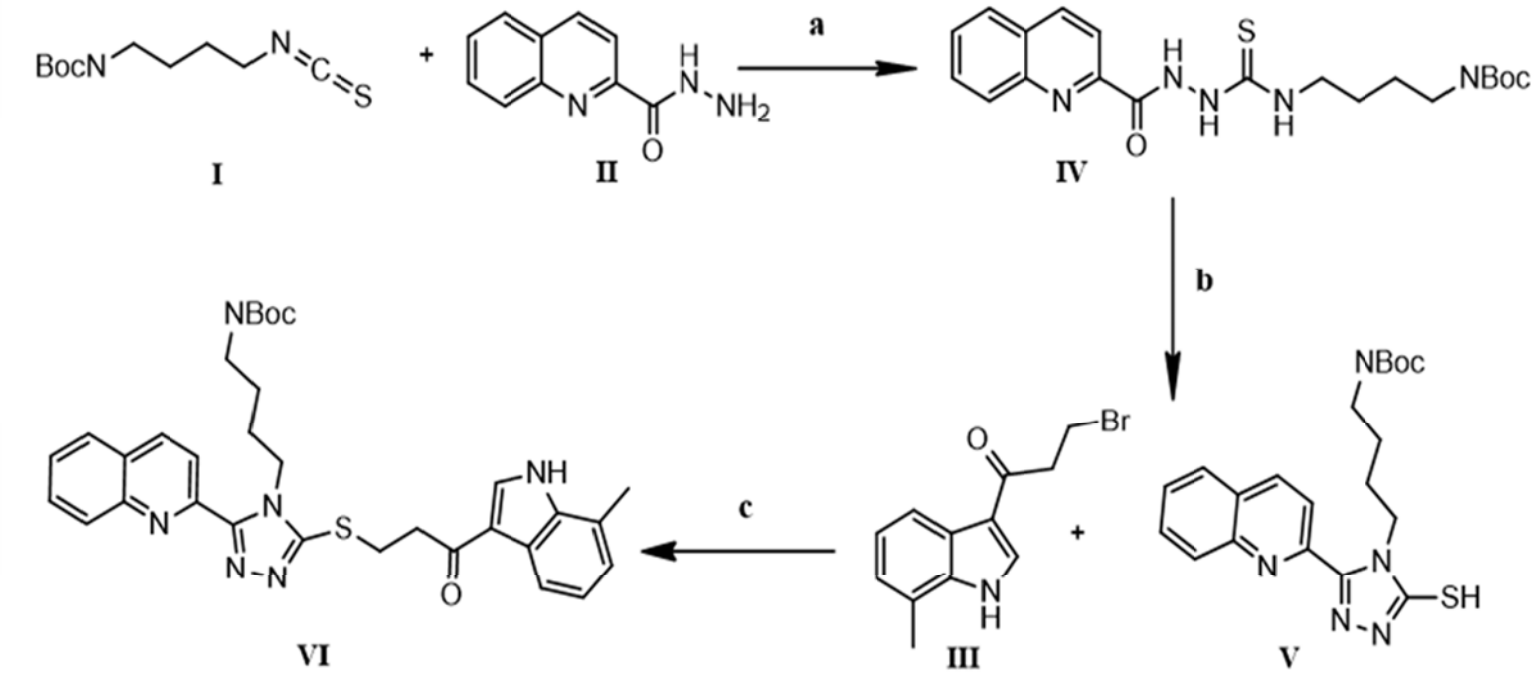

Figure 5.2. Overall synthetic route for the sst_2/sst_5 agonist, **VI**, shown in figure 5.1. Reagents and conditions: (a) DCM, 25°C, 18h; (b) 1M NaOH (1.5eq), EtOH, dioxane, 85°C, 4h; (c) PS-BEMP (3eq), 25°C, 10 min, followed by the addition of **III**, 25°C, 4h.

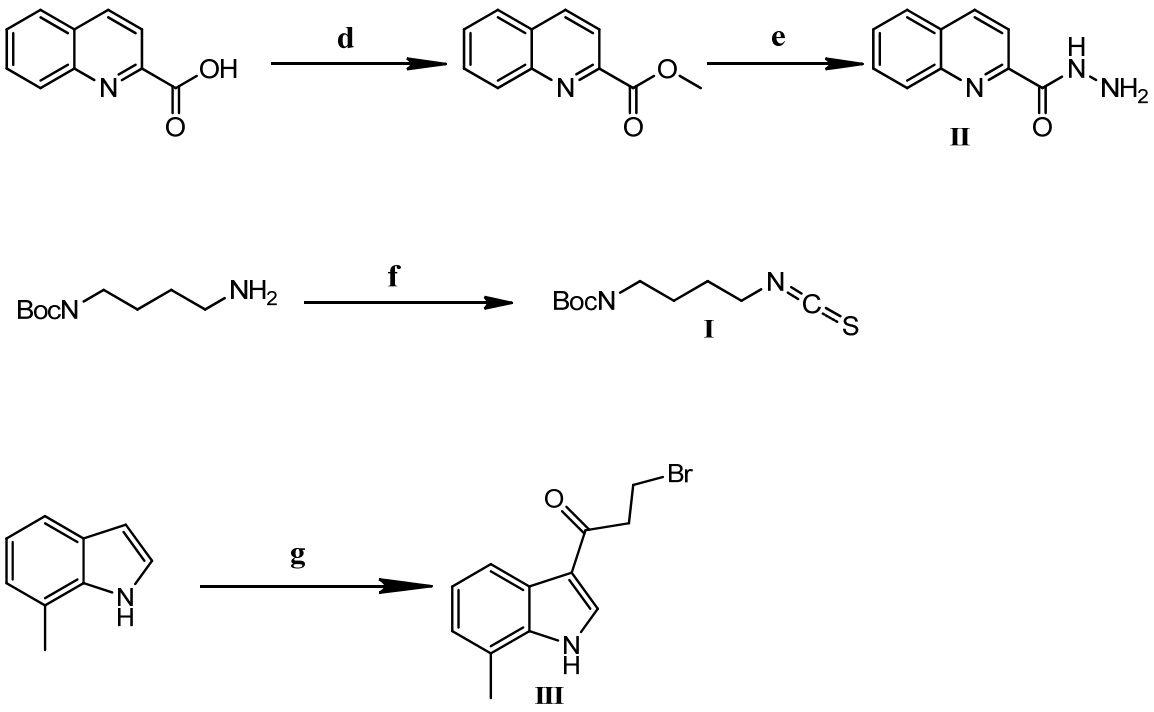

Figure 5.3. Preparation of the starting materials necessary for the synthesis of the final somatostatin ligand, **VI**, from commercially available reagents. Reagents and conditions: (d) $TMSCHN_2$ 2M in hexane (2eq), DCM/MeOH; (e) hydrazine monohydrate (10eq), MeOH, 25°C, 60h; (f) CS_2 (10eq), polymer supported *N*-cyclohexylcarbodiimide (1.1eq), DCM, 25°C, 3h; (g) EtMgBr, DCM, 0°C, 30min, $BrCH_2CH_2C(O)Cl$ (1.5eq), 25°C, 24h

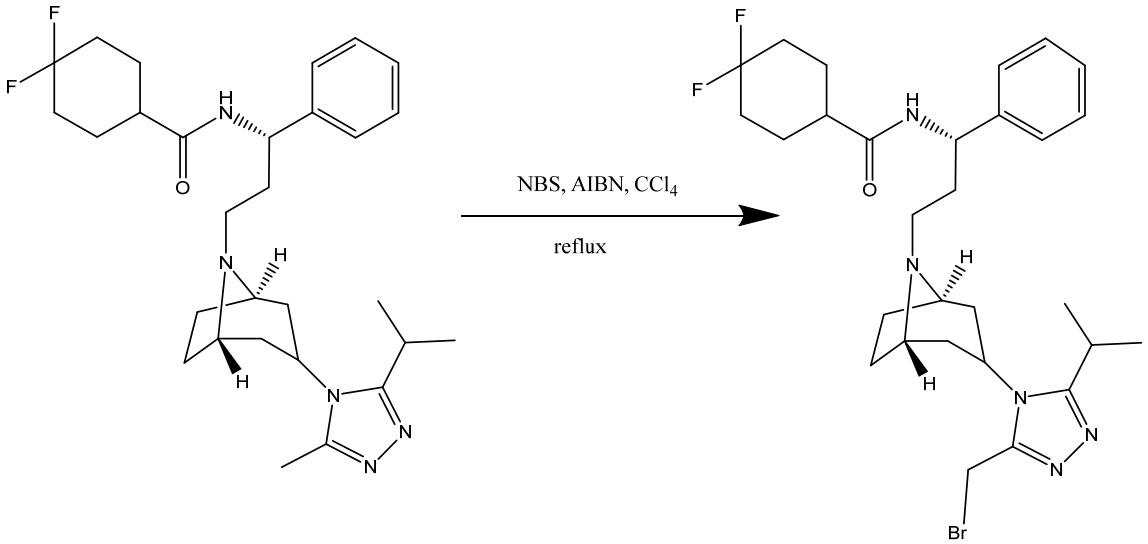

I

Figure 5.4. Synthetic step showing the desired addition of a bromine functional group to maraviroc. The resulting compound, **I**, is used in later steps to facilitate the addition of a fluorescent imaging agent to maraviroc. Maraviroc is the starting material shown in the reaction scheme.

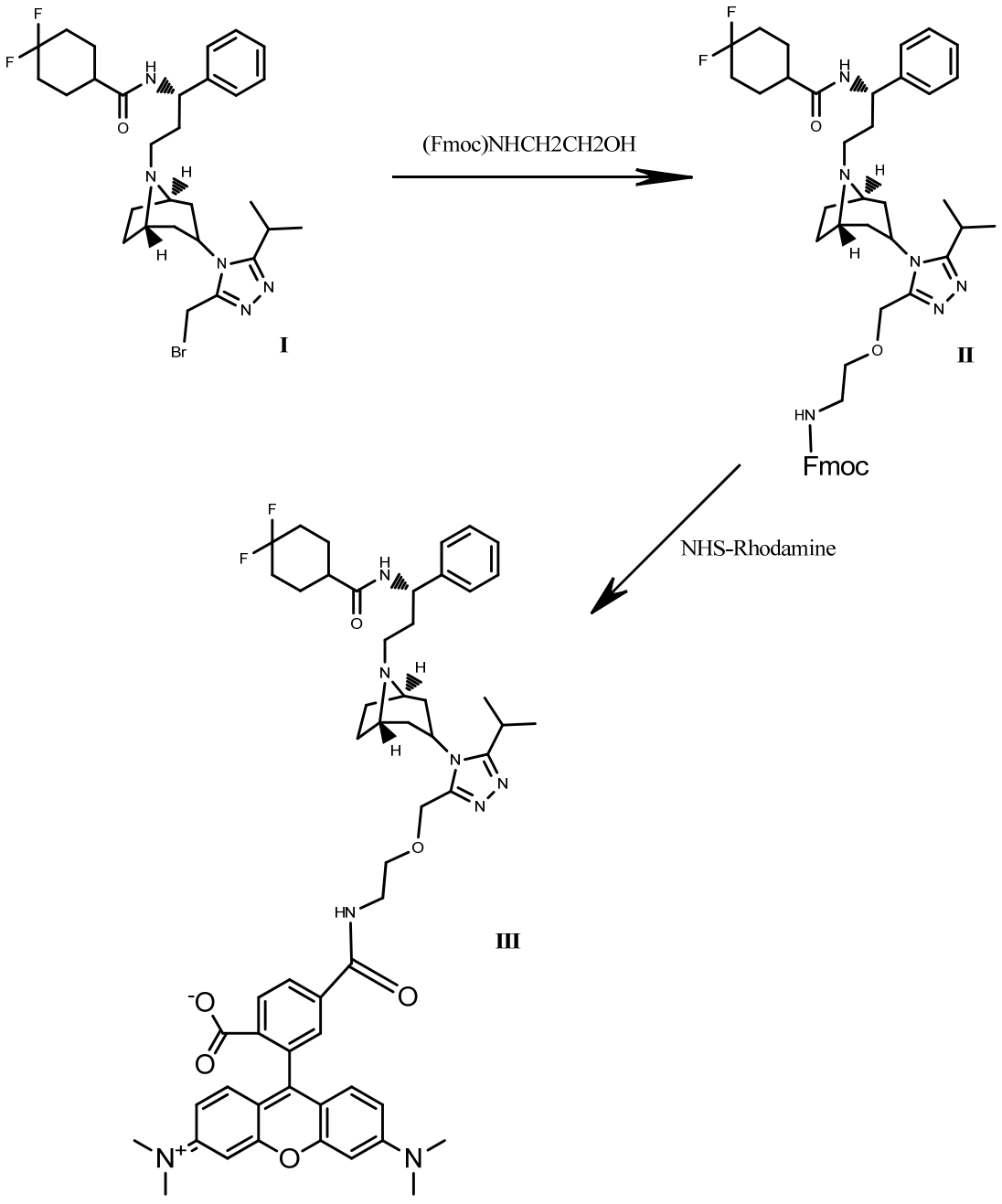

Figure 5.5. Reaction scheme detailing the steps involved in synthesizing the fluorescent maraviroc-rohodamine conjugate that will be evaluated in *in vitro* CCR5 binding studies. In the first step, an N-Fmoc-ethanolamine group is introduced to the bromine functionalized maraviroc in order to yield a free amine following deprotection. This product is then reacted with NHS-rhodamine, yielding the final maraviroc-rhodamine conjugate.

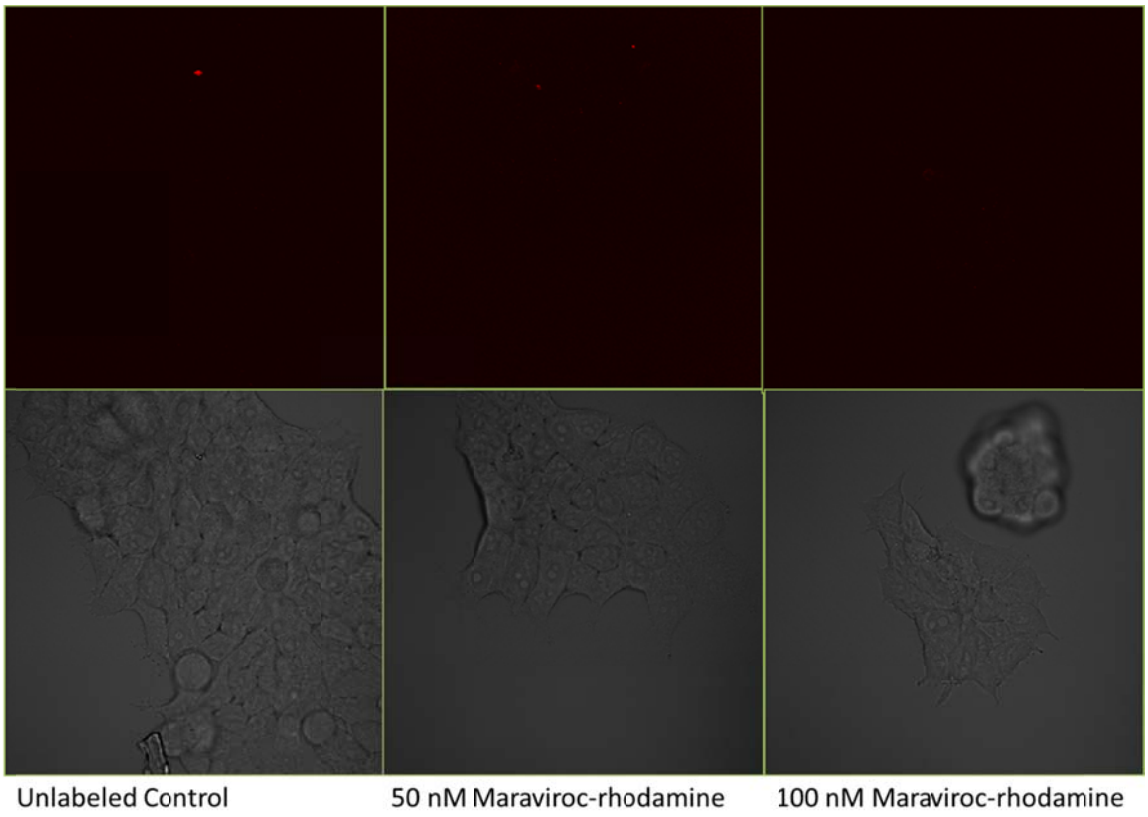

Figure 5.6. Images summarizing the confocal microscopy analysis of CCR5-expressing MCF-7 cells incubated with the maraviroc-rhodamine conjugate. Confluent wells of MCF-7 cells were incubated for 1h with two different concentrations of the maraviroc-rhodamine conjugate, washed, and imaged under an Olympus FV1000 confocal microscope using a 60X lens. The collected images indicate that modifying the maraviroc molecule by linking it to an imaging agent significantly diminishes its CCR5 affinity.

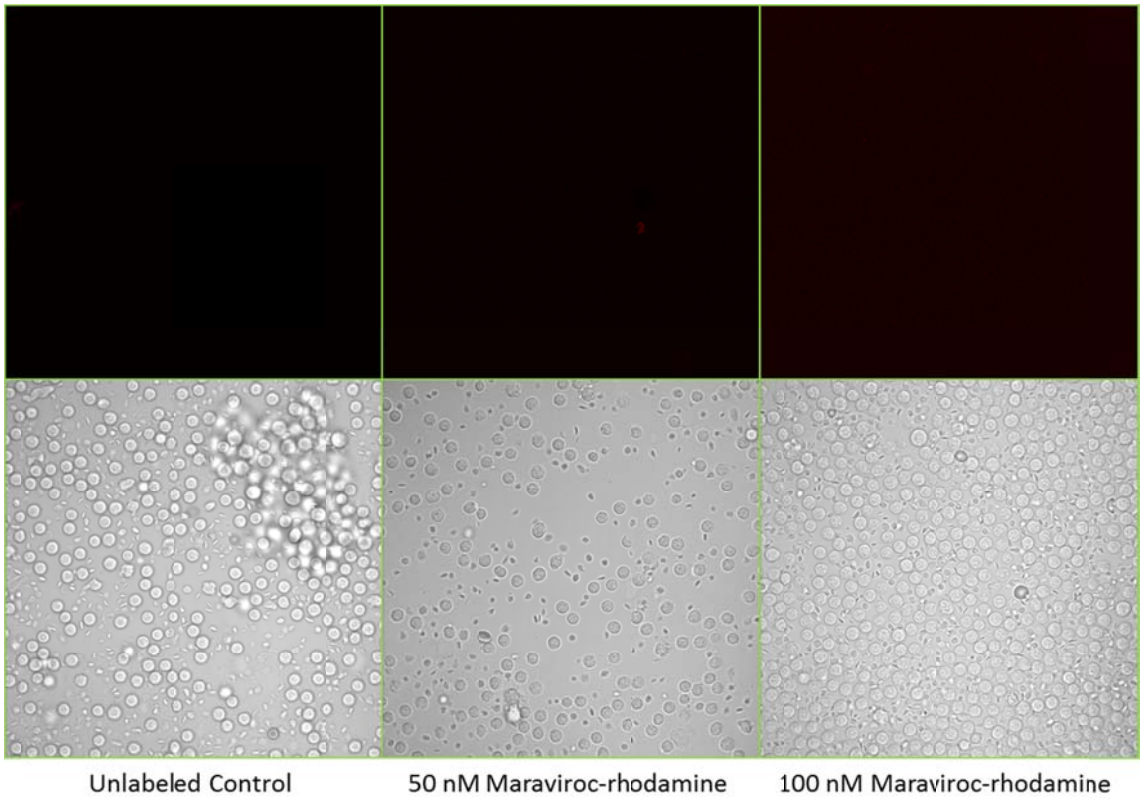

Figure 5.7. Images summarizing the confocal microscopy analysis of human white blood cells, some of which express CCR5 on their cell membrane, incubated with the maraviroc-rhodamine conjugate. 4-well confocal plates containing white blood cells were incubated for 1h with two different concentrations of the maraviroc-rhodamine conjugate, washed, and imaged under an Olympus FV1000 confocal microscope using a 60X lens. The collected images indicate that modifying the maraviroc molecule by linking it to an imaging agent significantly diminishes its CCR5 affinity.

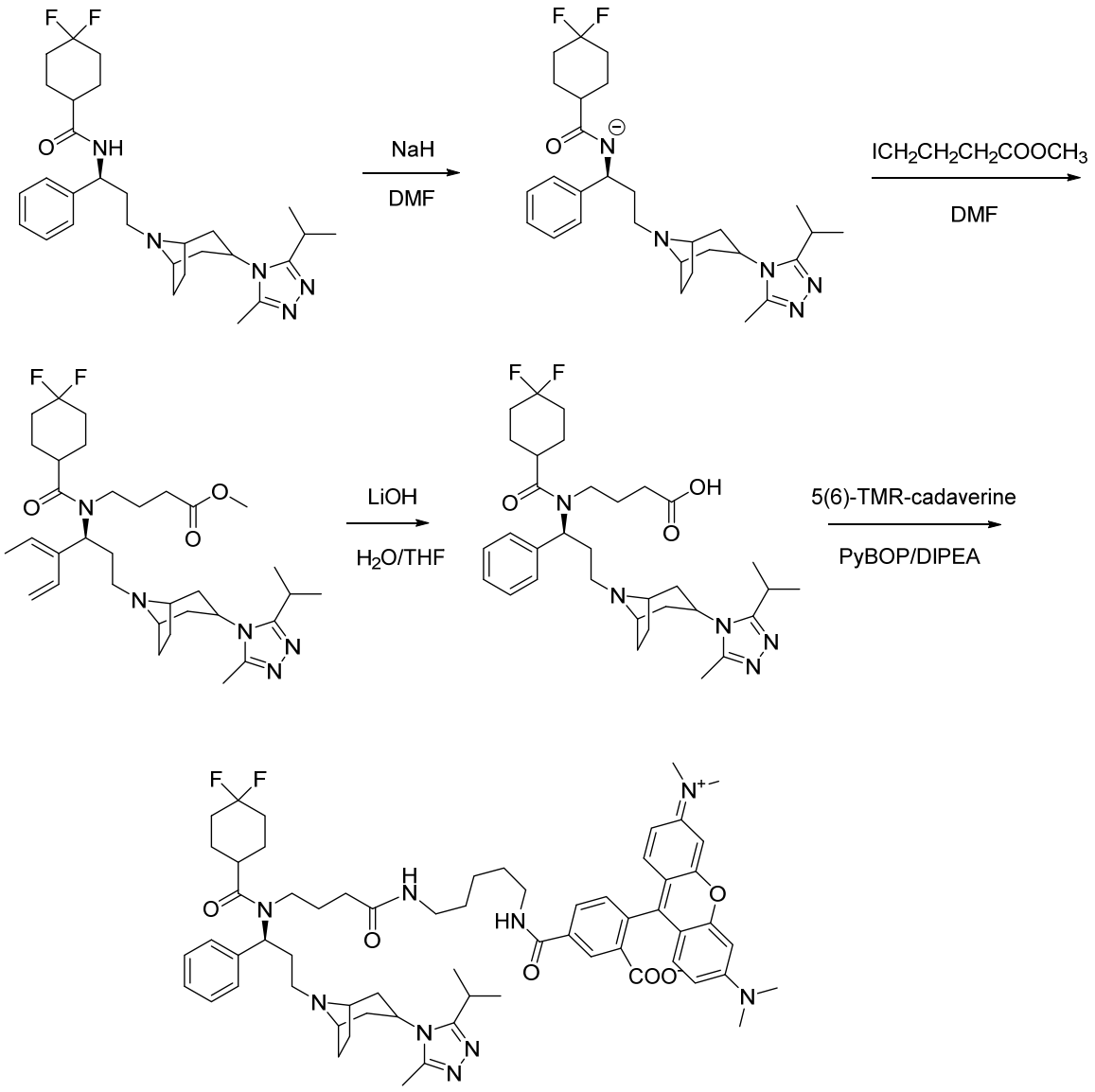

Figure 5.8. Reaction scheme detailing the steps involved in synthesizing the alternate fluorescent maraviroc-rohodamine conjugate that was evaluated in *in vitro* CCR5 binding studies to yield results very similar to those observed with the original fluorescent maraviroc compound **III**.

VITA

VITA

N. Achini Bandara is the oldest daughter of Nimal T. Bandara and Ajantha Kumari and was born in Peradeniya, Sri Lanka on February 15, 1988. Achini lived in Sri Lanka with her parents and two younger sisters, Sachini and Derani, for the first ten years of her life. She then moved with her family to a suburb of Harare, Zimbabwe where she lived till the age of fifteen. Achini attended Arundel Girls' School in Harare through Form III and first developed her interest in the sciences under the tutelage of her teachers while there. In 2003, she moved again with her family to Lexington, SC and finished her secondary education at Lexington High School, graduating in 2005. Achini spent the next four years as an undergraduate student on the beautiful campus of Wofford College in Spartanburg, SC and graduated *magna cum laude* in 2009 with a major in Chemistry and a minor in Mathematics. During the summer of 2009 she joined Dr. Philip Low's group in the Department of Chemistry at Purdue University where she worked on developing small molecule therapeutic and imaging agents for the treatment of somatostatin receptor subtype 2 and CCR5 overexpressing cancers as well as her thesis work focusing on the synergistic combination of folate receptor-targeted immunotherapy with immunomodulatory drugs for the treatment of cancer. She completed her Doctor of Philosophy degree in December 2014.